

THESIS ON MECHANICAL ENGINEERING E73

Advanced Multiphase Tribo-Functional PTA Hardfacings

ARKADI ZIKIN

TUT
PRESS

TALLINN UNIVERSITY OF TECHNOLOGY
Faculty of Mechanical Engineering
Department of Materials Engineering

This dissertation was accepted for the defence of the degree of Doctor of Philosophy in Engineering on April 23, 2013.

Supervisors: Leading researcher, Dr. Irina Hussainova, Department of Materials Engineering, Tallinn University of Technology, Estonia

Univ. Prof., Dipl.-Ing. Herbert Danninger, Faculty of Technical Chemistry, Vienna University of Technology, Austria

Advisors: Prof. Priit Kulu, Department of Materials Engineering, Tallinn University of Technology, Estonia

Dr. Ewald Badisch, AC2T research GmbH, Wiener Neustadt, Austria

Opponents: Prof. Petri Vuoristo, Department of Materials Science, Tampere University of Technology, Finland

Prof. Jaak Kikas, Institute of Physics, University of Tartu, Estonia

Defence of the thesis: June 13, 2013

Declaration:

Hereby I declare that this doctoral thesis, my original investigation and achievement, submitted for the doctoral degree at Tallinn University of Technology has not been submitted for any academic degree.

/Arkadi Zikin/



European Union
European Social Fund



Investing in your future

Copyright: Arkadi Zikin, 2013
ISSN 1406-4758
ISBN 978-9949-23-465-3 (publication)
ISBN 978-9949-23-466-0 (PDF)

MEHCHANOTEHNIKA E73

**Mitmefaasilised kulumiskindlad
PTA-keevispinded**

ARKADI ZIKIN

CONTENTS

LIST OF PUBLICATIONS	7
FOREWORD	8
PARTICIPATION AT INTERNATIONAL CONFERENCES	10
ABBREVIATIONS	11
1 REVIEW OF LITERATURE	12
1.1 Introduction.....	12
1.2 Surface treatment	12
1.2.1 Hardfacing as a method for surface treatment	12
1.2.2 Hardfacing processes	14
1.2.3 Plasma transferred arc (PTA) process.....	15
1.3 Trends in materials for PTA hardfacing	17
1.3.1 Iron based alloys	17
1.3.2 Cobalt-based and nickel-based alloys	18
1.3.3 Metal matrix composites (MMC's).....	20
1.4 Hardmetals, cermets and their application in coating technologies.....	24
1.5 Objectives of the study	26
2 MATERIALS AND EXPERIMENTAL	27
2.1 Starting materials	27
2.2 Hardfacing and main process parameters	28
2.3 Methods of characterisation.....	29
2.3.1 Microstructural characterisation	29
2.3.2 Phase analysis	30
2.3.3 Hardness at room and elevated temperature	30
2.3.4 Nanoindentation.....	31
2.4 Wear testing.....	32
2.4.1 Abrasive wear	32
2.4.2 Impact/abrasive wear	32
2.4.3 Erosive wear.....	33
2.5 High temperature corrosion	34
3 TECHNOLOGY, STRUCTURE AND PROPERTIES OF PTA HARDFACINGS	35
3.1 NiCrBSi matrix alloy	35
3.1.1 Hardfacing deposition and microstructural analysis	35
3.1.2 Mechanical characterisation.....	35
3.2 WC-Co particles reinforced NiCrBSi hardfacing	37
3.2.1 Chemical pre-treatment of hardmetal particles	37
3.2.2 Hardfacing deposition and microstructural analysis	38
3.2.3 Mechanical characterisation.....	39
3.2.4 Wear resistance	40
3.3 Cr ₃ C ₂ -Ni cermet particles reinforced NiCrBSi hardfacing	41
3.3.1 Chemical pre-treatment of milled Cr ₃ C ₂ -Ni particles	41
3.3.2 Hardfacing deposition and microstructure analysis	41
3.3.3 Mechanical characterisation.....	43
3.4 TiC-NiMo cermet particles reinforced NiCrBSi hardfacing.....	44

3.4.1 Hardfacing deposition and microstructure analysis	44
3.4.2 Mechanical characterisation.....	45
3.4.3 Wear resistance	46
3.5 TiC-Ni and ZrC-Ni cermet particles reinforced NiCrBSi hardfacings	48
3.6 High temperature wear.....	49
3.6.1 Impact/abrasive behaviour	49
3.6.2 Erosive behaviour	51
3.7 High temperature corrosion	53
4 CONCLUSIONS	55
REFERENCES.....	57
ACKNOWLEDGEMENTS	64
ABSTRACT.....	66
KOKKUVÖTE.....	68

APPENDIX

PUBLICATIONS.....	71
PUBLICATION I.....	71
PUBLICATION II.....	79
PUBLICATION III.....	91
PUBLICATION IV.....	103
PUBLICATION V.....	117
CURRICULUM VITAE.....	127
ELULOOKIRJELDUS	130

LIST OF PUBLICATIONS

The present dissertation is based on the following papers, which are referred in the text by their Roman numerals I-V.

I. Zikin, A., Ilo, S., Kulu, P., Hussainova, I., Katsich, C., Badisch, E., Plasma Transferred Arc (PTA) Hardfacing of Recycled Hardmetal Reinforced Nickel-matrix Surface Composites, *Mat. Sci. (Medžiagotyra)* 18-1, 2012, 12–17. DOI <http://dx.doi.org/10.5755/j01.ms.18.1.1334>

II. Zikin, A., Hussainova, I., Katsich, C., Badisch, E., Tomastik, C., Advanced chromium carbide based hardfacings, *Surf. Coat. Technol.* 206, 2012, 4270– 4278. DOI: <http://dx.doi.org/10.1016/j.surfcoat.2012.04.039>

III. Zikin, A., Badisch, E., Hussainova, I., Tomastik, C., Danninger, H., Characterisation of TiC-NiMo reinforced Ni-based hardfacing, *Surf. Coat. Technol.* 2013, In press. DOI: <http://dx.doi.org/10.1016/j.surfcoat.2013.02.027>

IV. Zikin, A., Antonov, M., Hussainova, I., Katona, L., Gavrilovic, A., High temperature wear of cermet particle reinforced NiCrBSi Hardfacings, *Tribol. Inter.* In press. 2012, DOI: <http://dx.doi.org/10.1016/j.triboint.2012.08.013>

V. Rojacz, H., Zikin, A., Mozelt, C., Winkelmann, H., Badisch, E., High temperature corrosion studies of cermet particle reinforced NiCrBSi hardfacings, *Surf. Coat. Technol.* 222, 2013, 90–96. DOI: <http://dx.doi.org/10.1016/j.surfcoat.2013.02.009>

FOREWORD

The degradation of materials through high-temperature processes such as oxidation, corrosion, and abrasive - erosive wear causes enormous costs for the European industry. It is crucial to avoid failure of various machine components which can entail catastrophic accidents. About 75 % of these costs are considered to be a consequence of wear-related losses. According to statistic reports, wear together with corrosion and fatigue are three main modes of materials failure. Therefore right selection of materials and cost-effective processes are a major focus for the industry in an era of global competition and environmental issues.

Recently hardfacing by welding has become a commonly used technique for improvement of material performance in extreme (high temperature, impact/abrasion, erosion, etc.) conditions. The possibility to apply hardfacing selectively and in pre-determined thickness to suit exact requirements in combating wear makes this method very attractive and cost effective.

The aim of the present work is to bring together knowledge on the manufacturing of surfaces of commercial interest, using hardfacing technique and surface engineering specialised in the characterisation of structures. Current research is concentrated on the development of novel wear resistant thick coatings (hardfacings) and their analysis in terms of microstructure, mechanical and tribological properties. Plasma transferred arc (PTA) welding is used as a hardfacings fabrication technology. During hardfacing process powders are transported to the surface of the substrate material, building protective thick metallurgically bonded coatings. Usually such coatings consist of metal matrix reinforced with coarse (up to 250 μ m) hard particles like tungsten carbides. In present research cermet particles are suggested as reinforcements for NiCrBSi matrix alloy. This can be named as a main novelty of current work. During this research formation of so-called double metal matrix composite structures is obtained.

Due to the extremely high temperature during PTA processing, the carbides are often dissolved in the matrix phase, subsequently recrystallised in form of precipitates, intermetallic phases or eta-carbides. Those material changes during the deposition process significantly influence (usually reduce) mechanical and wear properties of the hardfacings. In present work it was shown, that application of cermet particles as reinforcements can help to minimise the problem of carbide dissolution and provide thick wear resistant coatings with homogeneous distribution of cermet particles throughout the matrix.

Results indicate that TiC-NiMo and Cr₃C₂-Ni multiphase hardfacings have been proven to be the reliable candidates for high temperature tribo-applications: under the conditions of high-stress three-body abrasion TiC-NiMo reinforced hardfacings show significantly higher wear resistance as compared to the

commercial WC/W₂C reinforced coatings. Cermet reinforced hardfacings are also attractive candidates for applications in impact/abrasive conditions, especially at high temperatures. At elevated testing temperatures the volumetric wear rate values for the TiC-NiMo, TiC-Ni, ZrC-Ni and Cr₃C₂-Ni reinforced coatings are significantly lower as compared with commercially used alloys.

Based on the results of present research it is planned to deposit cermet particle reinforced NiCrBSi hardfacings as prototypes at industrial applications, particularly as wear resistant parts for iron ore sinter crushers, operating at temperatures close to 700°C in corrosive environments under impact/abrasion conditions.

PARTICIPATION AT INTERNATIONAL CONFERENCES

1. Materials Engineering & Balttrib 2010, Riga, Latvia, October 28-29, 2010.
2. IFHTSE - International Federation for Heat Treatment and Surface Engineering 19th congress: Glasgow, Scotland, October 17-20, 2011.
3. 20th International Baltic Conference "Materials Engineering" Kaunas, Lithuania, October 27-28, 2011.
4. 3rd International Symposium on Tribo-Corrosion, Atlanta, USA, April 19-20, 2012.
5. BALTMATTRIB - 21st International Baltic Conference: Engineering Materials & Tribology, Tallinn, Estonia, October 18-19, 2012.
6. IFHTSE - International Federation for Heat Treatment and Surface Engineering 20th congress, Beijing, China, October 23-25, 2012.
7. PLANSEE - 18th Plansee Seminar, Reutte, Austria, June 3-7, 2013.

ABBREVIATIONS

AC2T – Austrian Center of Competence for Tribology
ASTM – American Society for Testing and Materials
BSE – Backscattered Electron
CAT – Continues Abrasion Test
CIAT – Continues Impact-Abrasion Test
CTE – Coefficient of Thermal Expansion
CVD – Chemical Vapour Deposition
EDX – Energy Dispersive X-ray
ESAW – Electro-Slag Arc Welding
FCAW – Flux-Cored Arc Welding
GMAW – Gas Metal Arc Welding
GTAW – Gas Tungsten Arc Welding
HT-CIAT – High Temperature Cyclic Impact-Abrasion Test
HVOF – High Velocity Oxy-Fuel
MMAW – Manual Metal Arc Welding
MMC – Metal Matrix Composite
MML – Mechanically Mixed Layer
OM – Optical Microscopy
PTA – Plasma Transferred Arc
SAW – Submerged Arc Welding
SEM – Scanning Electron Microscopy
XPS – X-ray Photoelectron Spectroscopy
XRD – X-ray Diffraction
vol.% – volumetric percentage
wt.% – weight percentage

1 REVIEW OF LITERATURE

1.1 Introduction

The degradation of materials through high-temperature processes such as oxidation, corrosion, and abrasive - erosive wear causes enormous costs for the European industry. It is crucial to avoid failure of various machine components which can entail catastrophic accidents. About 75 % of these costs are considered to be a consequence of wear-related losses. According to statistic reports, wear together with corrosion and fatigue are three main modes of materials failure.

In many industrial processes such as in crushing, conveying, mixing and separating in the field of mining, steel and iron industry, cement industry, coal power plants, overground and underground working, recycling and environmental protection, the wear of tools and other work equipment plays a significant role contributing to final high costs of products. Therefore, the choice of materials that can sustain intensive wear and corrosion attacks of working instruments is of paramount importance.

1.2 Surface treatment

One of the successful methods for increasing tool durability is a surface treatment [1, 2]. Surface treatment or more commonly named “surface engineering” aims at enhancement of surface properties of the components without influencing bulk structure and properties. The processes by which a component can be surface engineered may be sub-divided into three basic groups [1]:

- Modification of existing surface without changing the composition. (Examples: shot peening, surface re-melting and transformation hardening).
- Modification of existing surface by changing the composition of a surface engineered layer. (Examples: carburising of steels, anodising and boronising).
- Modification of existing surface by application of new materials to the surface, usually named as coating process. (Examples: hardfacing, electroplating, thermal spraying, CVD).

1.2.1 Hardfacing as a method for surface treatment

One of the most economical surface treatment technology ways to increase the durability and efficiency of metal parts subjected to contact loading is hardfacing. There are many definitions for “hardfacing”; for example, according to the American Welding Society, “hard surfacing” or hardfacing is “the deposition of filler metal on a metal surface to obtain the desired properties

and/or dimensions; the desired properties are those that will resist abrasion, heat and corrosion” [3]. However, hardfacing by welding is best defined as the process of deposition by one of the various welding techniques; a layer or layers of metal of specific properties is deposited on certain areas of metal parts that are exposed to wear [4]. The possibility to apply such weld overlay coatings selectively and in various thicknesses to suit exact requirements describes hardfacing by welding also as a very economical method of combating wear. Figure 1.1 illustrates a typical wear resistant hardfacing deposited on a mild steel substrate and consisting of WC/W₂C hard particles uniformly distributed in NiCrBSi type of matrix.

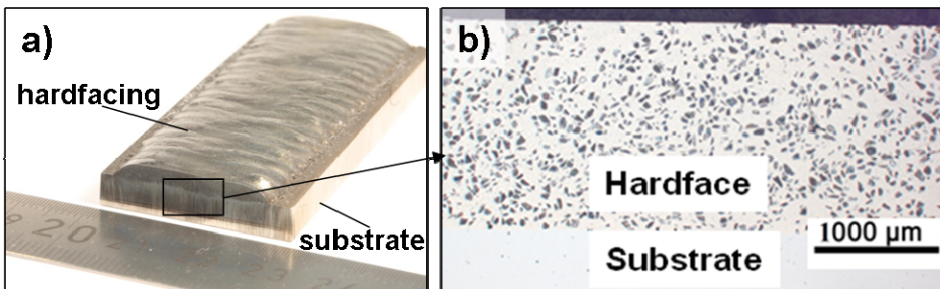


Figure 1.1 Examples of hardfacings: a) typical view of hardfacing deposited on steel substrate; b) optical microscopy cross-sectional image of NiCrBSi hardfacing reinforced with WC/W₂C carbides using PTA hardfacing process at AC2T research GmbH

Hardfacing by welding technologies offers more advantages than most of the other “anti-wear treatments” [2, 5–8]:

- Hardfacing by welding is a well established practice.
- Hardfacing can be applied in thickness levels to give long lasting protection.
- Hardfacing offers a wide variety of deposition types designed for any wear and service conditions.
- Hardfacing can be applied only to specific areas of metal parts that require high wear resistance.

There are basically two main areas where hardfacing is used [9–12]:

- To reclaim or build-up worn surfaces (use to return the part or component to its original size) as shown in Figure 1.2a. There are two solutions in that case: to replace the part or to reclaim it.
- To overlay a protective layer and protect metal parts against the loss of material (used by itself to give a component additional resistance to wear or corrosion) (Figure 1.2b).

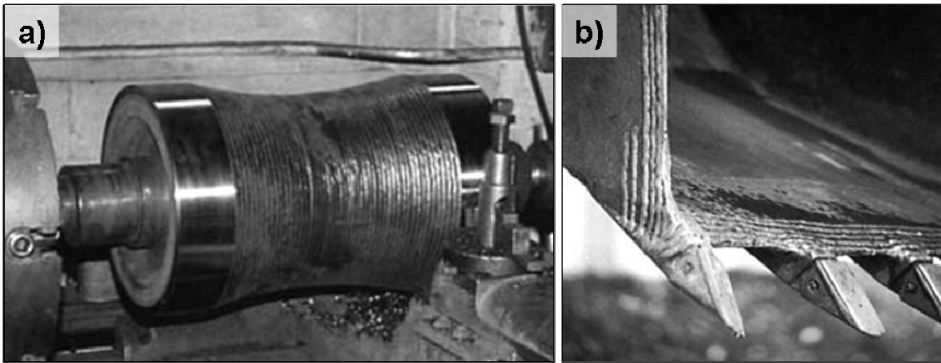


Figure 1.2 Examples of application: a) steel mill roll rebuilt to original dimensions (build-up); b) bucket lip hard surface as preventive maintenance (overlay) [10]

1.2.2 Hardfacing processes

Generally, most of the welding processes can be used for hardfacing. The weld surfacing can be classified as shown in Figure 1.3.

Solid phase bonding between metallic surfaces is obtained by cold or hot deformation processes. In fusion welding the abutting surfaces are joined by fusing the interfacial areas with or without additional consumable materials. With exception of gas and manual metal arc techniques, all other fusion welding processes can be automated. The commonly used processes include manual metal arc (MMAW), gas metal arc (GMAW), gas tungsten arc (GTAW), flux-cored arc (FCAW), electro-slag (ESW) and submerged arc (SAW) welding. Advanced processes with more intense heat sources include plasma transferred arc (PTA), laser and electron beam welding [7].

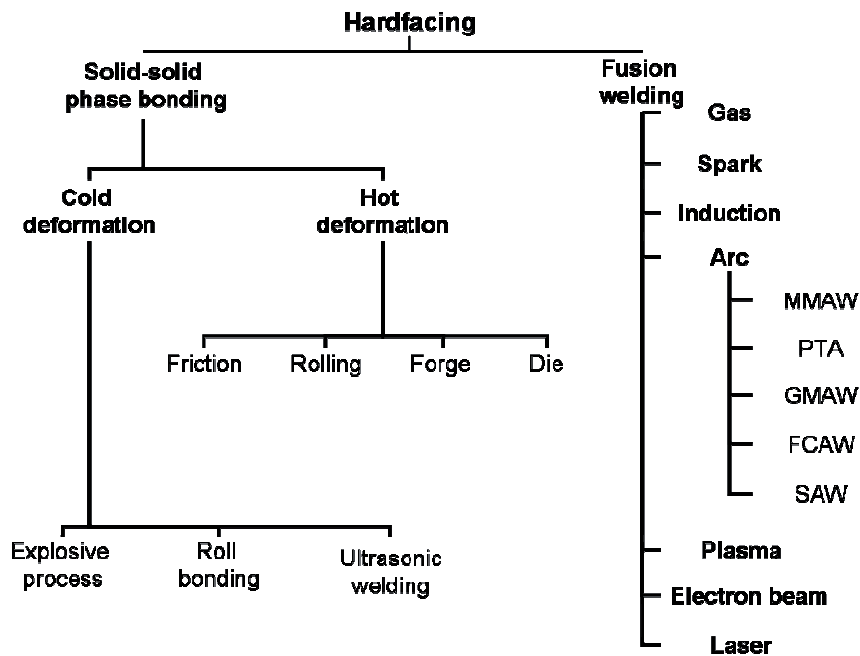


Figure 1.3 Classification of hardfacing (weld overlaying) processes, based on [7]

1.2.3 Plasma transferred arc (PTA) process

The plasma transferred arc (PTA) hardfacing process can be named as one of the most promising and cost-efficient technologies for production of thick wear resistant coatings [13–16]. This technology was developed as a modification of the GTAW and GMAW techniques in the 1960s and offers higher deposition rates and relatively low dilution. The possibility to use powder as coating consumables also increases the composition range of coatings to be deposited [15].

The detailed illustration of PTA technique is drawn in Figure 1.4. Basically this process employ a non-consumable tungsten electrode located inside the torch, a water-cooled constrictor nozzle, shield gas for the protection of the molten pool, transport gas for the delivering of powder consumables to the molten pool and the plasma gas.

A high frequency initiated non-transferred pilot arc is generated between a tungsten cathode and a water-cooled copper anode. Argon gas passes through an inner annulus between the cathode and anode and is ionised, forming a constricted plasma arc column. This ionised gas provides a current path for a transferred arc. Powder consumables are transported internally through the torch via a carrier gas and exit at orifices on the anode face, intersecting the plasma column at a distance above the substrate. The powder is introduced into a

molten pool that forms on the substrate surface. The weld pool is protected from oxidation by a shielding gas that flows from an outer annulus in the torch [15, 17].

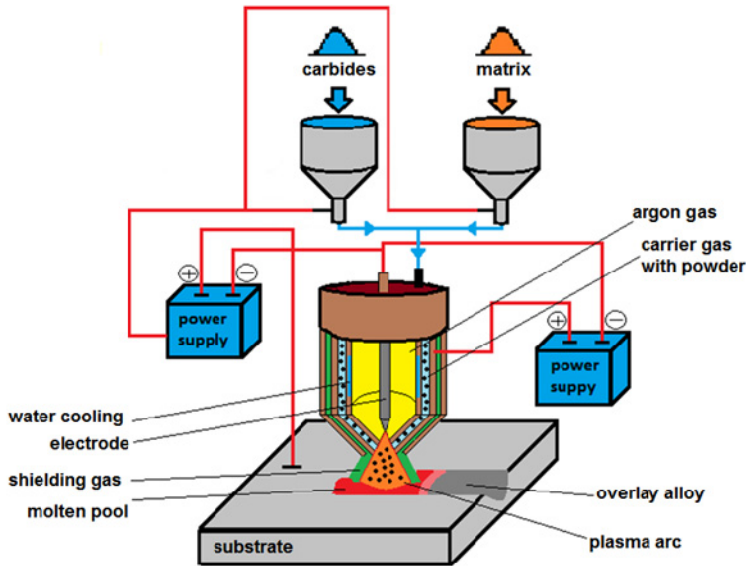


Figure 1.4 Schematic diagram of the PTA hardfacing process

The main advantages of PTA hardfacing process are [1, 7 and 15]:

- PTA provides metallurgical bonding between coating and substrate, ensuring good adhesion strength.
- PTA permits precise control of important weld parameters i.e. powder feed rates, gas flow rates, amperage, voltage, and heat input.
- PTA weld deposits are characterised by very low levels of inclusions, oxides, pores and discontinuities.
- PTA allows application of powder or combination of powders as coating consumables.
- PTA produces smooth deposits that significantly reduce the amount of post weld machining required.
- PTA parameters can be adjusted to provide a variety of deposits in thicknesses from 1.2 to 2.5 mm or higher.
- PTA offer high deposition rates with up to 15 kg/h.

The main disadvantages of this technology are not always controlled dilution and limited access to complex-shape tools.

1.3 Trends in materials for PTA hardfacing

The main feedstock materials used for the hardfacing are covered electrodes, solid wires, tubular cored wires and sintered strips [18–20]. By PTA hardfacing the main raw materials are powder consumables [15].

Generally hardfacing materials can be classified into the following main types: “build-up” alloys, metal-to-metal wear alloys, metal-to-earth-abrasion alloys, carbides and non-ferrous alloys [15, 22]. However, from a metallurgical viewpoint it is better to consider alloy types [1], where the main categories of PTA hardfacing could be selected as follows:

1. Iron-based alloys
2. Cobalt-based alloys
3. Nickel-based alloys
4. Metal matrix composites

1.3.1 Iron based alloys

The main advantage of iron-based hardfacing alloys can be attributed to their low cost and moderate wear resistance. Iron-based hardfacings are widely used in the industry, especially for the hardfacing of large equipment that undergoes severe wear, e.g. crushing, grinding, mining and earth-moving industry [1, 21–25]. There is a wide range of pearlitic, austenitic and martensitic hardfacing alloys established as industrial standards and commonly used in build-up processes, offering corrosion (austenitic alloys) and high-stress abrasion (martensitic alloys) resistance.

A very promising group of iron-based alloys belongs to cast irons. For harsh abrasive conditions the amount of Fe-Cr-C-based systems used is rapidly increasing because of the low production cost of the Fe-Cr-C powder and the growing market of high energy density powder sources for the different hardfacing techniques [26–29].

Fe-Cr-C hardfacings comprise hypo-, eutectic and/or hypereutectic structures [30, 31]. This fact depends on the energy input during the welding process due to the influence of the dilution and chromium/carbon ratio. If the carbon equivalent is less than 4.3 wt.% C, hardfacing is considered hypoeutectic and if it is above 4.3 wt.% it is considered to be hypereutectic. For both hypo- and hypereutectic structures with high carbon content (>2 wt.%) and chromium content (18-30 wt.%) formation of M_7C_3 pro-eutectic carbides is evident [33, 34]. Usually those primary carbides indicate a structure of $(Cr,Fe)_7C_3$ with rod-shape morphology. Those M_7C_3 type carbides are well known for their high hardness (about 1600 HV) combined with excellent abrasion and erosion resistance [29, 34–36]. The typical microstructure of a hypereutectic Fe-Cr-C alloy is shown in Figure 1.5a. The typical microstructure

of a complex highly alloyed Fe-Cr-C hardfacing, consisting of borides, carbides and carbo-borides in shown in Figure 1.5b.

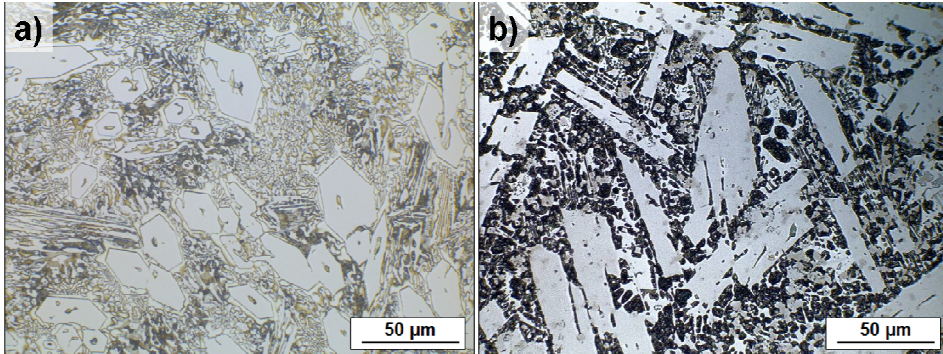


Figure 1.5 Microstructure of PTA-welded deposits: a) Fe-Cr-C hypereutectic alloy; b) Fe-Cr-C complex alloy with high amount of Nb, B, W and Mo. (powders courtesy of Castolin Eutectic GmbH; hardfacing produced at AC2T research GmbH)

The main disadvantage of iron-based alloys is their limited application at high temperature and in corrosive environments. Thus a series of alloys is available in which the iron matrix has been replaced by cobalt and nickel.

1.3.2 Cobalt-based and nickel-based alloys

For the Co-based hardfacings produced by PTA technology the main group of materials belong to the family of Stellites (carbide-containing cobalt-based alloys). The typical group of Stellite alloys used is presented in Table 1.1. High chromium levels are present for oxidation and corrosion resistance and tungsten or molybdenum provides increased matrix strength and carbide-forming ability. The main difference between these alloys is the carbon content which determines whether the alloys are hypoeutectic (for example Stellite 6), near eutectic (for example Stellite 12) or hypereutectic (for example Stellite 1). A typical microstructure of a hypoeutectic Co-based alloy is shown in Figure 1.6.

Low-carbon alloys (typically 0.25 wt.%) contain dispersed chromium-rich $M_{23}C_6$ and are reasonably ductile. These alloys provide metal-to-metal sliding wear resistance and cavitation resistance. At a carbon level of approximately 1 wt.% a network of $Co-M_7C_3$ eutectic is present. These alloys show limited ductility and may contain check cracks but have better abrasion resistance. At carbon levels of >2 wt.%, large primary carbides and $Co-M_7C_3$ eutectic are present [1].

Table 1.1 Nominal compositions of selected cobalt-based powders for PTA deposition [37]

Alloy	Nominal chemical composition of powders wt.%								
	Co	Cr	W	C	Ni	Mo	Fe	Si	other
Stellite 1	bal.	30	13	2.5	<2.0	<1.0	<2.0	<2.0	<1.0
Stellite 4	bal.	30	13.5	0.7	<2.5	<1.0	<2.5	<1.0	<1.0
Stellite 6	bal.	28.5	4.6	1.2	<2.0	<1.0	<2.0	<2.0	<1.0
Stellite 12	bal.	30	8.5	1.45	<2.0	<1.0	<2.0	<2.0	<1.0
Stellite 706	bal.	29	-	1.25	<2.0	4.5	<2.0	<1.0	<1.0
Stellite 712	bal.	29	-	2.0	<2.0	8.5	<2.0	<1.0	<1.0

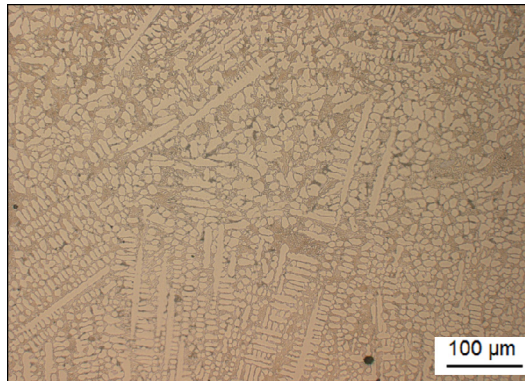


Figure 1.6 Microstructure of PTA-welded Co-based hypoeutectic hardfacing; (powder courtesy of Castolin Eutectic GmbH; hardfacing produced at AC2T research GmbH)

To achieve high temperature wear and corrosion resistance, Stellite 700 series alloys have been introduced. In this alloys tungsten is replaced by molybdenum. The molybdenum gives also an improvement in hot hardness [38].

Nickel-based materials are generally cheaper than cobalt-based alloys and have found many application fields by PTA and laser cladding technologies. Nickel-based alloys have a unique combination of properties that enables them to be used in a variety of special purpose applications. In particular, the NiCrBSi self-fluxing alloys provide adhesive wear and corrosion resistance at ambient and elevated temperatures similar to that of Co-based Stellite-type alloys. Moreover, because of the boride and carbide dispersions within their microstructures, these Ni/boride-based alloys also exhibit excellent resistance to abrasive wear. Therefore, NiCrBSi coatings are widely employed to improve the quality of components the surface of which is subjected to severe tribological conditions such as coal-fired boilers, heat exchangers, turbines, tools, extruders, plungers, rolls for rolling mills and agriculture machinery [39–43].

The typical microstructure of NiCrBSi alloys consists of borides and chromium carbides in a nickel-rich dendritic matrix [44]. At low chromium content (up to 5 wt.%) nickel boride (Ni_3B) is the main hard phase presented in the matrix; with increasing chromium concentration it is replaced by CrB and Cr_5B_3 .

Silicon provides self-fluxing characteristics and also forms the interdendritic phase with Ni-Si laminar eutectics or the intermetallic compound Ni₃Si [1, 44]. Complex carbides of M₂₃C₆ and M₇C₃ are also characteristic for the Ni-based alloys, and their fraction can be controlled by addition of Cr, B, and C and by the selection of deposition parameters [29, 45].

1.3.3 Metal matrix composites (MMC's)

Metal matrix composites have found application in many areas of daily life for quite some time [46,47]. The reinforcement of metals can have many different objectives like:

- Improvement of creep resistance
- Improvement of wear and corrosion resistance
- Improvement of high temperature properties
- Improvement of mechanical properties (hardness, yield strength, tensile strength, etc.)

MMCs can be classified as shown in Figure 1.7. For the hardfacing technologies MMCs are commonly used to reinforce the metal matrix with ceramic particles [15], building so called particle composites. Such ceramic particles as chromium, tungsten and titanium carbides can be added to cobalt- and nickel-based materials in various proportions (20–70%) to provide enhanced resistance to abrasion, impact and erosion, particularly at high temperatures [1, 8, 15, 17].

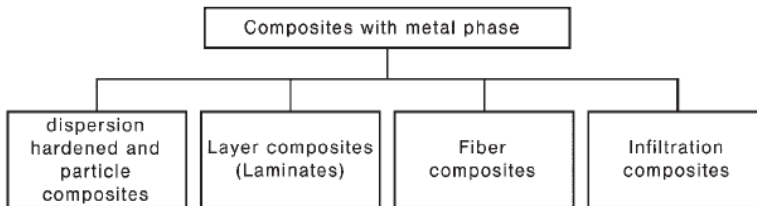


Figure 1.7 Classification of composite materials with metal matrixes [46]

Titanium carbide (TiC) can be considered as an attractive reinforcement for MMCs because of its high hardness, quite low density, good oxidation resistance and high wear resistance in erosion and abrasion environments [48–51]. Several attempts have been made to apply titanium carbide powders by hardfacing using different processing methods. For the powder feeding method, TiC-based powder and metal matrix powder are delivered into the laser or plasma beam, melted and deposited onto the substrate [4, 5, 52]. This method enables a uniform distribution of primary hardphases in the matrix and results in low carbide dissolution. Figure 1.8a illustrates a typical microstructure of laser clad TiC reinforced Fe-based alloy.

Alternative cladding methods include mixing TiC and metal matrix, pre-placing the powder mixture on the surface of the substrate with the help of an organic binder and forming a coating layer to be melted [53–55]. The coatings deposited by these techniques are mostly characterised by formation of a gradient distribution of hardphase and are highly affected by dilution and its influence on the microstructure of the final product. A promising method for the reinforcement of metal matrix with TiC particles using laser cladding involves in-situ synthesis of TiC by reaction of titanium and graphite during laser processing [56]. Such hardfacings are characterised by excellent metallurgical bonding between the coating and the substrate and the high quality of the deposited material. However, because of TiC's low density, a uniform distribution of hardphases is not easily achieved [20].

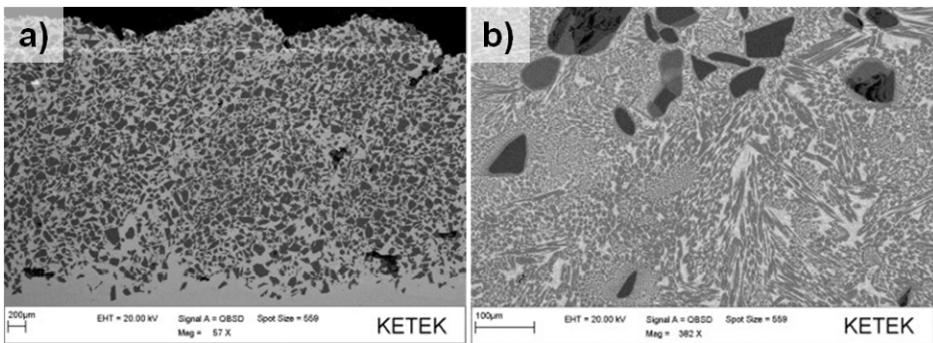


Figure 1.8 SEM cross-sectional micrographs of laser hardfaced coatings: a) 50 wt.% TiC reinforced M2 steel alloy; b) 50 wt.% Cr_3C_2 reinforced Inconel 625 alloy [7]

Several attempts have been performed to produce MMCs with Cr_3C_2 as reinforcing phase [8, 52, 57–59]. Due to the extremely high temperature of processing, the carbides are often dissolved in the binder phase and subsequently recrystallize and re-precipitate. This can have a positive effect on the low-stress abrasive wear resistance [8], but at the same time chromium carbide addition to matrix alloys can result in an increase in the propensity for thermal fatigue, cracks initiating at the incoherent carbides and propagating along their boundaries [1]. The typical micrograph of Cr_3C_2 reinforced Ni-based alloy is shown in Figure 1.8b, where the dissolution of primary carbides is evident and only few original carbides stay in the matrix.

Synthetic composite alloys consisting of a Fe or Ni-based matrix reinforced with fused eutectic tungsten carbide ($\text{WC}/\text{W}_2\text{C}$) are widely used to increase the lifetime of machinery equipment which is exposed to abrasion, erosion and impact [17, 60–62]. As compared with other carbides, tungsten carbide combines favourable properties such as high hardness, a certain amount of plasticity and good wettability by molten metals. Therefore the above mentioned alloys, mainly containing 40 to 60 wt.% tungsten carbides in a metal matrix, become dominant wherever the performance of chromium or titanium

carbides is not sufficient [63–66]. Typical micrographs of tungsten carbide reinforced Ni-based hardfacing are shown in Figure 1.9.

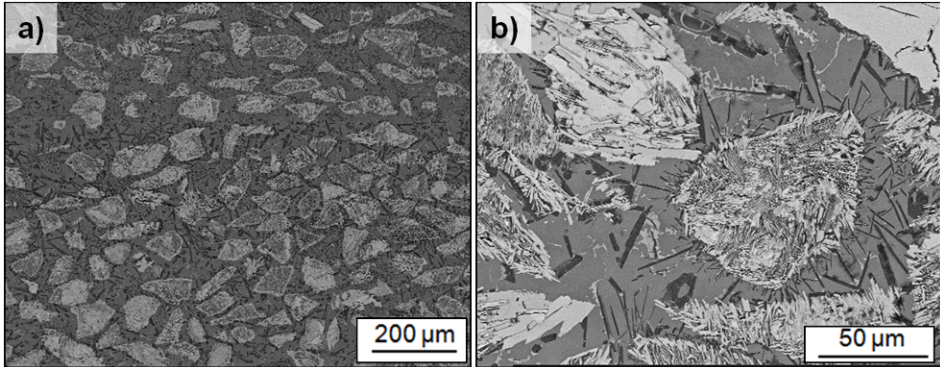


Figure 1.9 SEM cross-sectional micrographs of PTA hardfaced NiCrBSi matrix alloy reinforced with 60 wt.% of angular WC/W₂C particles (hardfacing produced at AC2T research GmbH): a) microstructure overview; b) higher magnification image

However, very much care must be taken to ensure that excessive dissolution of the tungsten carbides does not take place during the hardfacing operation. Dissolved tungsten carbide precipitates either as WC in nickel-based and cobalt-based alloys with a high carbon content, or as W₂C or eta-phase complex carbides in these melts with a low carbon concentration. The eta-carbides exist over a wide composition range and readily occur in the form of M₆C and M₁₂C in the Ni-W-C and Co-W-C systems. Both W₂C and eta-carbides are very brittle, and their corrosion and wear resistances are also inferior to those of WC [1].

A good example can be found in Ni-based matrices, where an extensive dissolution of primary carbides leads to the formation of eta-phases and intermetallic compounds such as Ni₂W₄C, which were identified as a prominent site for subsequent cracking [67, 68] and formation of so-called reaction zones (interfaces) on the grain boundary between matrix and reinforcements. The dissolution kinetic is influenced by hardfacing deposition energy. A detailed view on the carbide dissolution process for spherical WC/W₂C particles deposited by PTA with variation of welding current is shown in Figure 1.10.

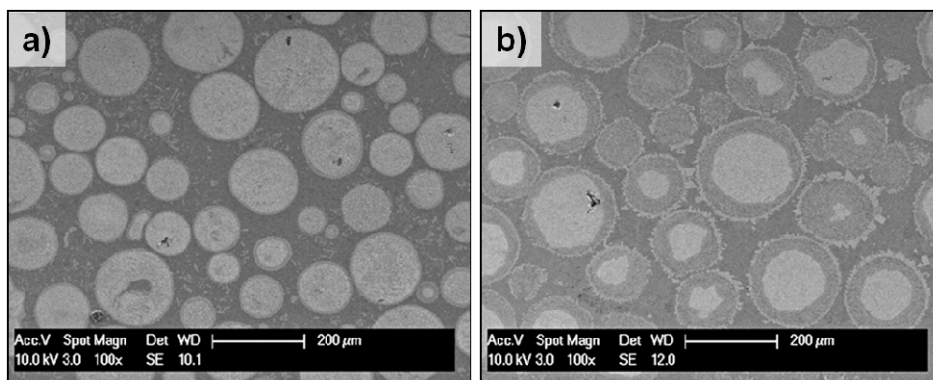


Figure 1.10 SEM cross-sectional micrographs of PTA hardfaced NiCrBSi matrix alloy reinforced with 60 wt.% of spherical WC/W₂C particles in dependence of welding current: a) welding current 50 A; b) welding current 80 A [17]

In addition, the wear rate of tungsten carbide reinforced MMCs under three-body abrasion have been shown to increase strongly with more pronounced degradation of the primary carbide during the deposition process [17, 69]. Influences of PTA processing parameters on the abrasive and impact behaviour of tungsten carbides hardfacings are shown in Figure 1.11. Under three-body low stress abrasion conditions, the wear rate of the hardfacing increases after PTA processing at higher welding current. By increasing of welding current from 50 A to 80 A, the wear rate doubles, and the highest wear rates under abrasive environments are observed for hardfacing deposited with welding current of 110 A (3 up to 4 times higher compared to 50 A). This can be explained by an increased dissolution of primary tungsten carbides. For the three-body abrasion of MMCs the major role for providing high wear resistance is played by microstructural parameter (e.g. amount of primary hardphases, their distribution in the matrix and their size); presence of eta-phases and secondary precipitates can also significantly reduce the wear resistance [69–72] and dissolution of primary carbides significantly influences most of the factors mentioned.

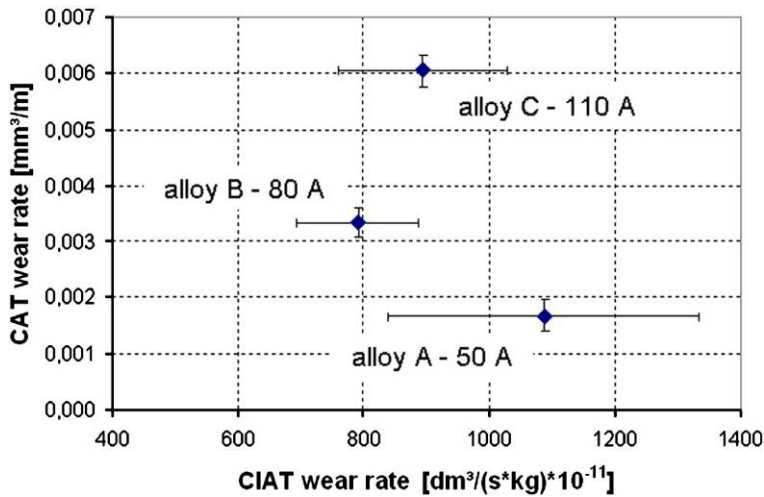


Figure 1.11 Three-body abrasion wear rate (CAT) and low energy impact (CIAT) wear rates for the PTA welded NiCrBSi matrix alloy reinforced with 60 wt.% of spherical WC/W₂C particles in dependence of welding current [17]

1.4 Hardmetals, cermets and their application in coating technologies

The term “ceramic metal composite” or “cermet” designates “a heterogeneous combination of metal(s) or alloy(s) with one or more ceramic phases” [73–75].

Hardmetals are one of the most known and successful powder metallurgical products mainly used for the manufacturing of machinery tools, which operate in environments where severe wear conditions prevail. Due to superior properties of tungsten carbide as hard phase in combination with different alloys of Fe, Co or Ni binder, it provides high wear resistance materials used in cutting, mining, drilling tools and other industrial equipment [1, 62, 76].

Cermets are very attractive candidates for applications in aggressive high temperature environments. Corrosion-oxidation resistance and wear behaviour at high temperature for TiC-based and Cr₃C₂-based cermets are widely studied. In oxidising environment and at high temperatures, the wear behaviour is influenced by rate of oxidation, adhesion of oxide layers and their resistance against impact. It was shown that TiC- as well as Cr₃C₂-based materials can be considered as suitable alternatives for WC-Co hardmetals due to their high temperature wear resistance and corrosion/oxidation stability [77–81].

Application of cermets in coating technologies is already established on the market. The main materials used there are WC-Co(Cr) and Cr₃C₂-Ni alloy powders. The process of cermet hard surfacing by thermal spraying according to the state-of-the-art is illustrated in Figure 1.12, using the HVOF spray technology as the most common process.

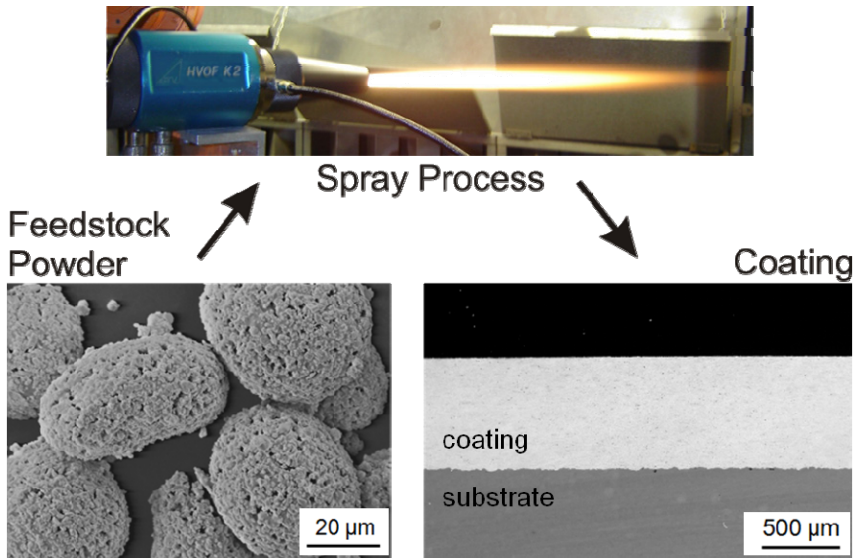


Figure 1.12 Illustration of tungsten carbide surfacing by the HVOF spray process: SEM of the feedstock powder, here an ‘agglomerated and sintered’ feedstock powder is shown (left); HVOF spray process (above); dense, WC-Co coating (right). Image courtesy of Fraunhofer IWS

Chromium carbides combined with metal matrix are often used as wear-resistant coatings on tool parts needing protection [77]. In thermal spray applications, chromium carbide is often combined with a nickel chromium matrix. The thermally sprayed $\text{Cr}_3\text{C}_2\text{-NiCr}$ coatings can serve as a barrier for high temperature wear [77, 82] and are therefore finding increasing application in many market sectors. They can be used to mitigate high temperature erosive wear in fluidised bed combustors and power generation/transport turbines, operating at temperatures to a maximum of 900-950 °C [82, 83]. $\text{Cr}_3\text{C}_2\text{-NiCr}$ thermal spray coatings can be used to protect power station boiler walls and other utility parts of coal-fired plants that are subjected to degradation by erosion-corrosion problems at high temperature aggressive atmospheres [84, 85]. Steam turbine components, in particular fittings, require high wear protection at temperatures up to 550 °C. $\text{Cr}_3\text{C}_2\text{-NiCr}$ thermal spray coatings have already entered this market, due to their excellent performances [86]. Another property that makes the application of $\text{Cr}_3\text{C}_2\text{-NiCr}$ coatings very attractive is the coefficient of thermal expansion (CTE) of chromium carbide that is almost equal to the CTE of steel, resulting in reduction in mechanical stress build-up at the boundary layer when coated on steel substrates [86].

1.5 Objectives of the study

Selection of materials and cost-effective processes are a major focus for the industry in an era of global competition and environmental issues.

The aim of the present work is to bring together knowledge on the manufacturing of surfaces of commercial interest and surface engineering specialised in the characterisation of structures.

The main objective is to develop advanced multiphase tribo-functional hardfacings and optimise the process of their deposition using PTA technology.

The main **technological goals** of the research work are:

- Development of cost-effective hardfacings for tribo-applications using recycled hardmetals as reinforcements for commercially available NiCrBSi matrix material.
- Development of multiphase hardfacings especially for high temperature applications using cermet precursor powders as reinforcements for commercially available NiCrBSi matrix material.
- Optimisation of the process of hardfacing deposition by PTA technology.

The main **scientific goals** are:

- Comprehensive structural, mechanical and tribo-chemical characterisation of the surfaces.
- Study of materials durability at extreme conditions of high temperature and corrosive media.

Throughout the thesis, the following scientific and technological aspects will be addressed:

- Pre-processing of cermets and hardmetals.
- Evaluation of the cermet and hardmetal particles as NiCrBSi matrix reinforcements.
- Deposition of the developed hardfacings.
- Microstructural characterisation of the coatings.
- Evaluation of the mechanical properties of the coatings.
- Assessment of the hardfacings as the tribo-functional materials for wear application at room and high temperatures as well as in corrosive media.

2 MATERIALS AND EXPERIMENTAL

2.1 Starting materials

Pre-processed cermet and hardmetal particles used as reinforcements for the NiCrBSi matrix alloy are listed in Table 2.1

Table 2.1: Starting powder data

Powder	Description	Particle size	Chemical composition, wt.%
NiCrBSi	Castolin Eutectic 16221	50–150 μm	0.2 C; 4 Cr; 1 B; 2.5 Si; 2 Fe; balance Ni
WC-Co	Recycled from bulk	150–310 μm	9–13 Co, 5–10 cont. *, balance WC
$\text{Cr}_3\text{C}_2\text{-Ni}$	Recycled from bulk	150–310 μm	20 Ni, 3-8 cont. *, balance Cr_3C_2
TiC-NiMo	Recycled from bulk	150–310 μm	20 Ni:Mo 2:1, 3–8 cont. *, balance TiC
WC/ W_2C	Castolin Eutectic PG6503**	45–210 μm	60 WC/ W_2C and 40 Ni-based matrix
WC/ W_2C	WOKA 50005**	45–90 μm	4 C; balance WC/ W_2C
Cr_3C_2	Sulzer Metco**	45–90 μm	-
TiC-Ni	heat treated	150–310 μm	10 Ni, balance TiC
ZrC-Ni	heat treated	150–310 μm	10 Ni, balance ZrC

* cont. – contaminations due to wear of grinding media

** powders used as reference materials

Recycling of hardmetal scrap requires applications of different processes for breakup, deagglomeration and purification of tungsten carbide particles. One of the effectively applied mechanical methods for recycling of cermets and hardmetal scrap is disintegrator milling [87, 88] providing particulates of uniform size and shape. Recycled powders can be successfully re-used for fabrication of protective coatings [89–91].

WC-Co hardmetals or cermets were milled with the help of centrifugal-type mill (DS-350, preliminary size reduction) and disintegrator milling system (DSL-175) to produce a powder. The principal scheme of the procedure applied in this work is shown in Figure 2.1, where tungsten carbide based hardmetal scrap was used as a starting material. WC-Co hardmetals were milled with the help of disintegrator technology to produce a powder and then chemically pre-treated (in acid solutions) to clean the surface of the received particles. Similar procedure was selected for the production of $\text{Cr}_3\text{C}_2\text{-Ni}$ and TiC-NiMo cermet particles from bulk.

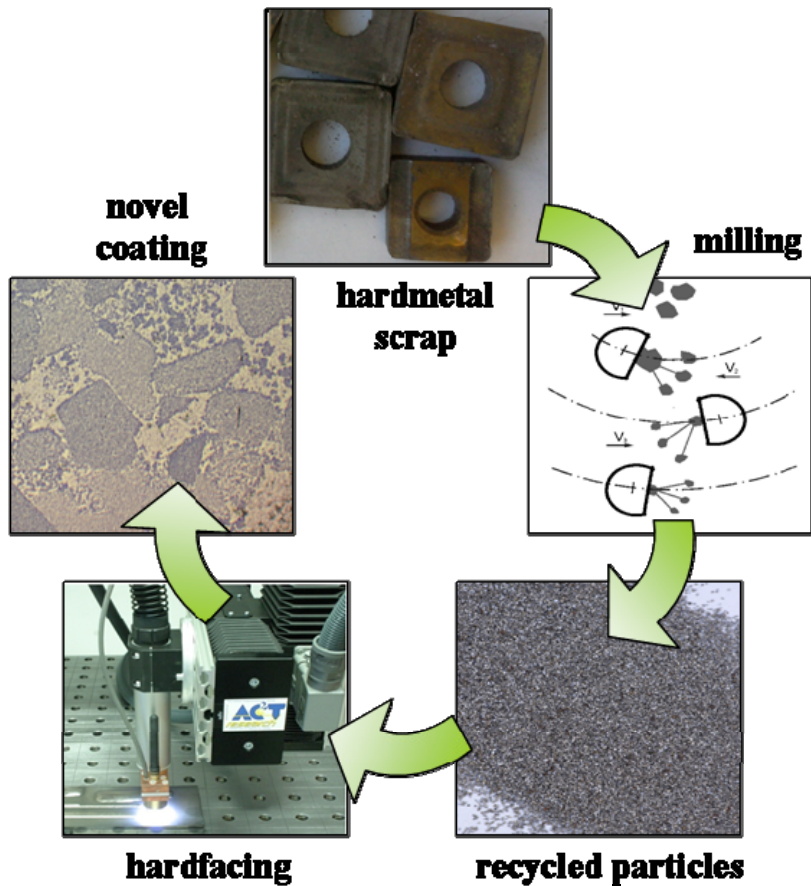


Figure 2.1 Schematic view of the work procedure

2.2 Hardfacing and main process parameters

PTA hardfacing was performed using a EuTronic® Gap 3001 DC apparatus (Figure 2.2). Welding parameters such as welding current, oscillation and welding speed, substrate, powder feed rate, nozzle distance to workpiece, process gas flow rates are the subjects of optimisation relating to the welding behaviour and practical welding procedures. A single layer welding procedure was carried out without preheating or heat control of the substrate.

40 vol.% of cermet particle reinforcements were used in this work. Two separately controlled powder feeders adjusted the required powder ratio. The powders were transported internally through the welding torch with the help of a carrier gas and then introduced into a molten weld pool which after solidification formed a metallurgically bonded layer on the surface of the base metal.

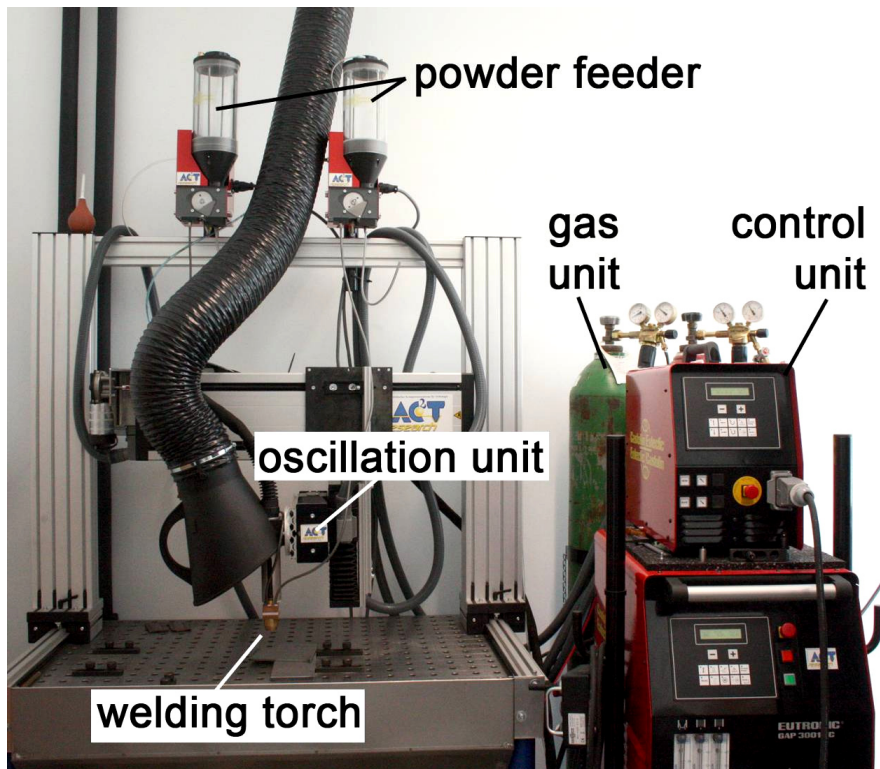


Figure 2.2 PTA welding plant at AC2T research GmbH (Castolin EuTronic® Gap 3001 DC apparatus)

2.3 Methods of characterisation

2.3.1 Microstructural characterisation

Prior to testing, the samples were slowly cut from large pieces using CBN disk, ground and subsequently polished using diamond paste. A comprehensive microstructural evaluation was performed by optical microscopy (OM) with a digital camera (MEF4A, Leica Microsystem) and scanning electron microscopy (SEM Philips XL 30 FEG), equipped with an energy dispersive X-ray analyser (EDX) with Dual BSE detector and operating at an accelerating voltage of 20 kV. For EDX quantification the standardless EDAX ZAF quantification method was used.

The microstructural examination was conducted on samples etched with a solution of HF and HNO₃ in volume ratio 1:12 at room temperature for 2 seconds. For the hardfacing with WC-Co reinforcements Murakami's etching reagent was used (K₃Fe(CN)₆ + KOH).

2.3.2 Phase analysis

X-ray diffraction (XRD) experiments were performed on an X-Pert powder diffractometer (PANalytical) in continuous mode using CuK α radiation in Bragg–Brentano geometry at 40 kV and 30 mA. The diffractometer was equipped with a secondary graphite monochromator, automatic divergence slits and a scintillation counter. Relative weight contributions (wt.%) for each crystalline phase as well as crystallite size were obtained with the help of Rietveld refinement procedure by using the commercial software TOPAS V3 [92]

X-ray photoelectron spectroscopy (XPS) experiments were performed on a Theta Probe[®] spectrometer (Thermo Fisher Scientific) using a monochromated AlK α X-ray source with the photon energy of 1486.6 eV. The vacuum chamber had a pressure of $\sim 10^{-10}$ mbar during the measurement. Survey spectra were recorded for binding energies between –10 and 1350 eV with a pass energy of 200 eV, the total dwell time of 0.25 sec per point and step size of 1 eV to determine the elements present in the particular measurement. For elements of special interest, measurements of higher resolution were also performed. The pass energy was set to 50 eV, the total dwell time per point to 0.75 s and the step size to 0.1 eV. The standard software of the Theta Probe[®] was used to evaluate the spectra. The evaluation of the data was done with help of the National Institute of Standards and Technology (NIST) database [93].

2.3.3 Hardness at room and elevated temperature

The hardness was determined by standard Vickers hardness testing. Average hardness values were calculated from 8 indents per specimen. Microhardness was measured under load of 0.01 kgf and microhardness (compound) was measured under load of 10 kgf and/or 50 kgf.

The hot hardness test is based on the Vickers HV10 test method, extended to elevated temperatures up to 800 °C (Figure 2.3) [94]. A load of 10 kgf was chosen to measure the compound hardness of multiphase materials. The whole test is performed under low vacuum (5 mbar) to protect the materials against oxidation. The sample position can be set by an actuator and hardness-vs-temperature curves can be measured. Five indents at each temperature were done for statistical evaluation.

The diagonals of the indent marks were measured by means of optical microscopy after cooling down, and Vickers hardness was calculated. The thermal expansion of the material at testing temperatures influences the hardness value <3 %. Hence, it is in the range of the test accuracy of the Vickers standard method. For this investigation the hot hardness was measured at room temperature (RT), 100, 300, 500, 600, 700 and 800 °C, respectively.

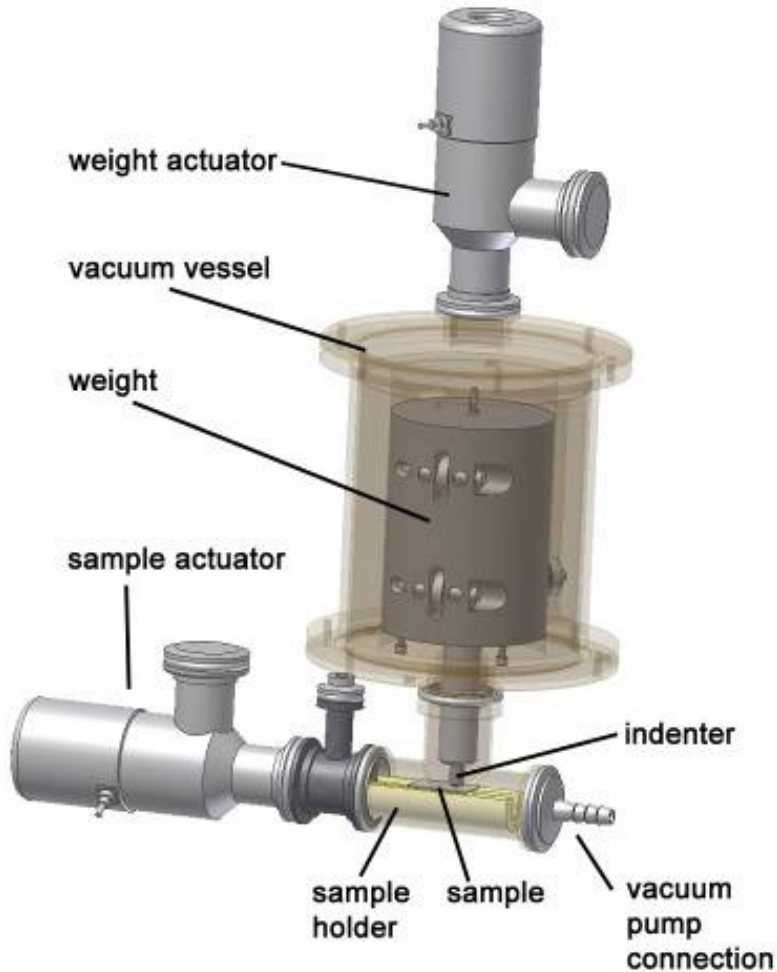


Figure 2.3 Schematic of hot hardness tester, developed at AC2T research GmbH [94]

2.3.4 Nanoindentation

To evaluate the mechanical properties of constituent phases, nanoindentation measurements were performed using a Hysitron Triboindenter TI900 equipped with a diamond Berkovich indentation tip with 100 nm tip radius. The load cycle comprised loading for 5 s to reach the peak load of 10 kfg and subsequent unloading for 5 s. The load vs. depth curves were analysed to determine the reduced elastic modulus and hardness using the procedure described elsewhere [95].

Micro-mechanical properties of separate phases (hardness and reduced Young's modulus) were determined by nanoindentation measurements and statistically analysed. The reduced Young's modulus (E_r) is described by following equation [95]:

$$1/E_r = (1-\nu_i^2)/E_i + (1-\nu_s^2)/E_s,$$

where ν is the Poisson's ratio, the index i denotes the values for the indenter tip and the index s the ones for the sample. For more details see PUBLICATION II and PUBLICATION III.

2.4 Wear testing

Tribological performances of the hardfacings were evaluated using different wear testing methods at room and elevated temperature. The wear behaviour under the following loading modes was investigated in the present study: abrasion; impact/abrasion and solid particle erosion.

2.4.1 Abrasive wear

The abrasive wear performance was evaluated using a three-body abrasion tester (as for ASTM G65) with variation of testing conditions:

- use of a dry-sand rubber wheel according to ASTM G65 requirements [96].
- application of a steel wheel to simulate high-stress wear behaviour of materials.

The main process parameters are listed in Table 2.2.

Table 2.2 Main three-body abrasion test work parameters

Parameter	Value
Wheel materials	rubber, steel
Rotation speed	200 rpm
Normal load	130 N
Sliding distance	4309 m
Abrasive material	SiO ₂
Abrasive particle size	0.2–0.3 mm

Before and after testing each specimen was cleaned with acetone, dried and weighed. At least three tests were run for each material to determine the wear resistance.

2.4.2 Impact/abrasive wear

Impact/abrasive wear tests were done on a cyclic impact abrasion tester (HT-CIAT) developed at AC2T research GmbH. The samples were mounted at 45° to the horizon, cyclically hit by a plunger at a given frequency in combination with an abrasive flow between the sample and the plunger (Figure 2.4) [94].

The samples were cleaned in an ultrasonic bath with isopropanol, dried and weighed before and after testing. Quantitative wear characterisation was conducted by measuring the gravimetric mass loss of the testing specimens. Tribo-tests parameters are listed in Table 2.3.

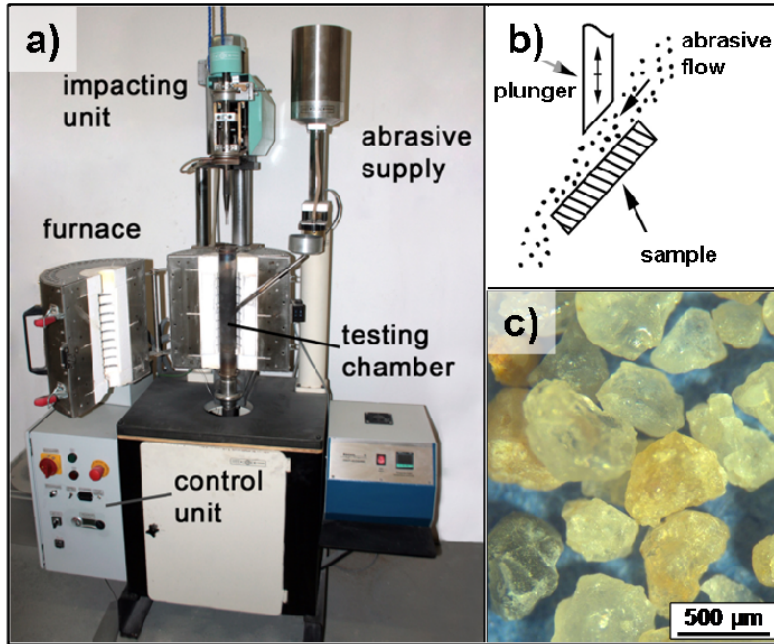


Figure 2.4 High temperature cyclic impact abrasion tester: a) view of testing device b) testing principle (45° impact angle with abrasives); c) abrasive silica particles [94]

Table 2.3 HT-CIAT test conditions

Parameter	Value
Impact energy	0.8 J
Impact angle	45°
Frequency	2 Hz
Testing cycles	7200
Abrasive material	SiO ₂
Abrasive flow	3 g/s
Abrasive particle size	0.4–0.9 mm
Abrasive hardness	1000–1200 HV1
Test temperatures	20 °C, 350 °C, 550 °C, 700 °C

2.4.3 Erosive wear

Erosion tests were performed on a centrifugal particle accelerator described elsewhere [97, 98]. The test parameters are listed in Table 2.4. Before and after testing each specimen was cleaned with acetone, dried and weighed. At least three tests were run for each material to determine the erosion resistance.

Table. 2.4 Erosion test conditions

Parameter	Values
Impact velocity	50 m/s
Impact angles	30°, 90°
Erodent	SiO ₂
Erodent particle size	0.1–0.3 mm, angular
Total quantity of erodent	6 kg
Test temperature	20 °C, 350 °C, 550 °C, 650 °C

2.5 High temperature corrosion

High temperature corrosion in solid salts was studied to examine the influence of different anions at elevated temperature. This study was performed to simulate the industrial conditions, for example of steel sinter plants and gas-oil industry, where high temperature corrosion is common wear mechanism.

The corrosion tests were performed at 700 °C to show stability against corrosion at high temperature and correlate the findings with the oxidation behaviour of the hardfacings. Both, corrosion and oxidation tests were performed over a period of 24 hours.

Chosen anions were:

- hydrogen carbonate HCO₃⁻
- chlorine Cl⁻
- hydrogen phosphate HPO₄²⁻
- hydrogen sulphate HSO₄⁻

The resulting salts were:

- sodium hydrogen carbonate NaHCO₃
- sodium chloride NaCl
- di-sodium hydrogen phosphate Na₂HPO₄
- sodium hydrogen sulphate NaHSO₄

For explicit oxidation, tests at the same temperature were carried out in air. After preparing the samples (fine ground condition) of 7×7×2 mm, they were cleaned with ethanol, weighed and put into small ceramic crucibles for assembly in the furnace. All samples were completely surrounded with 10 g of salts to guarantee full contact between the samples and the anions during high temperature corrosion tests at 700 °C. The corroded surfaces were investigated by OM/SEM/EDX.

3 TECHNOLOGY, STRUCTURE AND PROPERTIES OF PTA HARDFACINGS

3.1 NiCrBSi matrix alloy

3.1.1 Hardfacing deposition and microstructural analysis

The optimised deposition parameters for the NiCrBSi matrix alloy are listed in Table 3.1

Table 3.1 Main process parameters for the deposition of NiCrBSi matrix alloy

Parameter	Data
Welding current	80 A
Oscillation speed	20 mm/s
Oscillation width	20 mm
Welding speed	1.2 mm/s
Plasma gas	1.6 l/min
Substrate material	austenite steel (316L)
Substrate thickness	5 mm

XRD analysis of the original NiCrBSi matrix alloy indicated a high amount of $\gamma(\text{Fe,Ni})$ solid solution in Ni-based matrix with presence of small amount of Ni_3B and Cr_7C_3 hardphases (Figure 3.1a). Microstructural analysis has proven that NiCrBSi self-fluxing matrix alloy exhibits a nickel-rich dendritic matrix containing borides and carbides (Figure 3.1b), what is a typical phase composition for alloys with low chromium content [1]. According to the phase distribution analysis the content of Cr_7C_3 phase is 2 ± 1 wt.%, whereas the content of Ni_3B phase is 19 ± 1 wt.%. For more details see PUBLICATION II.

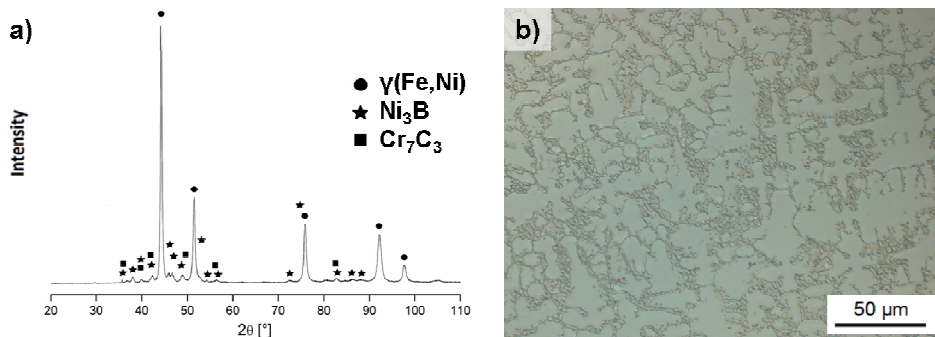


Figure 3.1 NiCrBSi hardfacing: a) XRD pattern; b) optical micrograph in cross-section

3.1.2 Mechanical characterisation

Vickers macro hardness of the NiCrBSi alloy was measured at 375 ± 6 HV10.

The measured hot hardness values for the original (monolithic) and the hard particle reinforced matrix alloy are presented in Figure 3.2. Hot hardness of the NiCrBSi alloy is 380 ± 40 HV10 at temperatures below 600 °C and rapidly decreases with increase in temperature. For more details see PUBLICATION II and PUBLICATION IV.

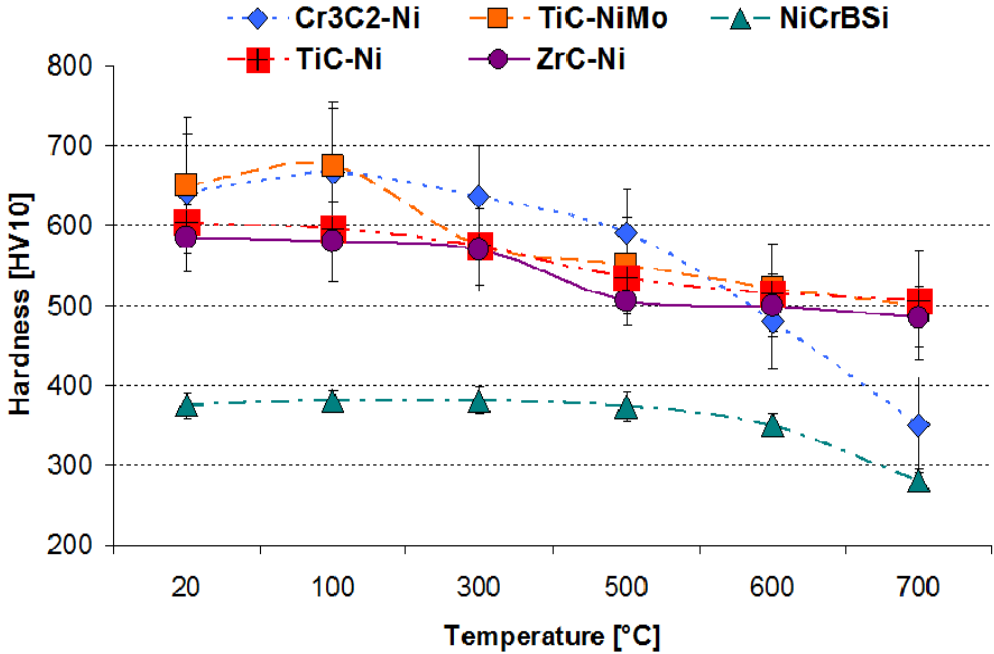


Figure 3.2 Hot hardness distribution curves for original NiCrBSi matrix alloy and Cr₃C₂-Ni, TiC-NiMo, TiC-Ni and ZrC-Ni reinforced NiCrBSi matrix alloy

3.2 WC-Co particles reinforced NiCrBSi hardfacing

3.2.1 Chemical pre-treatment of hardmetal particles

During the recycling process by disintegrator milling, the hard and dense hardmetals wear the mechanical grinding apparatus, contaminating the obtained powder. As a result the presence of iron-based particles and surface contaminations can be found in resulting hardmetal powder as shown in Figure 3.3.

Surface contamination, especially by oxides, can significantly influence quality, properties and performance (decrease weldability; increase porosity) of recycled hardmetal powder. During the PTA process, contaminants can cause CO or other gases to form, resulting in pores. This negative factor affects the final surface quality of nickel-based compositions. To produce reliable pore-free coatings, the quality of recycled powders needs to be improved.

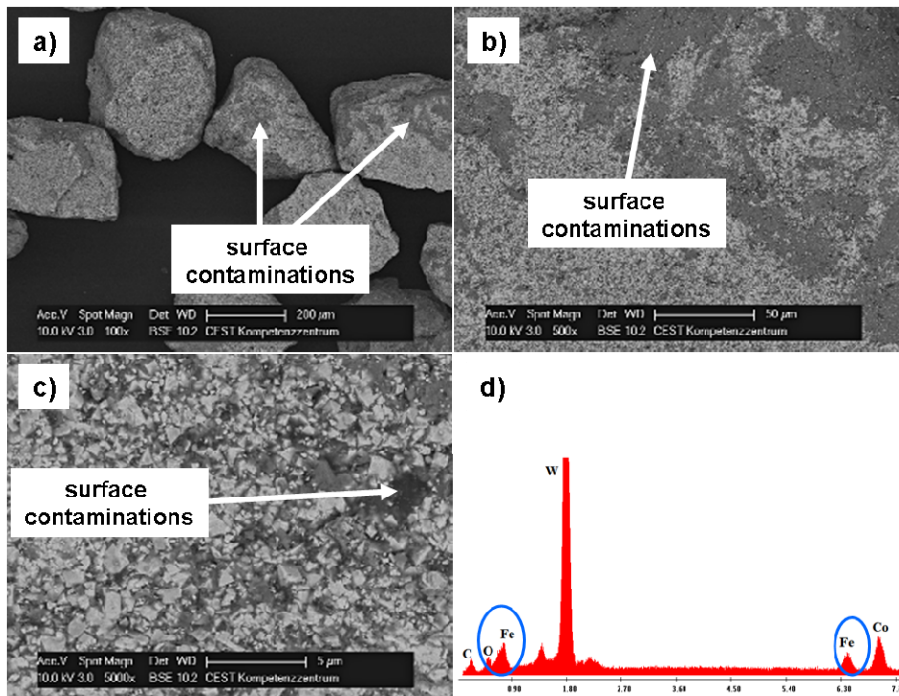


Figure 3.3 SEM micrographs: a) recycled WC-Co particles; b) and c) close view on the surface contaminations; d) EDX analysis of the area in c)

The present study has been focused on chemical pre-treatment of the powders produced from WC-Co scrap. The process of hardmetal scrap cleaning has been developed based on the commercially cheapest method of chemical pre-treatment and simplicity of experimental procedure that allows quick, efficient

and effective treatment of the recycled hardmetal powders to be used for PTA hardfacing process.

Cross-section image of both weld deposits (with chemically cleaned compared to not cleaned WC-Co particles) under the same deposition parameters are presented in Figure 3.4. The results indicate significant improvement of weld deposit quality. No porosity is found in either cross or longitudinal sections for the pre-treated weld. This chemical pre-treatment method has demonstrated to significantly improve the quality of recycled powders. For more details see PUBLICATION I.

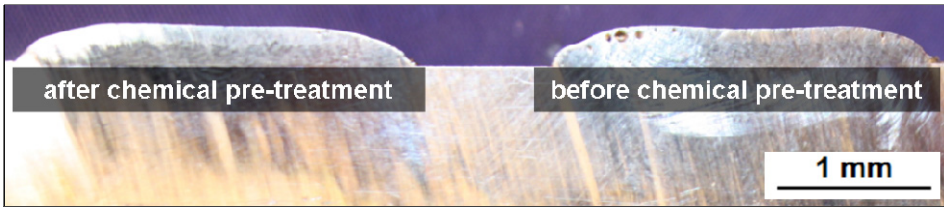


Figure 3.4 Cross-sectional images of PTA weld deposits for WC-Co particles reinforced NiCrBSi matrix alloy with treated and untreated hardmetal particles

3.2.2 Hardfacing deposition and microstructural analysis

The optimised deposition parameters for the WC-Co reinforced NiCrBSi hardfacing are listed in Table 3.2.

Table 3.2 Main process parameters for the deposition of WC-Co reinforced NiCrBSi hardfacing

Parameter	Data
Welding current	90–100 A
Oscillation speed	18–20 mm/s
Oscillation width	20 mm
Welding speed	0.7–1.0 mm/s
Plasma gas	1.6–2.0 l/min
Substrate material	mild steel (1.0037)
Substrate thickness	10 mm

Figure 3.5 illustrates a typical cross-sectional SEM micrograph of the deposited coating with 40 vol.% of hardmetal particles, where formation of three different main phases was observed: A complex matrix structure with Ni and Fe as the main elements and two different modifications of carbide grain structures (apparent phases B and C).

Microstructural analysis indicates penetration of the matrix elements (Fe and Ni) into the Co binder “into the” hardmetal agglomerates and partial dissolution of carbides. However, the carbides retain the angular grain shape developing the micro-sized MMC-particles in the coating with a “double-dispersed” MMC-structure (micro carbides with metal matrix).

The main difference between phases B and C is the matrix composition inside the hardmetal particle. Apparent phase C shows only 30 vol.% of carbide particles with average grain size of 1.3 μm (Figure 3.5b), whereas apparent phase B (Figure 3.5c) indicates mirrored structure of the metal matrix components with 70 vol.% of carbides and a factor of two coarser average particles size compared to phase C (2.5 μm). For more details see PUBLICATION I.

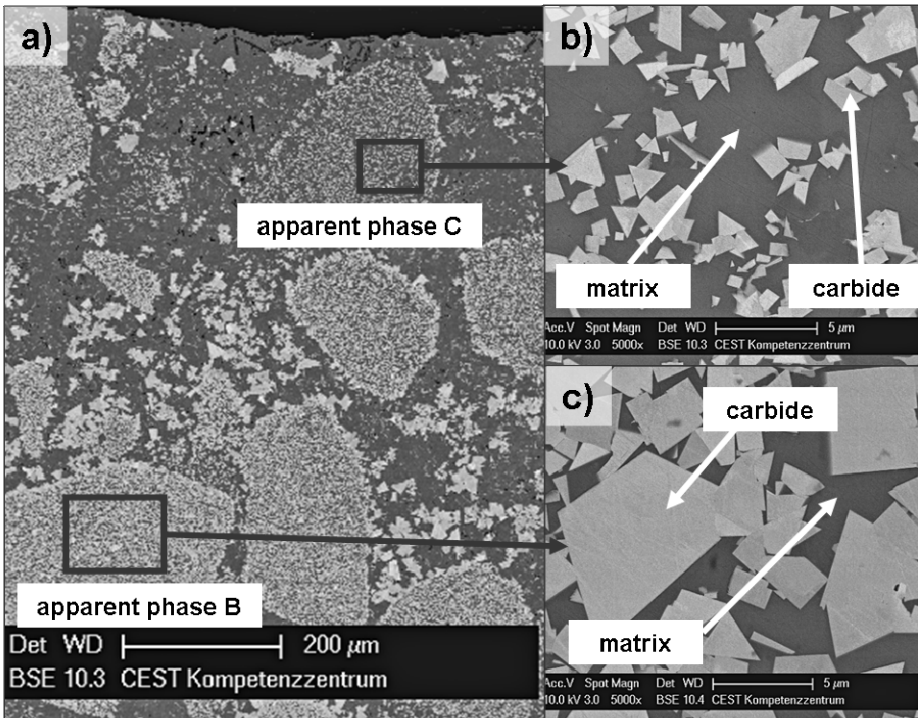


Figure 3.5 Cross-sectional SEM images of WC-Co reinforced NiCrBSi hardfacing: a) overview of the microstructure; b) detailed view on apparent phase C; c) detailed view on apparent phase B

3.2.3 Mechanical characterisation

Compound hardness is determined to be in the range between 380 HV10 and 550 HV10. Inside the apparent phases, the microhardness of apparent phase B (Figure 3.5c) was determined to be 760 ± 40 HV1 and hardness value of MMCs in apparent phase C (Figure 3.5b) is 1250 ± 55 HV1.

Micromechanical properties of the phases (hardness and reduced Young's modulus) were determined by nanoindentation measurements and statistically analysed using Box and Whisker plots (Figure 3.6). The results for the received coating showed mean nanoindentation hardness of 4.7 GPa in the matrix phase, whereas no significant difference were found for the hardness of micro carbides in apparent phases B and C (27.2 GPa). This hardness level was in close

approximation to hardness of WC/W₂C particles reinforced NiCrBSi hardfacing, measured as reference. For more of the details see PUBLICATION I.

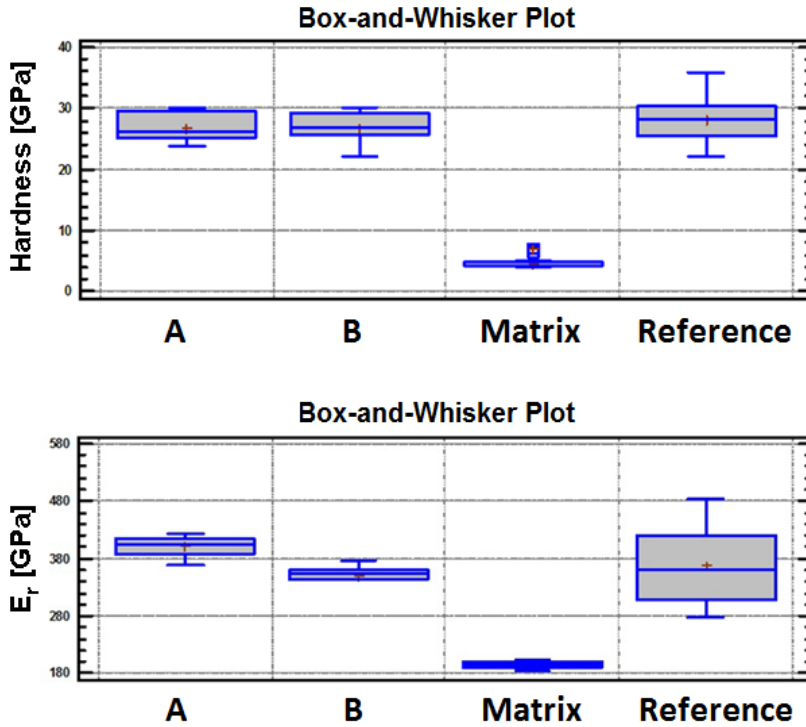


Figure 3.6 Box-and-Whisker plots of the measured hardness and reduced modulus: A – carbides in apparent phase B (less dissolved); B – carbides in apparent phase C (more dissolved); Matrix – apparent phase A; Reference – WC/W₂C

3.2.4 Wear resistance

Under three-body abrasion conditions with application of rubber wheel, the wear resistance of WC-Co reinforced hardfacing is two times lower compared to WC/W₂C (WOKA 50005) reinforced Ni-based alloy as shown in Table 3.3. Under impact/abrasion and steel wheel three-body abrasion conditions, the wear resistance of hardmetal scrap reinforced NiCrBSi hardfacing is higher compared to the reference material. For more detail see PUBLICATION I.

Table 3.3 Wear values for the WC-Co and WC/W₂C reinforced NiCrBSi hardfacings

Material	Volumetric wear [mm ³]	
	Three-body abrasion	Impact/abrasive wear
WC-Co	62 ± 6	6.6 ± 0.2
WC/W ₂ C	34 ± 4	7.3 ± 0.1

3.3 Cr₃C₂-Ni cermet particles reinforced NiCrBSi hardfacing

3.3.1 Chemical pre-treatment of milled Cr₃C₂-Ni particles

Purification of the Cr₃C₂-Ni powder was performed by chemical treatment in HCl acid and cleaning with ethanol and isopropyl alcohol. This operation was performed to remove trace elements from particle's surface after remilling in the disintegrator consisting of steel working chamber and WC-Co grinding bodies with the aim to improve the weldability of the powders and the mechanical properties of the produced materials. Effects of the purification process on the surface of Cr₃C₂-Ni particles are shown in Figure 3.7. For more details see PUBLICATION II.

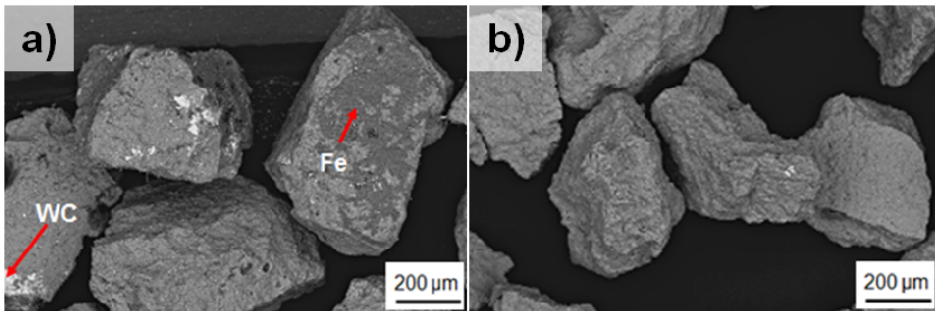


Figure 3.7 Particles of the cermet powders for PTA: a) untreated; b) chemically pre-treated particles

3.3.2 Hardfacing deposition and microstructure analysis

The optimised deposition parameters for the Cr₃C₂-Ni reinforced NiCrBSi hardfacing are listed in Table 3.4.

Table 3.4 Main process parameters for the deposition of Cr₃C₂-Ni reinforced NiCrBSi hardfacing

Parameter	Data
Welding current	80–100 A
Oscillation speed	15–18 mm/s
Oscillation width	20 mm
Welding speed	1.1–1.3 mm/s
Plasma gas	1.6–2.0 l/min
Substrate material	austenite steel (316L)
Substrate thickness	5 mm

Figure 3.8a presents the XRD pattern of the NiCrBSi alloy with addition of 40 vol.% Cr₃C₂-Ni particles. The matrix phase was identified as $\gamma(\text{Fe,Ni})$ with a high content of Cr₃C₂ and Cr₇C₃ hardphases. The presence of Cr₇C₃ can be explained by the structure of the precursor Cr₃C₂-Ni bulk cermet [99]. Some re-precipitation process takes places during deposition, forming M₇C₃ carbides,

especially on the border between cermet zone and matrix as shown in Figure 3.8b.

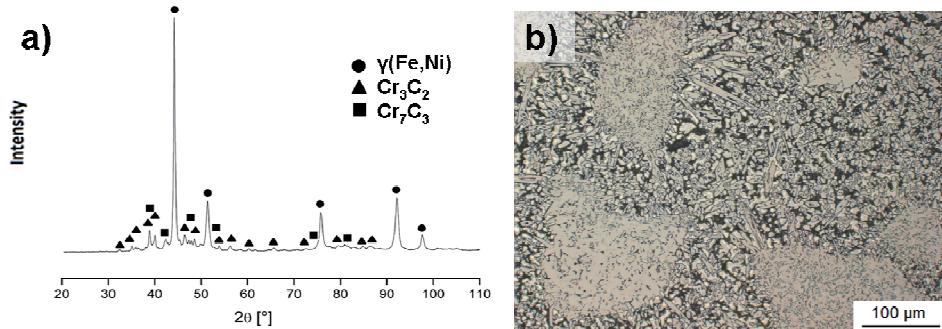


Figure 3.8 Cr_3C_2 -Ni reinforced NiCrBSi hardfacing a) XRD pattern; b) optical microscopy micrograph

SEM images of the structure (Figure 3.9) show Ni binder between the primary carbides. Growth and formation of spine-like carbides occurs mostly at the interfaces between matrix and cermet particles. No re-precipitated carbides were found inside the cermet phase (Figure 3.9b). The cermet particles (Figure 3.9c) represent the agglomerates of 2–5 μm sized Cr_3C_2 and Cr_7C_3 particles embedded into nickel matrix, i.e. the commonly reported structure of the reactive sintered Cr_3C_2 -Ni cermets [99]. For more details see PUBLICATION II.

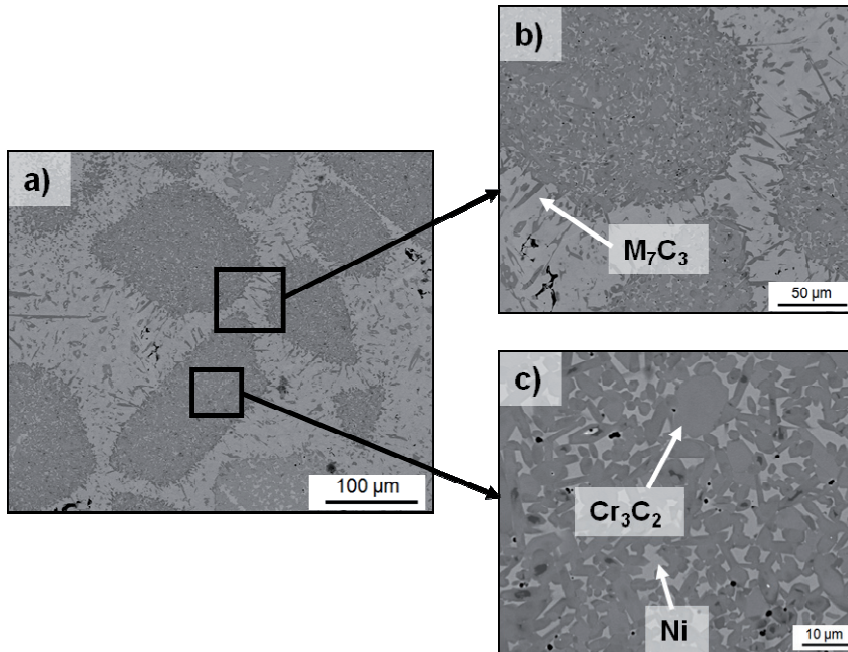


Figure 3.9 SEM images of Cr_3C_2 -Ni reinforced NiCrBSi hardfacing: a) overview; b) interface between particles and matrix; c) inner structure of the cermet particles

3.3.3 Mechanical characterisation

The cermet particle reinforced hardfacing reveals a hardness value of 730 ± 110 HV10.

Hot hardness values for the Cr_3C_2 -Ni reinforced hardfacing are shown in Figure 3.2 (section 3.1.2). For the Cr_3C_2 -Ni reinforced hardfacing, a slight decrease in hardness was observed in the interval between 300 °C and 600 °C. Rapid decrease in hardness starts from 600 °C; at the temperature of 700 °C the hardness is below 400 HV10. For more details see PUBLICATION IV.

Nanoindentation results obtained for the Cr_3C_2 -Ni reinforced coating are presented in Figure 3.10. The primary chromium hardphases Cr_3C_2 have a mean reduced Young's modulus of 378 ± 13 GPa and a hardness range from 21 GPa up to 28 GPa. This high spread of hardness values can be attributed to the presence of Cr_7C_3 phases. For more details see PUBLICATION II.

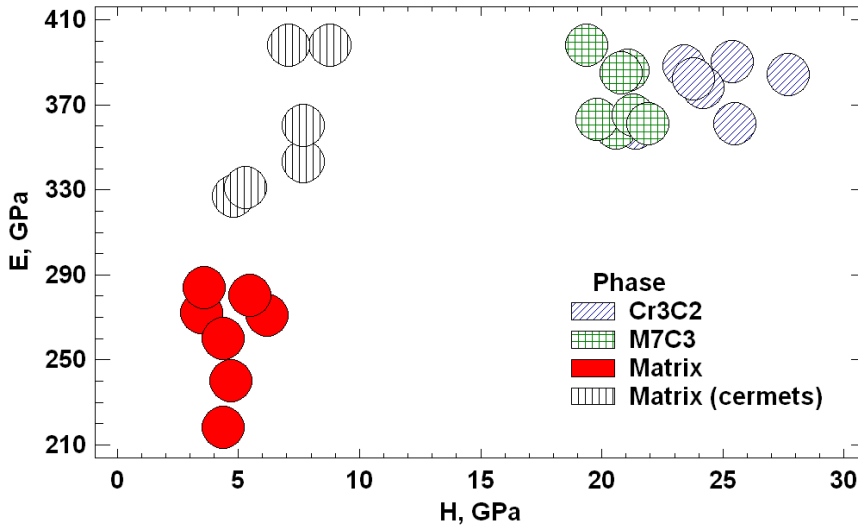


Figure 3.10 Nanoindentation measurements for Cr_3C_2 -Ni reinforced NiCrBSi hardfacing: Cr_3C_2 – carbides in cermet zone; M_7C_3 – spine-like carbides in matrix; Matrix – main phase in NiCrBSi matrix; Matrix (cermets) – Ni binder inside of the cermet particle

3.4 TiC-NiMo cermet particles reinforced NiCrBSi hardfacing

3.4.1 Hardfacing deposition and microstructure analysis

The optimised deposition parameters for the TiC-NiMo reinforced NiCrBSi hardfacing are listed in Table 3.5.

Table 3.5 Main process parameters for the deposition of TiC-NiMo reinforced NiCrBSi hardfacing.

Parameter	Data
Welding current	80–100 A
Oscillation speed	22–25 mm/s
Oscillation width	20 mm
Welding speed	0.9–1.2 mm/s
Plasma gas	1.6–2.0 l/min
Substrate material	austenite steel (316L)
Substrate thickness	5 mm

Figure 3.11a illustrates the TiC-NiMo reinforced NiCrBSi weld overlay. The welding seam examination reveals a uniform distribution of hardphases in the matrix, negligible porosity of the hardfaced layer and overall good quality of the welding seam with minimal dilution with the substrate of less than 5% according to the quantitative analysis.

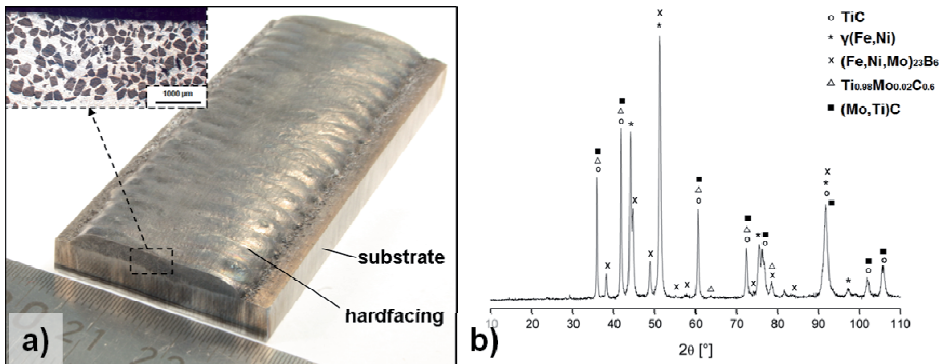


Figure 3.11 TiC-NiMo reinforced hardfacing: a) Weld seam analysis of TiC-NiMo reinforced NiCrBSi hardfacing; b) XRD pattern of the TiC-NiMo reinforced NiCrBSi hardfacing

The XRD pattern of TiC-NiMo reinforced NiCrBSi hardfacing is presented in Figure 3.11b. The analysis reveals five crystalline phases: Ni-rich dendritic matrix - $\gamma(\text{Fe,Ni})$; $(\text{Fe, Ni, Mo})_{23}\text{B}_6$, which is the most probable Fe-Ni-B hardphase located in dendrites with some traces of Mo in the crystal lattice; TiC phase; non-stoichiometric carbide $\text{Ti}_{0.92}\text{Mo}_{0.02}\text{C}_{0.6}$; and $(\text{Mo, Ti})\text{C}$. Formation of solid solutions of Mo in the TiC lattice results in development of so-called core-rim structured grains consisting of a TiC core surrounded by the rim of $(\text{Ti, Mo})\text{C}$ [100,101].

Figure 3.12 presents SEM micrographs of the TiC-NiMo reinforced hardfacing. The PTA welding process does not significantly influence the structure and composition of the cermet particles. However, it is found that besides a high amount of TiC-based angular precipitates (Figure 3.12d), TiC diffusing from the cermet zone to the matrix during deposition the structure of cermet particles along the interface (Figure 3.12b) differs from the microstructure of the cermet particles at the core (Figure 3.12c). The particles near the interface are partially dissolved showing decrease in grain size and modification in their shape. However, the chemical composition of the partially dissolved grains is kept uninfluenced. For more details see PUBLICATION III.

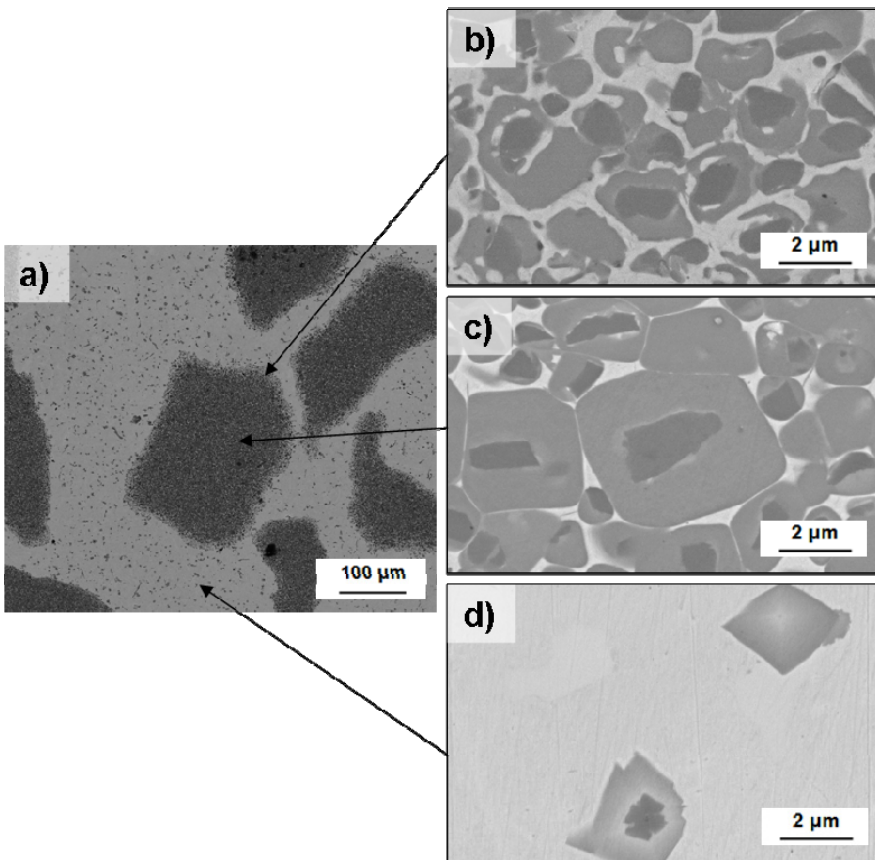


Figure 3.12 SEM micrographs of the TiC-NiMo reinforced NiCrBSi hardfacing: a) overview of the microstructure; b) interface cermet/matrix region; c) interior of the cermet particle; d) matrix region with TiC-based precipitates

3.4.2 Mechanical characterisation

The macrohardness of the TiC-NiMo reinforced hardfacing is 571 ± 25 HV50. Hot hardness values for the TiC-NiMo reinforced hardfacing are shown in Figure 3.2 (section 3.1.2). The hardness values stay at the same level in the temperature range from 20 °C to 300 °C and then start slightly to decrease in the

interval between 300 °C and 600 °C. Rapid decrease in hardness for TiC-NiMo reinforced hardfacings was measured at 700 °C.

Micro-mechanical properties of separate phases (hardness and reduced Young's modulus) were determined by nanoindentation measurements and statistically analysed. The corresponding hardness and reduced Young's modulus variations for the defined phases in TiC-NiMo reinforced NiCrBSi hardfacing are presented in a bubble chart in Figure 3.13. For more details see PUBLICATION III.

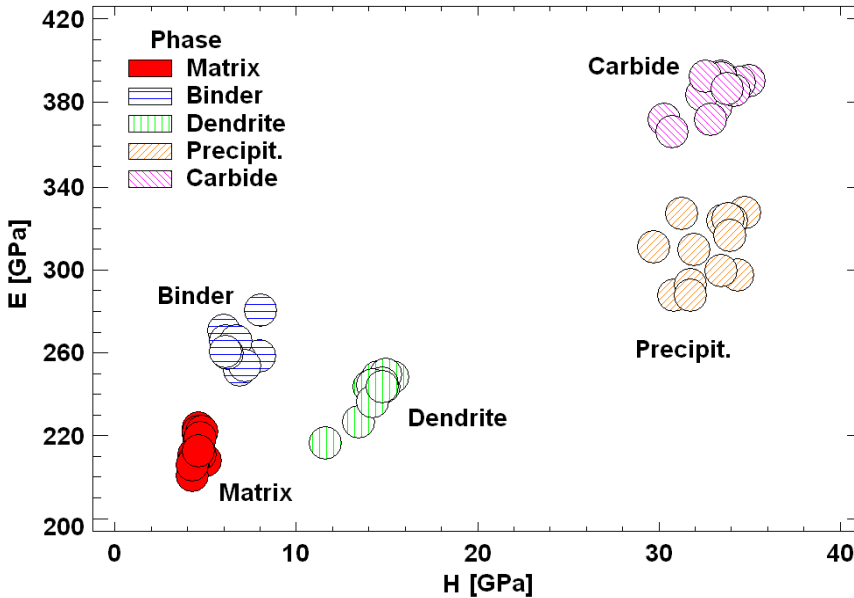


Figure 3.13 Nanoindentation measurements for TiC-NiMo reinforced NiCrBSi hardfacing: hardfacing (designations: carbide – TiC and (Ti,Mo)C phase; precipit. – TiC-based precipitates in matrix; dendrite – complex boride phase; binder – Ni-binder between carbide particles in the cermet zone; matrix – main matrix phase defined as $\gamma(\text{Fe,Ni})$)

3.4.3 Wear resistance

Wear tests exploiting steel and rubber wheels were carried out to reproduce three-body abrasion process. The relative wear resistance of the TiC-NiMo reinforced hardfacing was compared to conventionally used Ni-based reference hardfacing containing 40 vol.% of WC/W₂C particles (Castolin Eutectic EuTroLoy PG 6503 alloy). The wear values are listed in Table 3.6. For more details see PUBLICATION III.

Table 3.6 Three-body abrasion wear values for the TiC-NiMo and WC/W₂C reinforced NiCrBSi hardfacings

Material	Volumetric wear [mm ³]	
	Rubber wheel	Steel wheel
TiC-NiMo	22 ± 2	24 ± 2
WC/W ₂ C	15 ± 1	40 ± 3

SEM surface sectional images of the worn areas were examined as shown in Figure 3.14. Under rubber wheel testing conditions, for the WC/W₂C reinforced alloy high matrix hardness and dense distribution of coarse primary carbides ensure excellent wear resistance. For the TiC-NiMo reinforced alloy the increase in wear rate can be attributed to low hardness of the matrix material. The dominant wear mechanisms in this case are ploughing and cutting of ductile Ni-based matrix material. Under steel wheel testing conditions, for the WC/W₂C reinforced hardfacing the brittle fracture of both primary carbides and matrix precipitates was observed; extensive cracking and subsequent chip removal explains a significant increase in wear rate. For the TiC-NiMo reinforced alloy no pronounced brittle fracture of hard particles was detected: neither matrix precipitates nor cermet particles indicate extensive crack formation. For more details see PUBLICATION III.

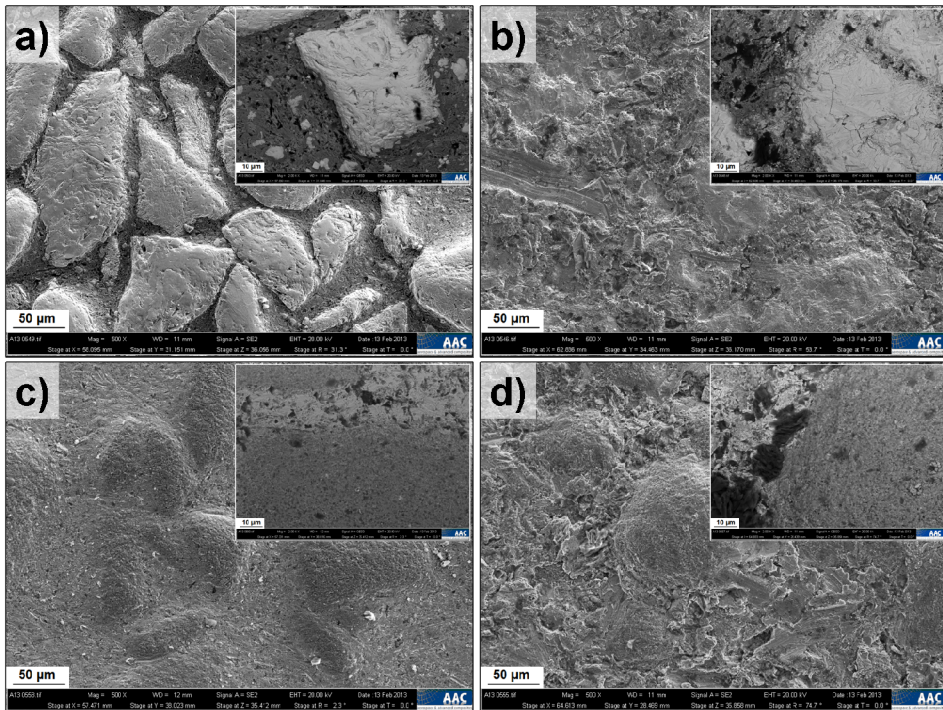


Figure 3.14 SEM worn surface micrographs of the hardfacings after three-body abrasion tests: a) and b) WC/W₂C reinforced coating - rubber and steel wheel; c) and d) TiC-NiMo reinforced coating - rubber and steel wheel

3.5 TiC-Ni and ZrC-Ni cermet particles reinforced NiCrBSi hardfacings

Process and deposition parameters for those materials are drawn in Table 3.7. The resulting hardfacing deposits and microstructure images are shown in Figure 3.15. The microstructures are characterised by dense distribution of primary hard phases in NiCrBSi matrix.

Table 3.7 Main process parameters for the deposition of ZrC-Ni and TiC-Ni reinforced NiCrBSi hardfacing

Parameter	ZrC-Ni	TiC-Ni
Welding current	80–85 A	65–75 A
Oscillation speed	15–17 mm/s	20–25 mm/s
Oscillation width	20 mm	20 mm
Welding speed	0.8–0.9 mm/s	1.3–1.5 mm/s
Plasma gas	1.6–2.0 l/min	1.0–1.2 l/min
Substrate material	austenite steel (316)	austenite steel (316)
Substrate thickness	5 mm	5 mm

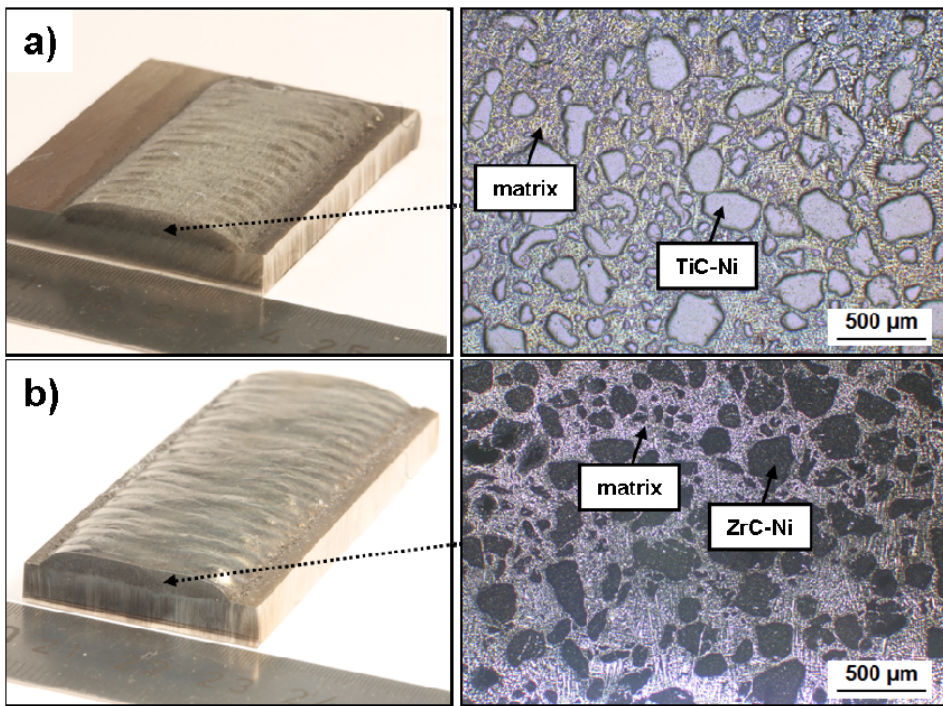


Figure 3.15 Weld seam analysis and optical microscopy images of a) TiC-Ni reinforced hardfacing; b) ZrC-Ni reinforced hardfacing

The details of those hardfacings are proprietary. Focused studies for the process optimisation and characterisation steps are not in the scope of present research.

3.6 High temperature wear

3.6.1 Impact/abrasive behaviour

Figure 3.16 shows the volumetric wear of the coatings tested at room temperature (RT), 300 °C, 550 °C and 700 °C. Commercially used multiphase coatings with Ni-based matrix and 60 wt.% of fused WC/W₂C (Castolin PG6503) hardphases were taken as a reference material. Good performance of the reference hardfacing at temperatures below 550 °C is evident; however, the volumetric wear increased significantly with increase in temperature, which can be attributed to hardphase oxidation and excessive fracture of the material [102]. In comparison, cermet particle reinforced hardfacings have better wear resistance starting from elevated temperatures. For more details see PUBLICATION IV. For the ZrC-Ni reinforced hardfacing the most promising results were detected, with a significant increase in wear resistance with higher testing temperature.

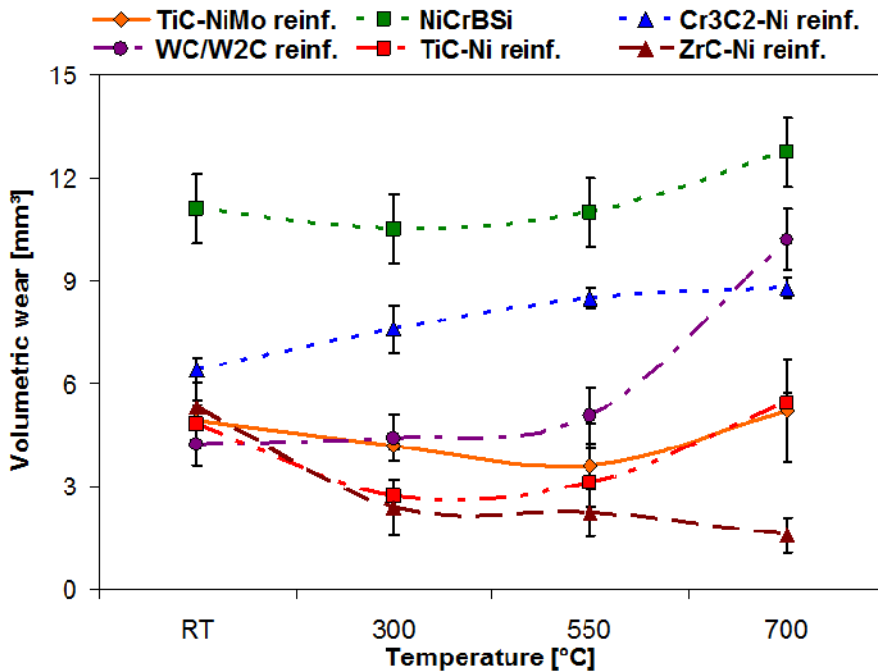


Figure 3.16 Volumetric wear values after HT-CIAT testing

For the Cr₃C₂-Ni reinforced NiCrBSi hardfacing (Figure 3.17a-c) with increase in testing temperature the presence of SiO₂ particles in the sub-surface layer of hardfacing is detected. Trans- and inter-granular cracking results in subsequent removal of the carbides and material chips from the surface especially when subjected to high testing temperatures. This could be one of the reasons of surface degradation. The Cr₃C₂-Ni reinforced hardfacing at 700 °C shows intensive plastic deformation and formation of oxide films (OF) with only fine

crushed ceramic particles found on the surface. For the TiC-NiMo reinforced coating (Figure 3.17d-f) with increase in testing temperature more than 50% of the hardfacing surface (almost all matrix regions and some cermet zones) is covered by SiO₂ particles. Low amount of precipitates in the matrix and their sub-micron size facilitate the penetration of silica into the soft matrix. At the highest test temperature (700 °C), the adhesion between silica particles and matrix is getting weaker due to oxidation of matrix resulting in higher wear rate. For more details see PUBLICATION IV.

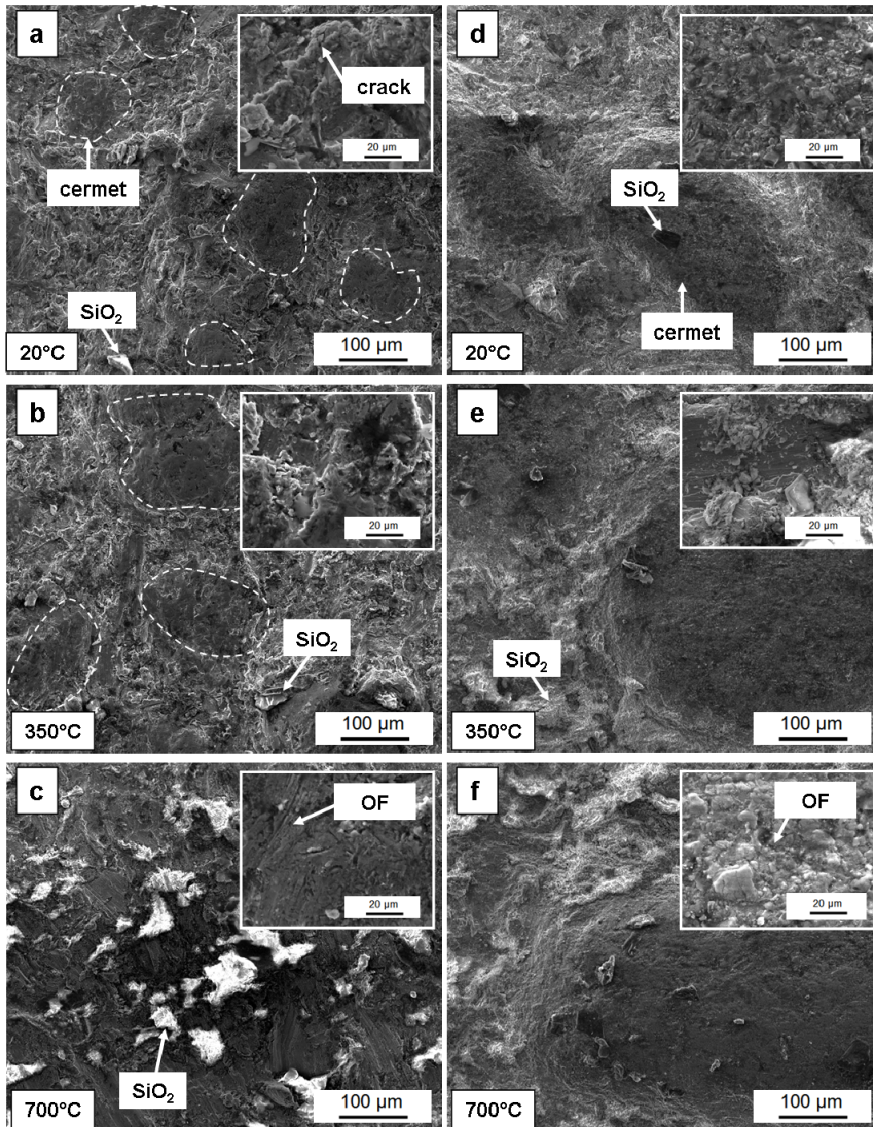


Figure 3.17 SEM micrographs of worn surface after HT-CIAT testing: a-c) Cr₃C₂-Ni reinforced NiCrBSi hardfacing at 20 °C, 350 °C and 700 °C; d-f) TiC-NiMo reinforced NiCrBSi hardfacing at 20 °C, 350 °C and 700 °C

3.6.2 Erosive behaviour

Volumetric wear rates for $\text{Cr}_3\text{C}_2\text{-Ni}$ and TiC-NiMo reinforced hardfacings are highlighted in Figure 3.18. On the abscissa the volumetric wear rate of the materials at the impact angle of 30° is drawn. The ordinate shows the wear rate of the tested materials at the impact angle of 90° . Both hardfacings show brittle mechanisms of behaviour, indication higher wear values under impact angle of 90° at all testing temperature.

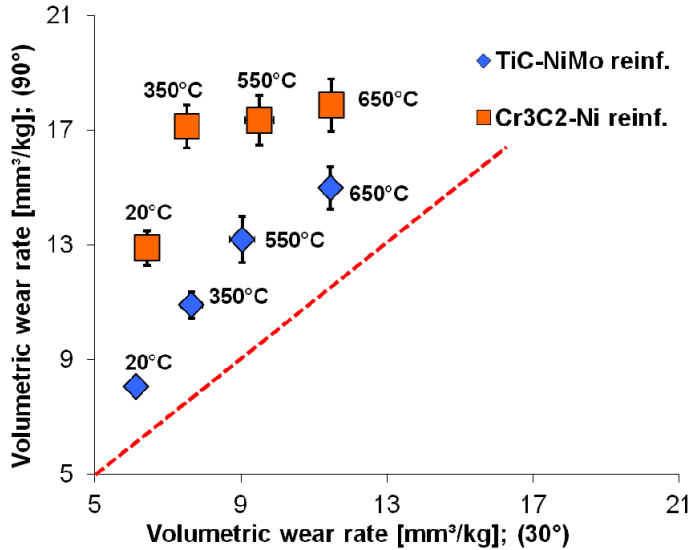


Figure 3.18 Wear rates after erosion testing for TiC-NiMo and $\text{Cr}_3\text{C}_2\text{-Ni}$ reinforced NiCrBSi hardfacing at constant impact velocity of 50 m/s

Wear mechanism of multiphase $\text{Cr}_3\text{C}_2\text{-Ni}$ and TiC-NiMo reinforced NiCrBSi hardfacings are schematically depicted in Figure 3.19 and supported by SEM micrographs in Figure 3.20. The main erosive wear mechanisms operating at given conditions are:

- ploughing and cutting of NiCrBSi matrix
- squeezing of a metal binder in cermet particles to the surface with formation of the rigid supporting compacted layer and top layer with higher metal content
- selective removal of a matrix binder from cermet particles by crushed abrasive particles pushed by the stream of particles
- fracturing and/or fragmentation of carbides
- removal of whole ceramic particles insufficiently supported by the metal matrix
- embedment of crushed abrasive particles mainly into the NiCrBSi matrix

- intermixing of cermet and NiCrBSi matrix constituents with formation of well developed mechanically mixed layer (MML) consisting of wear debris, fused silica dust, finely dispersed different oxides and highly deformed matrix alloy
- interaction of abrasive particles with formed oxide films at testing temperature of 650 °C. For more details see PUBLICATION IV.

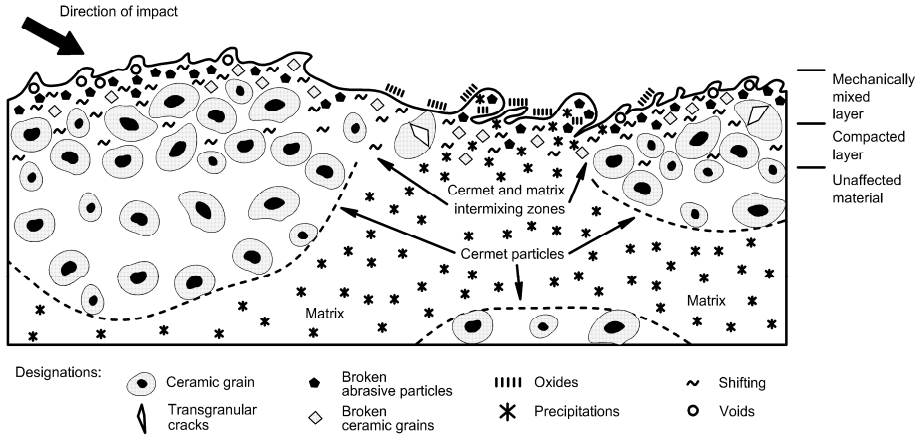


Figure 3.19 Features of cermet particle reinforced NiCrBSi hardfacings during high temperature solid particle erosive wear at the narrow impact angle

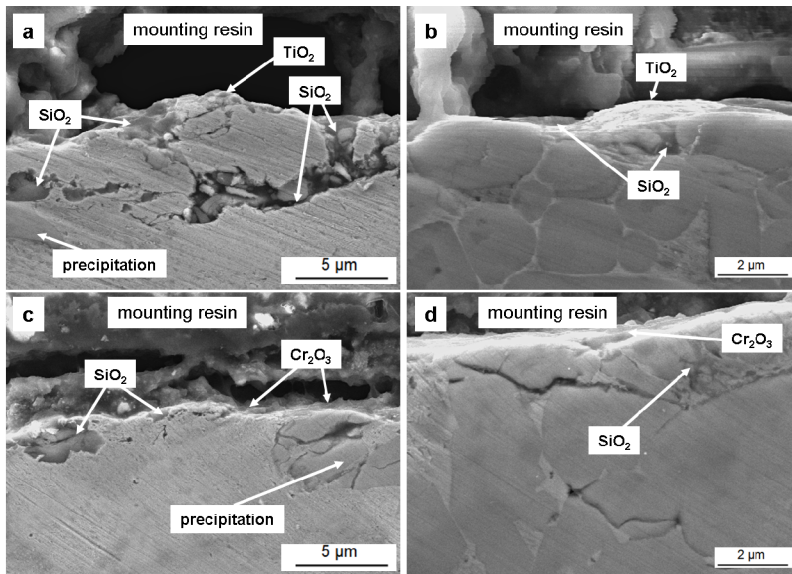


Figure 3.20 SEM cross-sectional images after erosion testing at 650 °C: a) TiC-NiMo reinforced NiCrBSi hardfacing matrix region; b) TiC-NiMo reinforced NiCrBSi hardfacing cermet region; c) Cr₃C₂-Ni reinforced NiCrBSi hardfacing matrix region; d) Cr₃C₂-Ni reinforced NiCrBSi hardfacing cermet region

3.7 High temperature corrosion

In the following subsections the effects of high temperature corrosion and oxidation of the $\text{Cr}_3\text{C}_2\text{-Ni}$ and TiC-NiMo reinforced hardfacings are shown and discussed. Figure 3.21 highlights the percentage mass change of both samples in all tested media. This diagram shows the excellent oxidation behaviour of both hardfacings. It can be said that the combination of the NiCrBSi matrix and both chosen hardphases results in high oxidation resistance. For more details see PUBLICATION IV and PUBLICATION V.

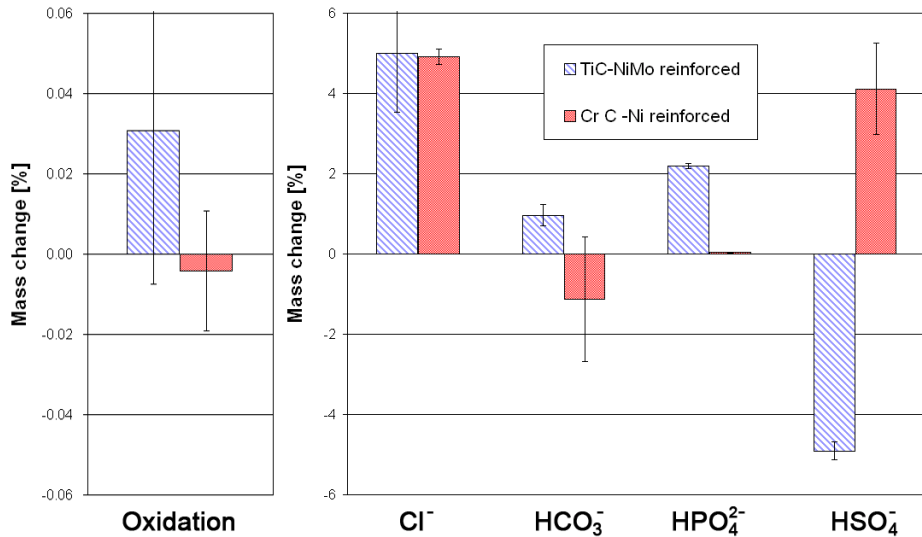


Figure 3.21 Percentage mass changes of $\text{Cr}_3\text{C}_2\text{-Ni}$ and TiC-NiMo reinforced NiCrBSi hardfacings after high temperature corrosion test

It was observed that chloride is highly corrosive to the $\text{Cr}_3\text{C}_2\text{-Ni}$ reinforced samples, which leads to intergranular corrosion in the matrix and total decomposition and oxidation of the carbides. As seen in Figure 3.22a chromium carbide oxidises, which is catalytic for the reaction with chlorine in high temperature environment. For the TiC-NiMo reinforced hardfacing the NiMo -binder of the TiC-NiMo hardphase degrades to NiCl_2 and more of MoCl_2 , which leaves small amounts of Ni in the TiC-NiMo cermet particles as seen in Figure 3.22b in detail. For more details see PUBLICATION V.

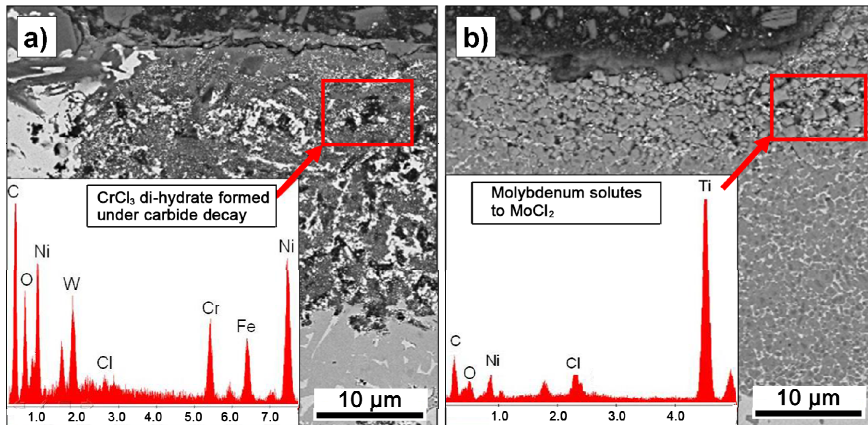


Figure 3.22 SEM/EDS cross-sectional analysis of the materials investigated after corrosion tests in chloride environment at 700 °C for 24 h: a) Cr_3C_2 -Ni particle reinforced; b) TiC-NiMo particle reinforced

Figure 3.23 shows a graphical draw of the areas of resistance for different corrosive anions at 700 °C. As seen, Cr_3C_2 -Ni reinforced hardfacings behave well in oxidative and sulphate/phosphate environment. TiC-NiMo hardfacings show good resistance against carbonate ions at 700 °C. Despite the high mass gain TiC-NiMo reinforced samples show better behaviour in chloride condition because of the better stability of the cermet phases. For more details see PUBLICATION V.

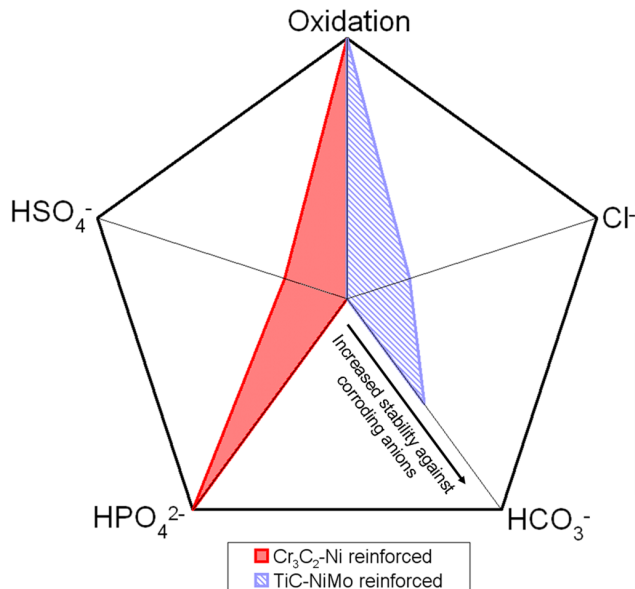


Figure 3.23 Proposing the field of application in for Cr_3C_2 -Ni and TiC-NiMo reinforced hardfacings in different corrosive and oxidative media at testing temperature of 700 °C

4 CONCLUSIONS

Based on the study within this work, the following conclusions can be drawn:

- The advanced multi-phase hardfacings based on the commercially available NiCrBSi matrix material and reinforced by recycled hardmetals and cermet particles has been developed and successfully introduced in the present study.
- Hardmetal scrap as well as chromium carbide and titanium carbide based cermet particles were successfully applied for fabrication of the wear resistant coatings using optimised PTA hardfacing technology. The produced hardfacings are characterised by minimal hardphase dissolution and homogeneous distribution of the reinforcements throughout the metal matrix.
- TiC-NiMo and Cr₃C₂-Ni multiphase hardfacings have been proven to be the reliable candidates for high temperature tribo-applications: under the conditions of high-stress three-body abrasion TiC-NiMo reinforced hardfacings show significantly higher wear resistance as compared to the commercial WC/W₂C reinforced coatings.
- The degradation of the NiCrBSi matrix due to oxidation and hardness loss at temperatures above 700 °C is a main limiting factor for the application of the TiC-NiMo and Cr₃C₂-Ni cermet reinforced coatings.
- Under conditions of high temperature erosion TiC-NiMo and Cr₃C₂-Ni reinforced hardfacings have revealed high wear resistance. Cr₃C₂-Ni reinforced hardfacing has exhibited tendency to a brittle failure; however, only moderate increase in wear rate at elevated temperatures up to 650 °C has been detected.
- Cermet reinforced hardfacings are attractive candidates for applications in impact/abrasive conditions, especially at high temperatures. At elevated testing temperatures the volumetric wear rate values for the TiC-NiMo, TiC-Ni, ZrC-Ni and Cr₃C₂-Ni reinforced coatings are significantly lower as compared with WC/W₂C reinforced hardfacings.
- Cermets reinforced hardfacings have shown stability against oxidation due to formation of the protective oxide layers on their surfaces. High temperature corrosion resistance of the developed hardfacings is influenced by the corroding anions to a great extent. The field of application for cermet reinforced hardfacings in dependence of the corrosive environment at 700 °C was proposed. Cr₃C₂-Ni reinforced

hardfacings exhibit high resistance against sulphate and phosphate environment, while the TiC-NiMo hardfacings show excellent behavior in carbonate environment.

The **novelty** of present research can be outlined by:

- Application of cermet and hardmetal recycling powders as reinforcements for NiCrBSi matrix alloy for hardfacing process.
- Chemical pre-processing of cermet particles for the PTA hardfacing.
- Development of novel wear resistant thick coatings, especially for high temperature harsh wear and corrosion conditions.
- Development of double-structured MMCs with fine carbide reinforcements.
- Optimised PTA process management for the deposition of cermet particles reinforced NiCrBSi hardfacings.
- Comprehensive mechanical and tribological characterisation of the coatings of novel compositions.
- Selection of potential fields of application for the cermet particles reinforced NiCrBSi hardfacings, based on the characterisation and wear testing results.

Based on the results of present research it is planned to deposit cermet particle reinforced NiCrBSi hardfacings as prototypes at industrial applications, particularly as wear resistant parts for iron ore sinter crushers, operating at temperatures close to 700°C in corrosive environments under impact/abrasion conditions.

REFERENCES

1. **Mellor, B.G.**, *Surface Coatings for Protection Against Wear*, Woodhead Publishing Limited, 2006, Cambridge, UK.
2. **Bach, F.W., Laarmann, A., Wenz, T.**, *Modern Surface Technology*, WILEY-VCH, 2004, Weinheim, Germany.
3. *CIGWELD: Technical information – Hardfacing information*, 2001, Comweld Group Pty Ltd., 338–359.
4. **Bulloch, J. H.**, Some considerations of wear and hardfacing materials, *Int. J. Pres. Ves. & Piping* 46, 1991, 251–267.
5. **Badisch, E., Kirchgaßner, M., Polak, R., Franek, F.**, The comparison of wear properties of different Fe-based hardfacing alloys in four kinds of testing methods, *Tribotest* 14, 2008, 225–233.
6. **Chatterjee, S., Pal, T. K.**, Solid particle erosion behaviour of hardfacing deposits on cast iron—Influence of deposit microstructure and erodent particles, *Wear* 261, 2006, 1069–1079.
7. **Chattopadhyay, R.**, *Advanced thermally assisted surface engineering processes*, Kluwer Academic Publishers, 2004, New York, USA.
8. **Nurminen, J., Nökki, J., Vuoristo, P.**, Microstructure and properties of hard and wear resistant MMC coatings deposited by laser cladding, *Int. J. Refract. Met. Hard Mater.* 27, 2009, 472–478.
9. **Ootes, W. R.**, *Welding Handbook*, vol. 8/e, American Welding Society, 1985.
10. *Welding Consumables – Hardfacing*. [Online] AFROX Product Reference Manual, Section 11, www.afrox.co.za.
11. *ASM Handbook: Volume 6: Welding Brazing and Soldering*, ASM, Materials Park OH, 1993.
12. **Dumovic, M.**, Repair and maintenance procedures for heavy machinery components, *Australasian Welding Journal* 46, *First Quarter*, 2001.
13. **Shin, J. C., Doh, J. M., Yoon, J. K., Lee, D. Y., Kim, J. S.**, Effect of molybdenum on the microstructure and wear resistance of cobalt-base stellite hardfacing alloys, *Surf. Coat. Technol.* 166, 2003, 117–126.
14. **Branagan, D.J., Marshall, M.C., Meacham B.E.**, High toughness high hardness iron based PTAW weld materials, *Mater. Sci. Eng. A* 428, 2006, 116–123.
15. **Deuis, R.L., Yellup, J.M., Subramanian, C.**, Metal-matrix composite coatings by PTA surfacing, *Compos. Sci. Technol.* 58, 1998, 299–309.
16. **D’Oliveira, A.S.C.M., Paredes, R.S.C., Santos, R.L.C.**, Pulsed current plasma transferred arc hardfacing, *Jour. Mater. Proc. Technol.* 171, 2006, 167–174.
17. **Katsich, C., Badisch**, Effect of carbide degradation in a Ni-based hardfacing under abrasive and combined impact/abrasive conditions, *Surf. Coat. Technol.* 206, 2011, 1062–1068.
18. *European Draft Standard EN 14700*, *Welding Consumables – Welding Consumables for Hard-facing*, British Standards Institution, London.

19. *AWS Specification A5.13:2000*, Specification for Surfacing Electrodes for Shielded Metal Arc Welding, *American Welding Society*, 2000, Miami, Florida.
20. *AWS Specification A5.21:2001*, Specification for Bare Electrodes and Rods for Surfacing, American Welding Society, 2001 Miami, Florida.
21. **Buchely, M.F., Gutierrez, J.C., León, L.M., Toro, A.**, The effect of microstructure on abrasive wear of hardfacing alloys, *Wear* 259, 2005, 52–61.
22. *ASM Handbook: Vol. 18, Friction, Lubrication and Wear Technology*, ASM, Materials Park OH, 1992.
23. **Uetz, H.**, *Abrasion und Erosion*, Carl Hanser Verlag, 1986, München, Germany.
24. **Berns, H.**, Microstructural properties of wear resistant alloys, *Wear* 181, 1995, 271–279.
25. **Hutchings, I.M.**, *Tribology: Friction and Wear of Engineering Materials*, 1992, Cambridge, UK.
26. **Liu, Y.F., Xia, Z.Y., Han, J.M., Zhang, G.L., Yang, S.Z.**, Microstructure and wear behavior of (Cr, Fe)₇C₃ reinforced composite coating produced by plasma transferred arc weld surfacing process, *Surf. Coat. Technol.* 201, 2006, 863–867.
27. **Dogan, O.N., Hawk, J.A., Laird II, G.**, Solidification structure and abrasion resistance of high chromium white irons, *Met. Mat. Trans. A* 28, 1997, 1315–1328.
28. **Kirchgaßner, M., Badisch, E., Franek, F.**, Behaviour of iron-based hardfacing alloys under abrasion and impact, *Wear* 265, 2008, 772-779.
29. **Flores, J.F., Neville, A., Kapur, N., Gnanavelu, A.**, Erosion-corrosion degradation mechanisms of Fe-Cr-C and WC-Fe-Cr-C PTA overlays in concentrated slurries, *Wear* 267, 2009, 1811–1820.
30. **Lu, L., Soda, H., McLean, A.**, Microstructure and mechanical properties of Fe–Cr–C eutectic composites, *Mater. Sci. Eng. A* 347, 2003, 214–222.
31. **Lin, C.M., Chang, C.M., Chen, J.H., Hsieh, C.C., Wu, W.**, Microstructural evolution of hypereutectic, near eutectic and hypereutectic high-carbon Cr-based hardfacing alloys. *Met. Mat. Trans. A* 40A, 2009, 1031–1038.
32. **Buchanan, V.E., Shipway, P.H., McCartney, D.G.**, Microstructure and abrasive wear behaviour of shielded metal arc welding hardfacings used in the sugarcane industry, *Wear* 263, 2007, 99–110.
33. **Zhou, Y.F., Yang, Y.L., Jiang, Y.W., Yang, J., Ren, X.J., Yang, Q.X.**, Fe-24 wt.% Cr-4.1 wt.% C hardfacing alloy: Microstructure and carbide refinement mechanisms with ceria additive, *Mater. Charact.*, 2012, doi:10.1016/j.matchar.2012.07.004
34. **Berns, H., Fischer, A.**, Microstructure of Fe-Cr-C hardfacing alloys with addition of Nb, Ti, and B, *Mater. Charact.* 39, 1997, 499–527.

35. **Chang, C.M., Chen, Y.C., Wu, W.**, Microstructure and abrasive characteristics of high carbon Fe-Cr-C hardfacing alloy, *Tribol. Int.* 43, 2010, 929–934.
36. **Badisch, E., Katsich, C., Winkelmann, H., Franek, F., Roy, M.**, Wear behaviour of hardfaced Fe-Cr-C alloy and austenitic steel under 2-body and 3-body conditions at elevated temperature, *Tribol. Int.* 43, 2010, 1234–1244.
37. *PTA Laser Powder*. [Online] Information to Kennametal Stellite powders 07.02.2013 www.stellite.co.uk
38. Properties of Deloro Stellite alloys. [Online] Technical Information, Deloro Stellite, 2004. www.stellite.co.uk
39. **Corchia, M., Delogu, P., Nenci, F., Belmondo, A., Corcoruto, S., Stabielli, W.**, Microstructural aspects of wear-resistant stellite and colmonoy coatings by laser processing, *Wear* 119, 1987, 137–152.
40. **Tylezak, J.H., Oregon, A.**, *Friction, Lubrication and Wear Technology, ASM Handbook*, vol. 18, 1995, 184–193.
41. **Navas, C., Colaco, R., Damborenea J., Vilar, R.**, Abrasive wear behaviour of laser clad and flame sprayed-melted NiCrBSi coatings, *Surf. Coat. Technol.* 200, 2006, 6854–6862
42. **Ming, Q., Lim, L.C., Chen, Z.D.**, Laser cladding of nickel-based hardfacing alloys, *Surf. Coat. Technol.* 106, 1998, 174–182.
43. **Conde, A., Zubiri, F., Damborenea, J.**, Cladding of Ni–Cr–B–Si coatings with a high power diode laser, *Mater. Sci. Eng. A* 334, 2002, 233–238.
44. **Badisch, E., Kirchgäßner, M.**, Influence of welding parameters on microstructure and wear behaviour of a typical NiCrBSi hardfacing alloy reinforced with tungsten, *Surf. Coat. Technol.* 202, 2008, 6016–6022.
45. **Liyanage, T., Fisher G., Gerlich, A.P.**, Influence of alloy chemistry on microstructure and properties in NiCrBSi overlay coatings deposited by plasma transferred arc welding (PTAW) *Surf. Coat. Technol.* 205, 2010, 759–765.
46. **Kainer, K.U.**, *Metal Matrix Composites*. [Online] Custom-made Materials for Automotive and Aerospace Engineering, *WILEY-VCH Verlag*, 2006, ISBN: 3-527-31360-5. <http://www.wiley-vch.de>
47. **Suresh, S., Mortensen, A., Needleman, A.**, *Fundamentals of Metal-Matrix Composites*, Butterworth-Heinemann, 1993, Stoneham, MA.
48. **Cardinal, S., Malchere, A., Garnier, V., Fantozzi, G.**, Microstructure and mechanical properties of TiC–TiN based cermets for tools application, *Int. J. Refract. Met. Hard Mater.* 27, 2009, 521–527.
49. **Hussainova, I.**, Effect of microstructure on the erosive wear of titanium carbide-based cermets, *Wear* 255, 2003, 121–128.
50. **Kübarsepp, J., Klaasen, H., Pirso, J.**, Behaviour of TiC-base cermets in different wear conditions, *Wear* 249, 2001, 229–234.
51. **Antonov, M., Hussainova, I.**, Cermets surface transformation under erosive and abrasive wear, *Tribol. Int.* 43, 2009, 1566–1575.

52. **Kathuria, Y. P.**, Nd-YAG laser cladding of Cr₃C₂ and TiC cermets, *Surf. Coat. Technol.* 140, 2001, 195–199.
53. **Sun, R.L., Lei, Y.W., Niu, W.**, Laser clad TiC reinforced NiCrBSi composite coatings on Ti–6Al–4V alloy using a CW CO₂ laser, *Surf. Coat. Technol.* 203, 2009, 1395–1399.
54. **Yang, S., Chen, N., Liu, W.J., Zhong, M.L., Wang, Z., Kokawa, H.**, Fabrication of nickel composite coatings reinforced with TiC particles by laser cladding, *Surf. Coat. Technol.* 183, 2004, 254–260
55. **Yang, S., Liu, W.J., Zhong, M.L., Wang, Z.**, TiC reinforced composite coating produced by powder feeding laser cladding, *Mater. Lett.* 58, 2004, 2958–2962.
56. **Wang, X.H., Song, S.L., Zou, Z.D., Qu, S.Y.**, Fabricating TiC particles reinforced Fe-based composite coatings produced by GTAW multi-layers melting process, *Mat. Sci. Eng. A* 441, 2006, 60–67.
57. **Dawei, Z., Li, T., Lei, T.C.**, Laser cladding of Ni–Cr₃C₂/(Ni+Cr) composite coating *Surf. Coat. Technol.* 110, 1998, 81–85.
58. **Dawei, Z., Lei, T.C., Li, F.J.**, Laser cladding of stainless steel with Ni–Cr₃C₂ for improved wear performance, *Wear* 251, 2001, 1372–1376.
59. **Huang, Z., Hou, Q., Wang, P.**, Microstructure and properties of Cr₃C₂-modified nickel-based alloy coating deposited by plasma transferred arc process, *Surf. Coat. Technol.* 202, 2008, 2993–2999.
60. **Van Acker, K., Vanhoyweghen, D., Persoons, R., Vangrunderbeek, J.**, Influence of tungsten carbide particle size and distribution on the wear resistance of laser clad WC/Ni coatings, *Wear* 258, 2005, 194–202.
61. **Gebert, A., Heinze, H., Schammer, S.**, Plasma-Pulver-Auftragschweissen = Wear protection by plasma powder build-up welding, *Metalloberfläche* 50, 1996, 56–60.
62. **Zum Gahr, K.-H.**, *Microstructure and Wear of Materials*, Elsevier Science Publishers, 1987, Amsterdam.
63. **Murthy, J.K.N., Venkataraman, B.**, Abrasive wear behaviour of WC–CoCr and Cr₃C₂–20(NiCr) deposited by HVOF and detonation spray processes, *Surf. Coat. Technol.* 200, 2006, 2642–2652.
64. **Vuoristo, P., Nieminen, R., Mäntylä, T., Tampere & Barbezat, G.**, Structure and wear characteristics of WC-Co(Cr) and Cr₂C₃-NiCr coatings sprayed by new potential HVOF process, *DVS-Berichte* 175, 1996, 301–305.
65. **Amado, J.M., Tobar, M.J., Alvarez, J.C., Lamas, J., Yáñez A.**, Laser cladding of tungsten carbides (Spherotene1) hardfacing alloys for the mining and mineral industry, *Appl. Surf. Sci.* 255, 2009, 5553–5556.
66. **Badisch, E., Kirchgaßner, M.**, Influence of welding parameters on microstructure and wear behaviour of a typical NiCrBSi hardfacing alloy reinforced with tungsten carbide, *Surf. Coat. Technol.* 202, 2008, 6016–6022.
67. **Ilo, S., Just, Ch., Badisch, E., Wosik, J., Danninger, H.**, Effects of interface formation kinetics on the microstructural properties of wear-

- resistant metal–matrix composites, *Mat. Sci. Eng.* 527, 2010, 6378–6385.
68. **Huang, S.W., Samandi, M., Brandt, M.,** Abrasive wear performance and micro-structure of laser clad WC/Ni layers, *Wear* 256, 2004, 1095–1105.
 69. **Zhou, R., Jiang, Y., Lu, D.,** The Effect of Volume Fraction of WC Particles on Erosion Resistance of WC Reinforced Iron Matrix Surface Composites, *Wear* 255, 2003, 137–138.
 70. **Leech, W.P., Li, S.X., Alam, N.,** Comparison of abrasive wear of a complex high alloy hardfacing deposit and WC-Ni based metal matrix composite, *Wear* 294–295, 2012, 380–386.
 71. **Polak, R., Ilo, S., Badisch, E.,** Relation between inter-particle distance and abrasion in multiphase matrix-carbide materials, *Trib. Lett.* 33, 2009, 29-35.
 72. **Colaco, R., Vilar, R.,** A model for the abrasive wear of metallic matrix particle-reinforced materials, *Wear* 254, 2003, 625–633.
 73. **Antonov, M.,** Assesment of cermets performance in aggressive media, PhD Thesis, 2006, Tallinn.
 74. **Tinklepaugh, J. R., Crandall, W. B.,** Cermets, *Reinhold Publishing Corporation*, 1960, New York.
 75. **Kisly, P. S.,** *Cermets. Naukova Dumka*, 1985, Kiev. [in Russian].
 76. **Ndlovu, S.,** *The Wear Properties of Tungsten Carbide-Cobalt Hardmetals from the Nanoscale up to the Macroscopic Scale*, PhD Thesis, 2009, Nürnberg.
 77. **Matthews, S., James, B., Hyland, M.,** The role of microstructure in the high temperature oxidation mechanism of Cr₃C₂-NiCr composite coatings, *Cor. Sci.* 51, 2009, 1172–1180.
 78. **Meng, J., Lu, J., Wang, J., Yang, S.,** Tribological behavior of TiCN-based cermets at elevated temperatures, *Mat. Sci. Eng. A* 418, 2006, 68-76.
 79. **Hussainova, I., Pirso, J., Antonov, M., Juhani, K.,** High temperature erosion of Ti(Mo)C-Ni cermets, *Wear* 2009, 267, 1894–1899.
 80. **Antonov, M., Hussainova, I., Veinthal, R., Pirso, J.,** Effect of temperature and load on three-body abrasion of cermets and steel, *Tribol. Inter.* 46, 2012, 261–268.
 81. **Antonov, M., Hussainova, I., Kübarsepp, J., Traksmäa, R.,** Oxidation-abrasion of TiC-based cermets in SiC medium, *Wear* 273, 2011, 23–31.
 82. **Dent, H., Horlock, A.J., McCartney, D.G., Harris, S.J.,** Microstructural characterisation of a Ni-Cr-B-C based alloy coating produced by HVOF thermal spraying, *Surf. Coat. Technol.* 139, 2001, 244–250.
 83. **Kamal, S., Jayaganthan, R., Prakash, S., Kumar S.,** Hot corrosion behaviour of detonation gun sprayed Cr₃C₂-NiCr coatings on Ni and Fe-

- based superalloys in Na_2SO_4 -60% V_2O_5 environment at 900 °C, *J. Alloy Compound* 463, 2008, 358–372.
84. **Kaur, M., Singh, H., Prakash, S.**, Surface engineering analysis of detonation-gun sprayed Cr_3C_2 -NiCr coating under high-temperature oxidation and oxidation–erosion environments, *Surf. Coat. Technol.* 206, 2011, 530–541.
 85. **Higuera Hidalgo, V., Belzunce Varela, J., Carriles Menendez, A., Poveda Martinez, S.**, High temperature erosion wear of flame and plasma-sprayed nickel–chromium coatings under simulated coal-fired boiler atmospheres, *Wear* 247, 2001, 214–222.
 86. **Mann, B.S., Prakash, B.**, High temperature friction and wear characteristics of various coating materials for steam valve spindle application, *Wear* 240, 2000, 223–230.
 87. **Kulu, P., Käerdi, H., Mikli, V.**, Retreatment of used hardmetals, *In Proc. TMS 2002 Recycling and Waste Treatment in Mineral and Metal Processing: Technical and Economic Aspects*, Lulea, 2002, 139–146.
 88. **Zimakov, S., Pihl, T., Kulu, P., Antonov, M., Mikli, V.**, Applications of recycled hardmetal powder, *Proc. Estonian Acad. Sci. Eng.* 9, 2003, 304–316.
 89. **Kulu, P., Zimakov, S.**, Wear resistance of thermal sprayed coatings on the base of recycled hardmetal, *Surf. Coat. Technol.* 130, 2000, 46–51.
 90. **Kulu, P., Hussainova, I., Veinthal, R.**, Solid particle erosion of thermally sprayed coatings, *Wear* 258, 2005, 488–496.
 91. **Surzhenkov, A., Kulu, P., Tarbe, R., Mikli, V., Sarjas, H., Latokartano, J.**, Wear resistance of laser remelted thermally sprayed coatings, *Estonian J. Eng.* 15, 2009, 318–328.
 92. TOPAS V3., General profile and structure analysis software for powder diffraction data, *Bruker AXS*, 2005, Karlsruhe.
 93. NIST - The National Institute of Standards and Technology [Online] www.nist.gov.
 94. **Winkelmann, H., Badisch, E., Kirchgaßner, M., Danninger, H.**, Wear mechanisms at high temperature. Part 1: Wear mechanisms of different Fe-based alloys, *Tribol. Lett.* 34, 2009, 155–166.
 95. **Pharr, G.M., Oliver, W.C., Brotzen, F.R.**, On the generality of the relationship between contact stiffness, contact area, and elastic modulus during indentation, *J. Mater. Res.* 7, 1992 613–617.
 96. *ASTM G65 - Standard Test Method for Measuring Abrasion Using the Dry Sand/Rubber Wheel Apparatus* 2010. DOI: 10.1520/G0065-04R10
 97. **Antonov, M., Hussainova, I., Pirso, J., Volobujeva, O.**, Assessment of mechanically mixed layer developing during high temperature erosion of cermets, *Wear* 263, 2007; 878–886.
 98. **Kleis, E., Kulu, P.**, *Solid Particle Erosion*, Springer, 2007, London.
 99. **Pirso, J., Viljus, M., Letunovits, S., Juhani, K.**, Reactive carburizing sintering – a novel production method for high quality carbide-nickel cermets. *Int. J. Refract. Met. Hard Mater.* 24, 2006, 263–270.

100. **Kim, Y.K., Shim, J.H., Cho, Y.W., Yang, H.S., Park, J.K.,** Mechanochemical synthesis of nanocomposite powder for ultrafine (Ti, Mo)C–Ni cermet without core-rim structure, *Int. J. Refract. Met. Hard Mater.* 22, 2004, 193–196.
101. **Hussainova, I., Kolesnikova, A., Hussainov, M., Romanov., A,** Effect of stressed state on erosive performance of cermets with core – rim structured ceramic grains, *Wear* 267, 2009, 177–185.
102. **Kuzmanovic, J.,** *WC-W₂C Particle Reinforced Powder Metallurgy Iron and Nickel Matrix Composites Produced by Pressing and Sintering*; MSc Thesis, 2011, Vienna University of Technology, Austria.

ACKNOWLEDGEMENTS

I would like to express my special thanks to my supervisors, Dr. Irina Hussainova and Prof. Herbert Danninger and to my technical advisors Dr. Ewald Badisch and Prof. Priit Kulu for their support, guidance and encouragement, which made this work possible.

I am deeply grateful to many of my colleagues at AC2T research GmbH and especially to Dipl.-Ing Christian Katsich for my integration in to the amazing world of hardfacings. I would also like to thank Peter Brunner, Kurt Pichelbauer, Philip Eidenberger, Markus Premauer, Harald Rojacz, Markus Varga, Cristopher Mozelt, Fjorda Xhiku, Werner Tschirk and Frank Schütze for their help during experiments. I am deeply grateful to Dr. Sotiraq Ilo and Dr. Christian Tomastik for the theoretical and practical help with nanoindentations. I would also like to thank Laszlo Katona, MSc for the help with X-ray photoelectron spectroscopy and fruitful discussions. I also would like to express my gratitude to Prof. Friedrich Franek and Dr. Andreas Pauschitz for their support and guidance.

I am also deeply grateful to the staff of Tallinn University of Technology and Vienna Technical University for their shared experience, fruitful and always enjoyable working atmosphere. I would like to thank Prof. Renno Veinthal for giving me an opportunity to work at AC2T research GmbH. I wish to express my most sincere gratitude and appreciation to Dr. Maksim Antonov for the interesting discussions on wear analysis and his overall support during my PhD studies. I also wish to extend my gratitude to Dr. Jüri Pirso for his enthusiasm during the explanation the principles of production technology of powder materials and very useful discussions. I would also like to thank Dmitrij Goljandin, MSc, for his support with samples milling and interesting lectures about principles of grinding by collision; I am also deeply grateful to Dr. Johannes Zbiral and Dr. Christian Edtmaier for interesting discussions on materials properties and microstructure.

Special thanks to Sten Vinogradov, BSc, Der-Liang Yung, MSc and Julijana Kuzmanovic, MSc, for being great students and for their contribution to my research.

I would also like to thank scientists from the CEST Kompetenzzentrum für elektrochemische Oberflächentechnologie GmbH and specially Dr. Aleksandra Gavrilović-Wohlmuther and Dr. Jarik Wosik for their help with XRD and SEM investigations and interesting discussions.

I would also like to express my gratitude to the scientists from Aerospace & Advanced Composites GmbH for the interesting discussions and especially to Dr. Christian Jogl for the world of micro-scale.

I would like to thank Castolin Eutectic GmbH for the cooperation and help with powder materials. I am deeply grateful to Johann Hornung, MSc for his advises and shared experiences on the welding technologies. I am also thankful to Dr. Martin Kirchgaßner and Dr. Gary Heath for their support.

I would like to thank TeroLab Surface Engineering GmbH and especially Franz Kreamsner for the fruitful discussions on the thermal spray topics.

I am also very grateful to Dr. Reinhard Polak for the mentoring and advising me at different stages of present work.

This work was funded by the Austrian COMET Programme (Project K2 XTribology, no. 824187) and carried out at the “Excellence Centre of Tribology” in cooperation with Tallinn University of Technology and Vienna University of Technology. This work has been also partially supported by graduate school „Functional materials and technologies“, receiving funding from the European Social Fund under project 1.2.0401.09-0079 in Estonia and following grants ETF 8211, ETF 8850, AR12132 and SIHT SF0140062s08.

Finally, I would like to thank my family and friends for their continuous direct and indirect support, patience, understanding and encouragement at different stages of the present work.

ABSTRACT

The degradation of materials through high-temperature processes such as oxidation, corrosion, and abrasive - erosive wear causes enormous costs for the European industry. It is crucial to avoid failure of various machine components which can entail catastrophic accidents. About 75 % of these costs are considered to be a consequence of wear-related losses. According to statistic reports, wear together with corrosion and fatigue are three main modes of materials failure.

Coatings and surface treatments have proved to be a successful approach for increasing machinery lifespan by preventing severe wear and corrosion of working tools. One of the attractive surface treatment methods is hardfacing by welding technique. This method offers the ability to apply thick protective coatings metallurgically bonded to the substrate material.

Current research is concentrated on the development of novel wear resistant thick coatings (hardfacings) and their analysis in terms of microstructure, mechanical and tribological properties. Plasma transferred arc (PTA) welding is used as a hardfacings fabrication technology. During hardfacing process powders are transported to the surface of the substrate material, building protective thick metallurgically bonded coatings. Usually such coatings consist of metal matrix reinforced with coarse (up to 250 μ m) hard particles like tungsten carbides. In present research cermet particles are suggested as reinforcements for NiCrBSi matrix alloy. This can be named as a main novelty of current work. During this research formation of so-called double metal matrix composite structures is obtained.

Due to the extremely high temperature during PTA processing, the carbides are often dissolved in the matrix phase, subsequently recrystallised in form of precipitates, intermetallic phases or eta-carbides. Those material changes during the deposition process significantly influence (usually reduce) mechanical and wear properties of the hardfacings. In present work it was shown, that application of cermet particles as reinforcements can help to minimise the problem of carbide dissolution and provide thick wear resistant coatings with homogeneous distribution of cermet particles throughout the matrix.

The aim of the present work is to bring together knowledge on the manufacturing of surfaces of commercial interest and surface engineering specialised in the characterisation of structures for two different fields of application: (i) cost-efficient wear resistant hardfacings reinforced with hardmetal scrap; (ii) cermet reinforcements for the high temperature (up to 700°C) wear resistant applications.

Throughout the thesis, the following scientific and technological aspects are addressed and solved:

- Pre-processing of cermets and hardmetals.
- Evaluation of the cermet and hardmetal particles as NiCrBSi matrix reinforcements.
- Deposition of the developed hardfacings.
- Microstructural characterisation of the coatings.
- Evaluation of the mechanical properties of the coatings.
- Assessment of the hardfacings as the tribo-functional materials for wear application at room and high temperatures as well as in corrosive media.

Keywords: hardfacing, PTA, tribology, high temperature wear, cermet, NiCrBSi

KOKKUVÕTE

Materjalide hävimine läbi kõrgtemperatuurse oksüdatsiooni, korrosiooni ja abrasiiverosiooni põhjustab Euroopa tööstusele ebanormaalselt suuri kulutusi. Seetõttu on ülioluline vältida masinaosade purunemist hoidmaks ära võimalikke õnnetusi. Statistikal põhinevad andmed kinnitavad, et kulumine koos korrosiooni ja väsimusega on peamised materjalide rivist välja langemise põhjused. Ligikaudu 75% seadme ekspluatatsiooniga seotud kulutustest on põhjustatud masinaosade kulumisest.

Pinded ja pinnatöötlus on tõestanud end eduka meetodina masinate eluea pikendamisel ning aitavad vältida tööriistade kulumist ja korrosiooni. Üks edukamaid pinnatöötlusmeetodeid on kõvapindamine keevitustehnoloogia abil. See meetod pakub võimalusi kanda alusmaterjalile pakse hea metallurgilise sidemega kaitsvaid pindeid.

Käesoleva töö eesmärkideks on: (i) kasutatud kõvasulamiga armeeritud säästlike kulumiskindlate kõvapinnete väljatöötamine; (ii) kõrgtemperatuursete (kuni 700°) kermistega armeeritud kulumiskindlate pinnete loomine.

Käesolev uurimistöö keskendub uudsete kulumiskindlate pakside kõvapinnete arendamisele: tehnoloogia optimeerimisele, pinnete mikrostruktuuri, mehaaniliste ja triboloogiliste omaduste uurimisele. Plasmakaarkeevitus (*PTA-welding*) on üks levinud mooduseid kõvapinnete valmistamisel. Kõvapindamise käigus kantakse pulbrid alusmaterjali/toote pinnale, tekitades nii metallurgilise sidemega paksu kaitsva pinde. Tavaliselt koosnevad sellised pinded jämedate kõvade osakestega (kuni 250 µm), näiteks volframkarbiidiga armeeritud raua või nikli baasil metallmaatriksist. Käesolevas töös uuritakse keraamilis-metalsete komposiitmaterjalide kasutamist NiCrBSi-sulamist maatriksi armeerimiseks. See on ka käesoleva töö peamiseks uudseks lahenduseks. Uurimistöö käigus saavutati nn. topeltarmeeritud WC-Co kõvasulami või TiC-NiMo ja Cr₃C₂-Ni kermise osakestega metallmaatriksstruktuuriga komposiitpinded.

Erakordselt kõrge temperatuuri tõttu PTA-keevituse käigus karbiidid sageli sulavad metalses maatriksis ja rekristalliseeruvad disperssete osakestena, intermetalliididena või muude ühenditena. Need materjali muutused pindamisprotsessi käigus mõjutavad oluliselt (tavaliselt vähendavad) kõvapinnete mehaanilisi ja kulumisomadusi. Käesolevas töös näidatakse, et keraamilis-metalsete komposiitmaterjalide (kermiste) kasutamine armeerimisel aitab vähendada karbiidide lahustumist ning tekitada homogeenelt jaotunud osakestega paksu kulumiskindla kaitsekihi kogu maatriksi mahus.

Käesolevas doktoritöös käsitletakse ja lahendatakse järgmiseid teaduslikke ja tehnoloogilisi aspekte:

- kõvasulami ja kermiste ümbertöötlus;
- kõvasulami ja kermiste sobivuse hindamine NiCrBSi-baasil pinnete armeerimisel;
- uutest komposiitpulbritest kõvapinnete saamine;
- pinnete mikrostruktuuri kirjeldamine;
- pinnete mehaaniliste omaduste hindamine;
- kõvapinnete sobivuse hindamine tribofunktsionaalsete materjalidena kulumise ja korrosiooni tingimustes toa- ja kõrgetel temperatuuridel.

Võtmesõnad: kõvapindamine, PTA-keevitus, triboloogia, kõrgtemperatuurne kulumine, kõvasulam, kermised, iseräbustuv NiCrBSi-sulam

PUBLICATIONS

PUBLICATION I

Zikin, A., Ilo, S., Kulu, P., Hussainova, I., Katsich, C., Badisch, E., Plasma Transferred Arc (PTA) Hardfacing of Recycled Hardmetal Reinforced Nickel-matrix Surface Composites, *Mat. Sci. (Medžiagotyra)* 18-1, 2012, 12-17. DOI: <http://dx.doi.org/10.5755/j01.ms.18.1.1334>¹

¹ Copyright 2012, reprinted with permission from Medžiagotyra

Plasma Transferred ARC (PTA) Hardfacing of Recycled Hardmetal Reinforced Nickel-matrix Surface Composites

Arkadi ZIKIN^{1,2*}, Sotiraq ILO¹, Priit KULU², Irina HUSSAINOVA²,
Christian KATSICH¹, Ewald BADISCH¹

¹ AC²T research GmbH, Viktor-Kaplan-Straße 2, 2700 Wiener Neustadt, Austria

² Department of Materials Engineering, Tallinn University of Technology, Ehitajate tee 5, 19086 Tallinn, Estonia

crossref <http://dx.doi.org/10.5755/j01.ms.18.1.1334>

Received 27 May 2011; accepted 09 September 2011

The aim of this work was to apply coarse recycled hardmetal particles in combination with Ni-based matrix to produce wear resistant metal matrix composite (MMC) thick coatings using plasma transferred arc hardfacing (PTA) technology. Assignment of hardmetal waste as initial material can significantly decrease the production costs and improve the mechanical properties of coatings and, consequently, increase their wear resistance. The microstructure of MMC fabricated from a recycled powder was examined by optical and SEM/EDS microscopes, whereas quantitative analyses were performed by image analysis method. Micro-mechanical properties, including hardness and elastic modulus of features, were measured by nanoindentation. Furthermore, behaviour of materials subjected to abrasive and impact conditions was studied. Results show the recycled powder provides hardfacings of high quality which can be successfully used in the fabrication of wear resistant MMC coatings by PTA-technology.

Keywords: tribology, hardfacing, recycling carbide, PTA, MMC, wear behaviour, chemical treatment.

1. INTRODUCTION

Tungsten carbide hardmetals are one of the most known and successful powder metallurgical products mainly used for manufacturing of machinery tools, which operate in environments where severe wear conditions prevail. Due to superior properties of tungsten carbide as hardphases in combination with different alloys of Fe, Co or Ni basis, it provides high wear resistance materials used in cutting, mining, drilling tools and other industrial equipment [1–3]. However, the high marked requirements lead to permanently increasing price and wastage of cemented tungsten carbide. Therefore research and development on alternative solutions such as reuse or recycling of the hardmetal scrap containing tungsten carbide became significantly important in recent years.

Recycling technology of hardmetal scrap with worn cermets requires applications of different processes for breakup, disjunction and purification of tungsten carbide particles. One of effectively applied mechanical methods for recycling of worn cermets and hardmetal scrap is disintegrator milling [4–7], which provides particle powders of uniform size and shape. Also, this method offers some more advantages in preservation the chemical composition and mechanically activation of materials. Received hardmetal powders by application of disintegrator milling process are successfully used in the fabrication of thin protective coatings by HVOF thermal spray technology [8–11]. The studies have shown importance of narrow granulometry and spherical shape of particles on wear resistance of coating. Particle size and shape depend on the duration of milling. An increase in time results in larger sized particle shape approaching spherical with a smooth

surface [4]. However increased amount of cycles leads to extensive wear of a grinding media and increased content of contaminations (Fe, Fe-based particles) in powder that significantly influence quality and properties of recycled hardmetal powder. Therefore to decrease content of impurities by processing of coarse, angular (up to 0.4 mm) particles plasma transferred arc (PTA) technology was suggested in present work.

The PTA-process is an efficient technology commonly used for the fabrication of wear resistant metal matrix composites (MMCs) [12–14]. PTA as an unique heat source for surface modification exhibits an enormous potential because of its low cost, easy operation and no need in a special surface treatment. Single or multilayer depositions provide strong metallurgical bonding between the deposit and the base metal, as well as porosity-free coating and relatively low dilution with substrate. In the PTA process, the heat of the plasma (arc of ionised gas) is used to melt the surface of the substrate and the welding powder, where the molten weld pool is protected from the atmosphere by the shielding gas. The variations in processing parameters such as preheat temperature, arc current and welding rate affect the welding performance (e.g. deposition rate) and the MMC's quality in terms of cermets homogeneity and hardness. PTA hardfacing is a promising approach for fabricating metallurgically bonded thick coatings of low alloyed steels using recycled cermets powders.

The main purpose of this work was to apply recycled cermets (cutting tools) in combination with metal matrix by PTA routine to produce novel advanced MMCs. It should be noted that this is a novel experimental process with no similar precedent found in literature. The principal scheme of the procedure applied in this work is shown in Fig. 1, where tungsten carbide based hardmetal scrap was used as an initial material. WC-Co hardmetals were milled

*Corresponding author: Tel. +43-262281600322, Fax. +43-26228160099.
E-mail address: zikin@ac2t.at (A. Zikin)

with the help of disintegrator technology to produce a powder and chemically treated to clean the surface of the received grains. Then blends were mixed with Ni-based matrix and overlaid on steel substrate, producing wear resistant thick coating.

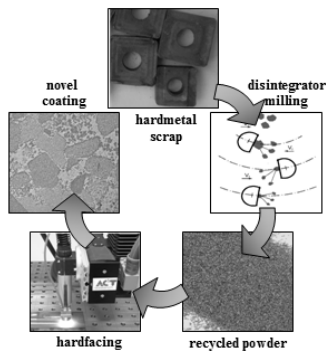


Fig. 1. Schematic view of the work procedure

2. EXPERIMENTAL DETAILS

Powder preparation and characterisation. Recycled WC-Co hardmetal powders were produced from hardmetal scrap by disintegrator milling as described in [5]. Purification of powders was performed by chemical treatment in concentrated sulphuric acid and successive cleaning with water and isopropyl alcohol. These processing steps were done to clean the particle surface after milling and to improve the weld ability and mechanical properties of material.

Table 1. Characteristics of initial powders

Type of powder	Particle size [μm]	Composition [wt %]
WC-Co	150–410	9–13 Co; 6–10 Fe; 2–4 Cr; rest WC*
Matrix**	32–125	0.2 C; 4 Cr; 1 B; 2.5 Si; 2 Fe; 1 Al; rest Ni
Reference***	45–90	4 C; rest WC/W ₂ C

* Various due to wear of grinding media and Co binder content.

** Castolin 16221 PTA powder.

*** Sulzer WOKA 50005.

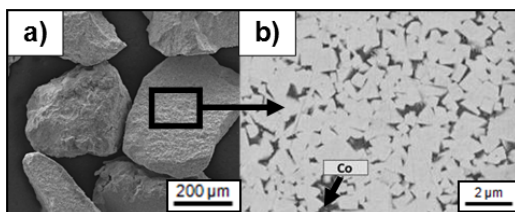


Fig. 2. SEM micrographs of recycled hardmetal particles: a – SE image of WC-Co particles; b – BSE image of grinded and polished grain surface

Castolin Ni-based 16221 powder was selected as a matrix material in the PTA processing of the recycled WC-Co hardmetal powders. The choice of this matrix can be explained by sufficient knowledge about powder

properties combined with experience by PTA cladding of this powder with tungsten carbide. Chemical composition and grain size of recycled powder, matrix and reference powder are presented in Table 1. It should be noticed, that coarse carbide grains are agglomerates of fine (3 μm–5 μm) tungsten carbide particles bonded together by Co-binder. Characterisation of microstructure of powders was performed by optical microscopy (OM) after etching as well as scanning electron microscopy (SEM/EDS). Typical microstructure of recycled WC-Co particles is shown in Fig. 2.

Hardfacing. PTA hardfacing was performed using a EuTronic® Gap 3001 DC apparatus (Fig. 3). Welding parameters such as welding current, oscillation and welding speed, substrate, powder feed rate, nozzle distance to workpiece, process gas flow rates are optimised related to the welding behaviour concerning to practical welding procedures. Welding procedure was carried out in a single layer welding without preheating or heat control of the substrate for reduced dilution. The mean welding parameters used in the present study are given in Table 2. The provided PTA-welded specimens were prepared by water jet cutting for further characterisations. This method of metallographic sample preparation avoids overheating of the probes that may induce changes in the properties of substrate and hardfacing [15].

Table 2. Summary of PTA welding parameters

Parameters	Values
Welding current	90/(100) A
Welding speed	0.9 mm/s
Oscillation speed	19.5 mm/s
Oscillation width	20 mm
Substrate material	mild steel (1.0037)
Substrate thickness	10 mm
Plasma gas	1.8 l/min
Carrier gas	carbide: 0.8 l/min; matrix 1.2 l/min
Shielding gas	15 l/min
Powders feed rate	35 g/min

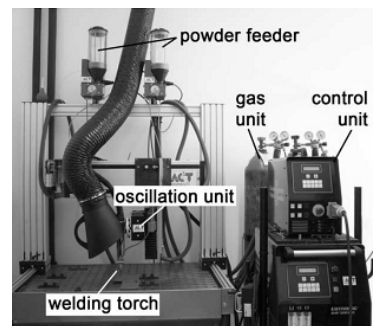


Fig. 3. PTA welding plant at AC²T (European Centre of Tribology)

Materials characterisation and wear examination. Test samples were cut, grinded and finished by 1 μm polish. Hardness measurements were carried out with standard Vickers hardness technique HV10. To determine hardness of each phase in the microstructure, e.g.

hardphases and metallic matrix, micro-hardness HV0.1 tests were applied. Four determinations of the micro- and macro-hardness were repeated for each considered sample for statistic calculation. Characterisation of microstructure was performed by OM after etching with Murakami's reagent as well as by SEM/EDS. The Leica QWin image analysis software (Leica microsysteme GmbH, Austria) was adapted and used to measure carbides/matrix content and grain size of carbides in MMCs. Mechanical properties were determined using nanoindentations. The preparation of samples for nanoindentation was done using standard methods without etching. The nanoindentation measurements of carbides and matrix were performed using a Hysitron TriboIndenter® apparatus (Hysitron inc., USA) equipped with Berkovich indenter operating in line-scan mode. For indentation an applied normal load of 5 mN was used.

In order to simulate field conditions in lab-scale as realistic as possible, wear tests were performed with the ASTM standard G65 method for 3-body-abrasion and the Cycling Impact Abrasion Test (CIAT) for combined impact-abrasion behaviour developed at the Austrian Centre of Competence for Tribology (AC²T) and described elsewhere [16–18].

3. RESULTS AND DISCUSSION

Pretreatment of powders. Certain percent of impurities, oxides and wasted adherences on the surface of the recycled tungsten carbide were indicated by EDS (Fig. 4, a). These impurities can influence weldability of the powders and influence the quality of the provided hardfacing, especially aggravate the coating porosity and decrease mechanical properties.

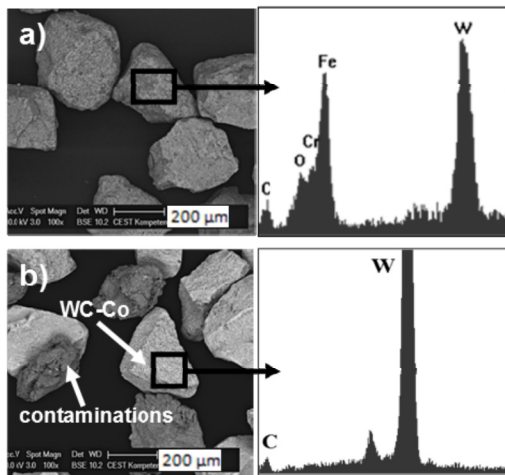


Fig. 4. Effect of cleaning process on surface composition of recycled WC-Co powder: a – SEM image and EDS analysis without chemical treatments of powder; b – SEM image and EDS analysis with chemical treatments of powders

A method of fast chemical treatment was developed for cleaning of the milled powder, which significantly improves the properties of recycled WC-Co powders. The impurities in the powder surface were removed by the

treatment, whereas no dilution of the main elements (WC with Co binder) was observed. Fig. 3, b, presents EDS analysis of the surface of recycled powder particles after the chemical treatment where no additional elements on the grain surface were indicated. The measured weight lost during the chemical processing of the powders is less than 1.5%. Cleaning is found to significantly improve the hardfacing weld layer quality by decreasing porosity (Fig. 5).

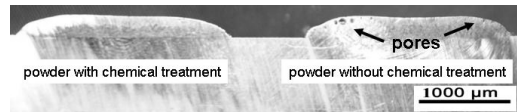


Fig. 5. Cross-section of weld deposit: effects of cleaning process on hardfacing quality

Formation of pores and concaved form of hardfacing during PTA-process can be explained by additional energy required to oxidise the adhered surface contaminations by the reaction with plasma. It should be noticed that chemical treatment of hardmetal powder surface is an experimental process and future investigations with process improvement steps are required.

Microstructure and hardness. For the developing of high quality MMCs certain amount of hard particles homogeneously distributed in the matrix and low dissolution of carbides in the matrix material are required. Preliminary investigations with 25 vol.%–30 vol.% of hardmetal powder provide no homogenous distribution of carbides in the hardfacings caused by sinking of the heavy carbide particles (Fig. 6, a) leaving a huge area of the deposit without particles. Similar problems were observed by laser cladding of WC in combination with Ni-matrix [19]. In the present study a homogeneous distribution of carbides was performed only by addition of 40 vol.% of hardmetal powder in coating (Fig. 6, b).

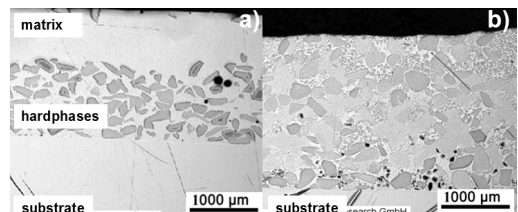


Fig. 6. OM micrographs of coatings: a – 30 vol.% of hardphases unetched; b – 40 vol.% of hardphase etched with Murakami's reagent

Fig. 7 illustrates a typical cross-sectional SEM micrograph of the received coating with 40 vol.% of hardmetal powder, where formation of three different main phases was observed. Phase A responds to a complex matrix structure with Ni and Fe as the main elements. Chemical composition of the matrix phase A is shown in Table 3 as indicated by the dispersive X-ray analyser (SEM/EDS). The certain content of Fe and Cr in the matrix can be explained by contamination with Fe and FeCr containing wear particles of grinding media in the recycling process. Tungsten carbide and Co inclusions inside the matrix are dissolved and re-precipitated WC-Co

grains are formed the double-dispersed structures. Hardness of the matrix is determined to be in the range between 380 HV10 and 550 HV10.

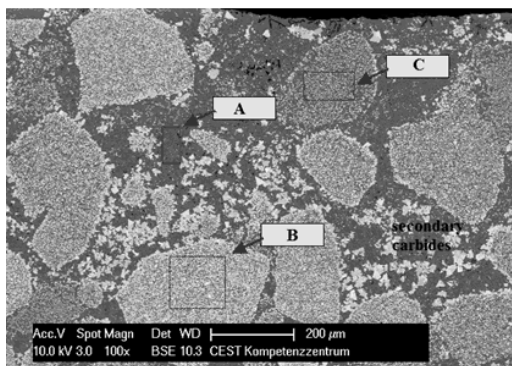


Fig. 7. SEM image of typical microstructure of PTA hardfacing with 40 vol. % of recycled hardmetal powder

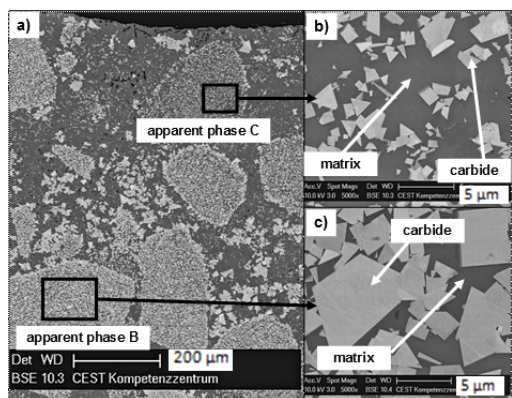


Fig. 8. SEM image of typical cross-section of received coating with detailed phases' analysis: a – overview image of weld deposit; b – BSE image of apparent phase C (more dissolved hardmetal particles); c – BSE image of apparent phase B (less dissolved hardmetal particles)

Two different modifications of carbide grain structures (apparent phases B and C) were received after hardfacing process. Microstructural analysis indicates penetration of the matrix elements (Fe and Ni) into Co binder between hardmetal agglomerates and partial dissolution of carbides. However carbides retain the angular grain shape developing the micro-sized MMC-particles in the coating with a “double-dispersed” MMC-structure (micro carbides with metal matrix). The main difference between phases B and C is matrix composition inside the carbide MMC and average grain size reduction of micro carbides in hardmetal MMC (Fig. 8). It was assumed that various level of hardphases dissolution is due to different binder element content in recycled powder grains. The difference between binder content responds to quality of recycled powder, whereas the Co content is always dependent on cutting tools waste material.

Apparent phase C shows only 30 vol.% of carbide particles with average grain size of 1.3 μm (Fig. 8, b), whereas apparent phase B (Fig. 8, c) indicates mirrored

structure of the metal matrix components with 70 vol.% of carbides between matrix and a factor of two coarser average particles size compared to phase C (2.5 μm). The micro hardness of more dissolved matrix was determined to be 750 HV0.1 and hardness value of MMCs in phase C is 1240 HV0.1. This difference in hardness can be explained by influence of matrix content. Table 3 illustrates analysis of chemical composition by EDS of matrix region in both hardmetal MMC phases, which showed differences in elements content (especially Co and W).

Table 3. Chemical composition of matrix in phase A, B and C

Element	Matrix, phase A	Matrix, phase B	Matrix, phase C
	wt %	wt %	wt %
W	9	8	12
Co	10	9	20
Ni	50	52	43
Fe	28	28	22
Cr	3	3	3

Nanoindentation. Micro-mechanical properties of the phases (hardness and reduced Young's modulus) were determined by nanoindentation measurements and statistically analysed using Box and Wisher plots (Fig. 9). The results for the received coating showed mean nanoindentation hardness of 4.7 GPa in the matrix phase, whereas no significant difference were found for the hardness of micro carbides in apparent phases B and C (27.2 GPa). This hardness level was in close approximation to hardness of tungsten carbide (whole WC/W₂C particles) measured as reference.

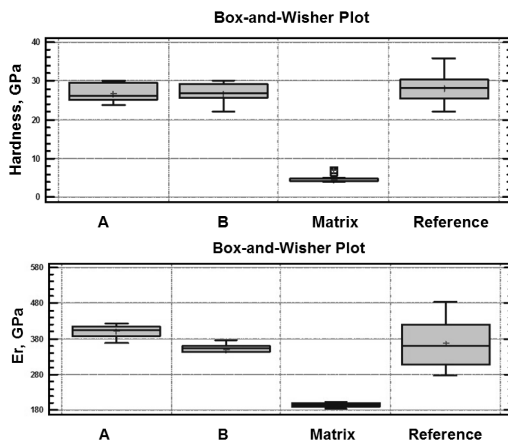


Fig. 9. Box and Whisker plots of the measured hardness and reduced modulus: A – carbides in apparent phase B (less dissolved); B – carbides in apparent phase C (more dissolved); Matrix – apparent phase A; Reference – WC/W₂C

Some differences in values of the reduced elastic modulus were observed between hardmetal with less dissolved micro carbides (A) and hardmetal with more dissolved micro carbides (B). This decrease from 320 GPa to 290 GPa of the elastic parameter can be explained by

influence of the increased content of matrix elements (Ni, Co, Fe, etc.) and formation of solid solutions in the more dissolved hardmetal regions. However, the elastic modulus of these both recycled phases was within the measured values of the reference carbide (conventionally used WC/W₂C). These results indicate the micro-mechanical properties of the recycled hardphases were close to the micro-mechanical properties of the tungsten carbides used as the reference. However, the distribution broadness as indicated by standard deviation (Fig. 9) for the measured micro-mechanical properties of the recycled hardphases show close values as the measurements for the reference tungsten carbides. These indicate the high quality of the obtained hardphases in the recycling process of the present study.

Wear testing. It is generally assumed that abrasive wear behaviour of materials influenced by their hardness, microstructural features and wear conditions. Some previous studies [20–22] have shown the importance of hardness of both the matrix and the hardphases, whereas type, content, homogeneous distribution and size of the hardphases have a significant influence on wear properties of the material. The microstructure of investigated coating consists of coarse carbide MMCs, homogeneously distributed throughout the matrix. The relatively large difference in hardness due to partial dilution of some hardmetal grains leads to a higher wear rate. However, decrease in hardness corresponds to changes in material ductility. In conditions where impact wear is a dominative factor, increased plasticity and high content of fine grained hardphases result in improved wear resistance of a material [18].

Quantitative wear analysis was determined by volume loss and the results are given in Fig.10, where the summary of wear data obtained in different tests is listened. The relative wear resistance of the coating was compared to Ni-based reference hardfacing consisting 40 vol. % of WC/W₂C grains.

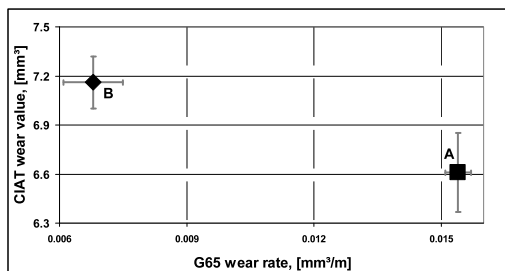


Fig. 10. ASTM G65 and CIAT wear values: A – produced MMC coating; B – reference material with 40 vol. % of WC/W₂C

The volume loss of the produced material under abrasive conditions is increased by a factor of two as compared to the reference coating, which is in a good agreement with [23]. Representative worn surfaces of the produced material are presented in Fig. 11, a. The predominant wear mechanism is dissection of tungsten carbides resulted in matrix material's wear. In the present study it was found that there is no significant wear of secondary MMCs regions with high carbides content (Fig. 11, b). From the other hand the hardmetal regions

containing more dissolved hardphases do not give enough protection against wear, resulting in ductile deformation of the matrix showing microcutting scars on the surface and failure of small carbide particles (Fig. 11, c). Therefore the reason for the increased volume loss can be found in the lack of secondary MMCs regions with high carbides content in the surface regions which are exposed directly to abrasive wear attack.

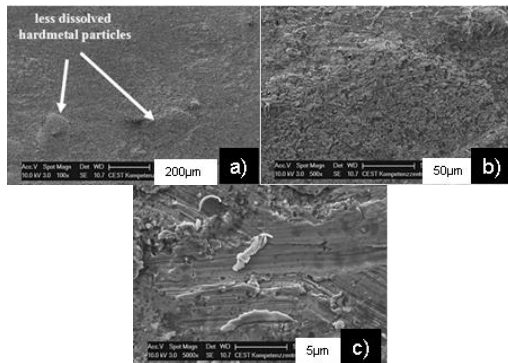


Fig. 11. Typical SEM images of worn of produced MMC coating after abrasion testing

The results observed after cycling impact abrasion test (Fig. 10) show relatively low wear rate of the produced material and higher wear resistance as compared to the reference material. The main mechanisms of material damage are related to plastic deformation of surface through microploughing and microcutting, whereas the brittle fracture of carbides region and breakouts of carbides is negligible as compared to reference material (Fig. 12).

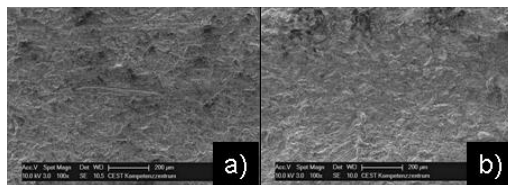


Fig. 12. Typical SEM images of worn surface after impact/abrasion testing: a – produced MMC coating; b – reference material with 40 vol. % of WC/W₂C

4. CONCLUSIONS

Based in the study within this work, the following conclusions can be drawn:

1. Hardmetal scrap was successfully applied by fabrication of wear resistant coatings using PTA hardfacing technology.
2. Chemical treatment of the milled powders has significantly improved quality of the produced hardfacings.
3. A certain amount of WC-Co particles is required (min. 40 vol. %) to achieve homogeneous distribution of carbides in the matrix during PTA processing.
4. Formation of two different secondary MMC apparent phases with different microstructure and mechanical properties in both matrix/carbide areas was observed.
5. Under pure abrasion conditions, reduced wear resistance by a factor of two as compared to conventionally

used WC/W₂C was obtained. This fact can be explained by significant difference in hardness in secondary MMCs (less dissolved hardmetal grains – 1250 HV0.1; more dissolved hardmetal grains – 780 HV0.1) as well as by certain percent of contaminations (up to 10 % of Fe and FeCr particles inside of recycled powder).

6. Under combined impact/abrasion conditions produced coating has shown promising results with high wear resistance.

Acknowledgments

This work was funded from the “Austrian Comet-Program” (governmental funding program for pre-competitive research) via the Austrian Research Promotion Agency (FFG) and the TecNet Capital GmbH (Province of Niederösterreich) and has been carried out within the “Austrian Center of Competence for Tribology” (AC²T research GmbH) and partially supported by graduate school „Functional materials and processes“, receiving funding from the European Social Fund under project 1.2.0401.09-0079 in Estonia. Estonian Science Foundation under grant No. 8211 is also acknowledged for the support of this study. The authors are also grateful to Dr. Jaroslav Wosik for SEM/EDS analysis of samples and to MSc Andrei Surzenkov and MSc Dmitrij Goljandin for powders preparation and research cooperation.

REFERENCES

- Zum Gahr, K.-H., *Microstructure and Wear of Materials*. Elsevier, Amsterdam, 1987.
- Ndlovu, S. The Wear Properties of Tungsten Carbide-Cobalt Hardmetals from the Nanoscale up to the Macroscopic Scale *PhD Thesis* Der Technischen Fakultät der Universität Erlangen, Nürnberg, 2009.
- Mellor, B. G. *Surface Coatings for Protection against Wear*. Woodhead Publishing, Cambridge, 2006.
- Kulu, P., Mikli, V., Käerdi, H., Besterci, M. Characterization of Disintegrator Milled Hardmetal Powder *Powder Metallurgy Progress* 3 (1) 2003.
- Tümanok, A., Kulu, P., Mikli, V., Käerdi, H. Technology and Equipment for Production of Hardmetal Powders from Used Hardmetal *In: Proc. 2nd International DAAAM Conference* Tallinn, Estonia 2000: pp. 197–200.
- Kulu, P., Käerdi, H., Mikli, V. Retreatment of Used Hardmetals *In: Proc. TMS 2002 Recycling and Waste Treatment in Mineral and Metal Processing: Technical and Economic Aspects* 1 Lulea 2002: pp. 139–146.
- Zimakov, S., Pihl, T., Kulu, P., Antonov, M., Mikli, V. Applications of Recycled Hardmetal Powder *Proceedings of The Estonian Academy of Sciences. Engineering* 9/4 2003: pp. 304–316.
- Kulu, P., Zimakov, S. Wear Resistance of Thermal Sprayed Coatings on the Base of Recycled Hardmetal *Surface and Coatings Technology* 130 2000: pp. 46–51.
- Kulu, P., Hussainova, I., Veinthal, R. Solid Particle Erosion of Thermal Sprayed Coatings *Wear* 258 2005: pp. 488–496.
- Surzenov, A., Kulu, P., Tarbe, R., Mikli, V., Sarjas, H., Latokartano, J. Wear Resistance of Laser Remelted Thermally Sprayed Coatings *Estonian Journal of Engineering* 15 (4) 2009: pp. 318–328.
- Mikli, V., Käerdi, H., Kulu, P., Besterci, M. Characterisation of Powder Particle Morphology *Proceedings of The Estonian Academy of Sciences. Engineering* 7/1 2001: pp. 22–34.
- Shin, J. C., Doh, J. M., Yoon, J. K., Lee, D. Y., Kim, J. S. Effect of Molybdenum on the Microstructure and Wear Resistance of Cobalt-base Stellite Hardfacing Alloys *Surface and Coatings Technology* 166 2003: pp. 117–126.
- Branagan, D. J., Marshall, M. C., Meacham, B. E. High Toughness High Hardness Iron Based PTAW Weld Materials *Materials Science and Engineering A* 428 2006: pp. 116–123. <http://dx.doi.org/10.1016/j.msea.2006.04.089>
- Gurumoorthy, K., Kamaraj, M., Prasad Rao, K., Sambasiva Rao, A., Venugopal, S. Microstructural Aspects of Plasma Transferred Arc Surfaced Ni-based Hardfacing Alloy *Materials Science and Engineering A* 456 2007: pp. 11–19.
- Bhaduri, A. K., Albert, S. K. Developemnt of Hardfacing for Fast Breeder Reactors *Materials Science Research Horizons* Chapter 5 Nova Science Publishers 2007: pp. 149–169
- Badisch, E., Katsich, C., Winkelmann, H., Franek, F., Roy, M. Wear Behaviour of Hardfaced Fe-Cr-C Alloy and Austenitic Steel under 2-body and 3-body Conditions at Elevated Temperature *Tribology International* 43 2010: pp. 1234–1244.
- Sarkar, S., Badisch, E., Mitra, R., Roy, M. Impact Abrasive Wear Response of Carbon/Carbon Composites at Elevated Temperature *Tribology Letters* 37 2010: pp. 445-451.
- Winkelmann, H., Badisch, E., Kirchgäßner, M., Danning, H. Wear Mechanisms at High Temperatures. Part 1: Wear Mechanisms of Different Fe-based Alloys at Elevated Temperature *Tribology Letters* 34 2009: pp. 155–166.
- Nurminen, J., Näkki, J., Vuoristo, P. Microstructure and Properties of Hard and Wear Resistant MMC Coatings Deposited by Laser Cladding *International Journal of Refractory Metals & Hard Materials* 27 2009: pp. 472–478.
- Zhou, R., Jiang, Y., Lu, D. The Effect of Volume Fraction of WC Particles on Erosion Resistance of WC Reinforced Iron Matrix Surface Composites *Wear* 255 2003: pp. 137–138.
- Colaco, R., Vilar, R. A Model for the Abrasive Wear of Metallic Matrix Particle-reinforced Materials *Wear* 254 2003: pp. 625–633.
- Kirchgäßner, M., Badisch, E., Franek, F. Behaviour of Iron-based Hardfacing Alloys under Abrasion and Impact *Wear* 265 2008: pp. 772–779.
- Badisch, E., Kirchgäßner, M. Influence of Welding Parameters on Microstructure and Wear Behaviour of a Typical NiCrBSi Hardfacing Alloy Reinforced with Tungsten Carbide *Surface & Coatings Technology* 202 2008: pp. 6016–6022. <http://dx.doi.org/10.1016/j.surfcoat.2008.06.185>

Presented at the 20th International Baltic Conference "Materials Engineering 2011" (Kaunas, Lithuania, October 27–28, 2011)

PUBLICATION II

Zikin, A., Hussainova, I., Katsich, C., Badisch, E., Tomastik, C., Advanced chromium carbide based hardfacings, *Surf. Coat. Technol.* 206, 2012, 4270 - 4278. DOI: <http://dx.doi.org/10.1016/j.surfcoat.2012.04.039>²

² Copyright 2012, reprinted with permission from Elsevier



Advanced chromium carbide-based hardfacings

A. Zikin^{a,b,*}, I. Hussainova^b, C. Katsich^a, E. Badisch^a, C. Tomastik^a

^a AC2T Research GmbH, Viktor-Kaplan-Straße 2, 2700 Wiener Neustadt, Austria

^b Department of Materials Engineering, Tallinn University of Technology (TUT), Ehitajate tee 5, 19086 Tallinn, Estonia

ARTICLE INFO

Article history:

Received 7 February 2012

Accepted in revised form 13 April 2012

Available online 21 April 2012

Keywords:

PTA

Hardfacing

Cr₃C₂-Ni

Nanoindentation

High temperature wear

Tribology

ABSTRACT

Ceramic metal composite powders are widely used in thermal spray technologies; however, application of such hardphases in cladding systems has not been strongly developed yet. In the present study, two different hardfacings produced by the plasma transferred arc (PTA) process were analysed and compared to reveal differences between NiCrBSi coatings reinforced with standard chromium carbide and chromium-based cermet powders. The coatings were produced from a mixture of hardphases (Cr₃C₂ or Cr₃C₂-Ni) and nickel based powder with a ratio of 40/60 vol.%. The coatings' thickness was set to 2–2.5 mm on an austenite substrate. Hardfacings were characterised in terms of their microstructures, mechanical properties and impact-abrasion wear resistance at room and elevated temperatures. The manufactured Cr₃C₂-Ni reinforced hardfacing alloy has shown promising microstructural features with a low level of carbide dissolution and high temperature wear performance.

© 2012 Elsevier B.V. All rights reserved.

1. Introduction

Ceramic metal composites or cermets are known to combine the hardness of ceramics and the fracture toughness of metals. The widely used tungsten carbide (WC) based cermets, for example, have both high hardness and high fracture toughness, making them useful in severe wear applications such as for cutting tools and drill bits. WC based cermets, however, degrade at temperatures above 500 °C. Chromium carbide has been a potentially suitable ceramic phase for use in cermets due to excellent oxidation resistance of its three polymorphs – the cubic (Cr₂₃C₆), the hexagonal (Cr₇C₃), and the orthorhombic (Cr₃C₂). Chromium carbide-based composites are widely used tribological materials in high-temperature applications requiring high resistance to wear and corrosion-oxidation [1–3].

Chromium carbides combined with metal matrix are often used as wear-resistant coatings on tool parts needing protection [4]. In thermal spray applications chromium carbide is often combined with a nickel chromium matrix. The thermally sprayed CrC-NiCr coatings can serve as a barrier for high temperature wear [5,6] and are therefore finding increasing application in the aerospace market.

Another property that makes the application of CrC-NiCr coatings very attractive is the coefficient of thermal expansion of chromium carbide that is almost equal to the coefficient of thermal expansion of steel, resulting in a reduction in mechanical stress build-up at the layer boundary when coated on steel substrates.

Several attempts have been made to improve the mechanical properties and tribological performance of chromium carbide based coatings by varying the deposition techniques, processing parameters and characteristics of the feedstock powder [7]. Hardfacing techniques such as plasma transferred arc (PTA), gas tungsten arc welding (GTAW) and laser cladding have been widely accepted in industry to improve the corrosion and erosion resistance of materials in aggressive environments [9–11]. The PTA process exhibits enormous potential because the PTA overlays have a lower production cost and a higher productivity compared to thermal sprayed coatings, as well as easy operation and no need for any special surface treatment [8–12]. Furthermore, the PTA technique allows the production of high quality coatings (good metallurgical bonding and low level of porosity) consisting of metal matrix and carbide hardphases.

Although Cr₃C₂-20–25% NiCr systems are widely known as wear protective coatings, only a few studies [13–17] have been concentrated on the processing of chromium carbide reinforcements in combination with a nickel-based matrix by cladding technologies. Due to the extremely high temperature of processing, the carbides are often dissolved in the binder phase and subsequently recrystallised and re-precipitated. This influences the oxidation behaviour during high-temperature applications and leads to changes in wear properties of the coating [18,19]. At the same time there is a lack of information about the deposition of Cr₃C₂-Ni systems with the PTA process.

For the present study the chromium carbide-based hardfacings were produced by the PTA technique from (i) Cr₃C₂ hardphase particles; and (ii) Cr₃C₂-Ni cermet powder blended with NiCrBSi matrix to overcome the problem of carbide dissolution. The coatings were deposited on austenitic stainless steel substrate. The aim of the work was twofold: (1) to develop a reliable process to produce hardfacings

* Corresponding author at: AC2T Research GmbH, Viktor-Kaplan-Straße 2, 2700 Wiener Neustadt, Austria. Tel.: +43 2622 81600 322; fax: +43 2622 81600 99.

E-mail address: zikin@ac2t.at (A. Zikin).

of defined microstructure and properties; and (2) to characterise coating performance as a function of starting powder composition. Two hardphase reinforced coating systems (chromium carbide particles reinforced and cermet particles reinforced) with NiCrBSi matrix were examined and compared.

2. Experimental details

2.1. Powders

Two hardphase powders were used in the present research: standard Cr_3C_2 powder with particle size with mesh $-45 + 90 \mu\text{m}$ (Sulzer Metco) and pre-processed powder chromium carbide-based and pure nickel bonded cermet particles. These cermet particles were remilled from the bulk of $\text{Cr}_3\text{C}_2-20 \text{ wt.}\% \text{ Ni}$ and then sieved with mesh $-150 + 310 \mu\text{m}$.

Purification of the $\text{Cr}_3\text{C}_2-\text{Ni}$ powder was performed by chemical treatment in HCl and cleaning with ethanol and isopropyl alcohol. This operation was performed to remove trace elements (W, Fe) from the particles' surface after remilling in the disintegrator consisting of steel working chamber and WC-Co grinding bodies with the aim to improve the weldability of the powders and the mechanical properties of the produced materials [20]. Fig. 1 demonstrates the difference between untreated and chemically treated cermet powders.

NiCrBSi alloy powder (0.2% C, 4% Cr, 1% B, 2.5% Si, 2% Fe, 1% Al, rest Ni) with particle size with mesh $-50 + 150 \mu\text{m}$ was used as matrix material for the PTA hardfacing process.

2.2. Plasma transferred arc hardfacing

PTA hardfacing of Cr_3C_2 and $\text{Cr}_3\text{C}_2-\text{Ni}$ particles in combination with NiCrBSi matrix was carried out using a EuTronic® Gap 3001 DC apparatus (Fig. 2). To prevent oxidation of the substrate material at high temperature, austenitic stainless steel was used as substrate. The coatings' thickness was set to 2–2.5 mm. Welding parameters such as welding current, oscillation and welding speed, powder feed rate, nozzle distance to substrate, carrier, shielding and plasma gas

flow rates are optimised with respect to practical welding conditions. Main process parameters are given in Table 1.

To adjust the requested ratio of carbide and metal powder, two powder feeders are controlled separately. A powder consumable was transported internally through the torch via a carrier gas and exited at orifices on the anode face, intersecting the plasma column some distance above the substrate. The powder was introduced into a weld pool that forms on the substrate surface. The weld pool is protected from oxidation by a shielding gas that flows from an outer annulus in the torch. The metallurgical bond between coating and substrate is a characteristic feature of the process. The welding deposition was performed in a single layer without preheating or heat control of the substrate for reduced dilution.

2.3. Characterisation

Prior to testing the samples were cut from large pieces, ground and subsequently polished down to $1 \mu\text{m}$ roughness using diamond paste.

A comprehensive microstructural evaluation of the plasma hardfacing was carried out by optical microscopy (OM) equipped with a digital camera (MEF4A, Leica Microsystem) and scanning electron microscopy (SEM; Philips XL 30 FEG equipped with an energy dispersive X-ray analyser) on the surface and cross-section of the coatings. The microstructural studies were performed on samples etched with a solution of HF and HNO_3 in volume ratio 1:12 at room temperature for 10 s.

X-ray diffraction (XRD) studies were carried out using X-Pert powder diffractometer (PANalytical, Netherlands) and $\text{CuK}\alpha$ radiation in Bragg-Brentano geometry at 40 kV and 30 mA. The measurements were conducted in continuous mode. This diffractometer is equipped with a secondary graphite monochromator, automatic divergence slits, and a scintillation counter.

Hardness of the hardfacings was measured using standard Vickers hardness tester at a load of 10 kg (HV10). An average hardness was estimated from 10 indentations per specimen.

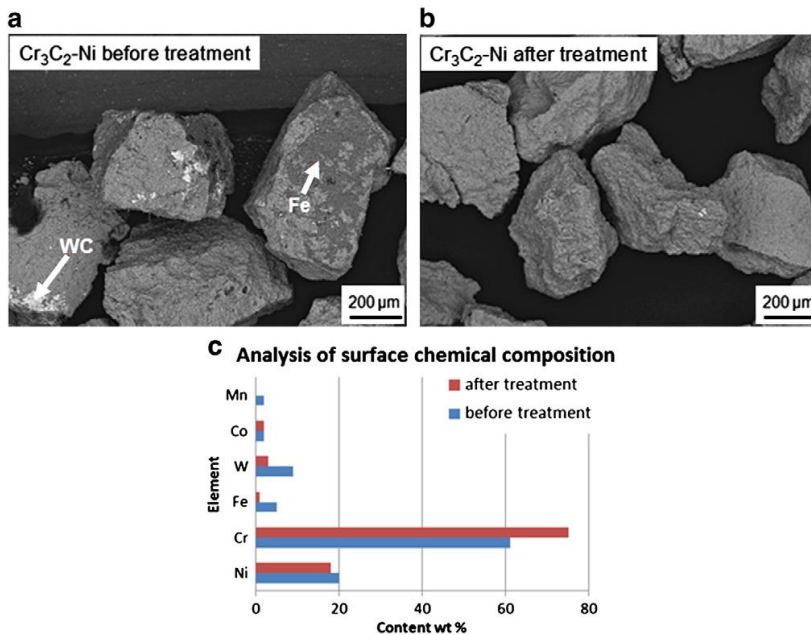


Fig. 1. Particles of the cermet powders for PTA: a) untreated; b) chemically treated particles; c) surface analysis before and after treatment.

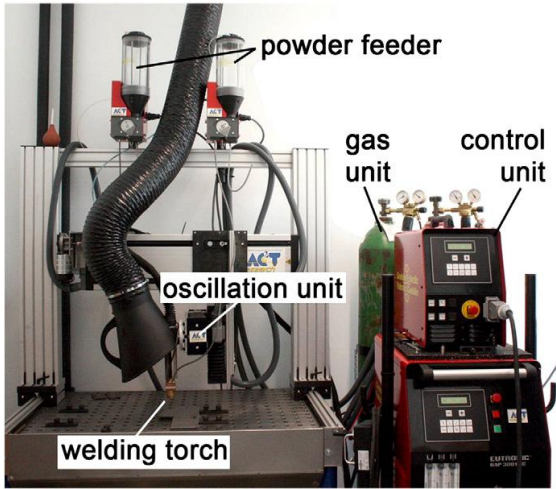


Fig. 2. PTA welding plant at AC2T research GmbH.

Vickers hardness test rig [21] specially developed by AC2T was used to measure the hardness of materials at high temperatures. The diagonals of the indent marks were measured by OM. The testing chamber was kept under vacuum to exclude oxidation during the test. All samples were loaded by 10 kg to measure HV10. The mean value of hardness at each test temperature was calculated by averaging of the results obtained on at least 8 indents.

To determine the hardness of each phase in the composite and analyse the mechanical properties of each constituent phase, nanoindentation measurements were carried out using a Hysitron Triboindenter T1900 (Minneapolis, MN, USA) equipped with a diamond Berkovich indentation tip with 100 nm tip radius. The load cycle involved loading for 5 s to reach the peak load of 10 mN and subsequent unloading for 5 s. The load vs. depth curves were analysed to evaluate the elastic modulus and hardness using the procedure described in [22].

2.4. Impact/abrasion testing

The wear rates of the hardfacings were evaluated with the help of Cyclic Impact Abrasion Tester (HT-CIAT) developed at the Austrian Centre of Competence for Tribology (AC2T, Austria) for studying combined impact–abrasion action and described elsewhere [21]. Tests were performed at room and elevated (300, 550 and 700 °C) temperatures. The samples were fixed at 45° and cyclically hit by a plunger while constant abrasive flow was running between the sample and the plunger.

Table 1
Main parameters of PTA processing.

Parameter	Value
Welding current	100 Å
Oscillation speed	1.5 mm/s
Oscillation width	20 mm
Welding speed	1.1 mm/s
Substrate material	Austenite steel
Substrate thickness	5 mm
Nozzle distance to the substrate	8 mm
Plasma gas	Ar; 1.7 l/m
Shielding gas	Ar/H ₂ ; 15 l/m
Carrier gas	Ar/H ₂ ; 2 l/min

Samples to be tested were cleaned in an ultrasonic bath with isopropanol, dried and weighed before testing. Quantitative wear characterisation was done by gravimetric mass loss of the testing specimens. Tribo-test parameters are listed in Table 2. Upon completion of testing the topography of the worn surfaces was analysed by SEM.

3. Results and discussion

3.1. Microstructural analysis

In the present study, two different hardfacings produced by the identical PTA process tools operating with identical parameters (Table 1) were analysed and compared to reveal differences between coatings obtained from standard chromium carbide and cermet powders. The coatings were produced from a mixture of hardphases (Cr₃C₂ or Cr₃C₂–Ni) and NiCrBSi matrix powder with a ratio of 40/60 vol.%.

The XRD patterns of the Cr₃C₂ and Cr₃C₂–Ni reinforced alloys and NiCrBSi matrix alloy are shown in Fig. 3. XRD analysis of the original NiCrBSi matrix alloy indicated a high amount of FeNi₃ solid solution in Ni-based matrix with presence of small amount of Ni₃B and Cr₇C₃ hardphases (Fig. 3a). When 40 vol.% Cr₃C₂ particles were added to the NiCrBSi alloy, Cr₃C₂, Cr₇C₃ and M₂₃C₆ phases could be detected by XRD analysis in the hardphased layer as shown in Fig. 3b. Intensive dissolution of carbides results in an increased content of free Cr and C in the liquid alloy [15], which influences the matrix composition and leads to the formation of an austenite Ni_{2.9}Cr_{0.7}Fe_{0.36} phase. The complex phase Cr₇C₃ is formed in the alloy as re-precipitated carbides during the rapid solidification process. It should be outlined that XRD peaks for many chromium carbides and borides are very closely placed and with significant alloying in these phases, confirmation of the type of carbides from XRD alone is difficult. Therefore the presence of M₂₃C₆ phase is very doubtful. Almost all peaks of M₂₃C₆ match with Cr₇C₃ and Cr₃C₂ peaks. Furthermore M₂₃C₆ phase is usually not formed by high free carbon levels and the microstructural analysis has not revealed any M₂₃C₆ carbides in the hardfacing matrix. Most probably those peaks correspond to some mixed Cr–B–Ni phase presented as precipitations in the matrix. Fig. 3c presents the XRD analysis of the NiCrBSi alloy with addition of 40 vol.% Cr₃C₂–Ni powder. In this case, due to the Ni binder in the cermet particles, the dissolution of chromium carbides is negligible and the matrix phase was identified as FeNi₃ with a high content of Cr₃C₂ and Cr₇C₃ hardphases. The presence of Cr₇C₃ can be explained by the structure of the precursor Cr₃C₂–Ni bulk cermet [23], where a certain amount of Cr₇C₃ was formed during sintering.

Fig. 4 illustrates the typical cross-sectional OM micrographs of the coatings. The reference material (NiCrBSi self-fluxing matrix alloy) exhibits a nickel-rich dendritic matrix containing borides and carbides (Fig. 4a) that is a typical phase composition for alloys with low chromium content [9]. According to phase distribution analysis the content of Cr₇C₃ phase is 2 ± 1 wt.%, whereas the content of Ni₃B phase is 19 ± 1 wt.%.

Table 2
Tribo-test parameters.

Parameter	Value
Impact energy	0.8 J
Impact angle	45°
Frequency	2 Hz
Testing cycles	7200
Abrasive material	Silica sand
Abrasive flow	3 g/s
Abrasive size, shape	0.4–0.9 mm, angular
Abrasive hardness	1000–1200 HV
Test temperatures	RT, 300 °C, 550 °C, 700 °C

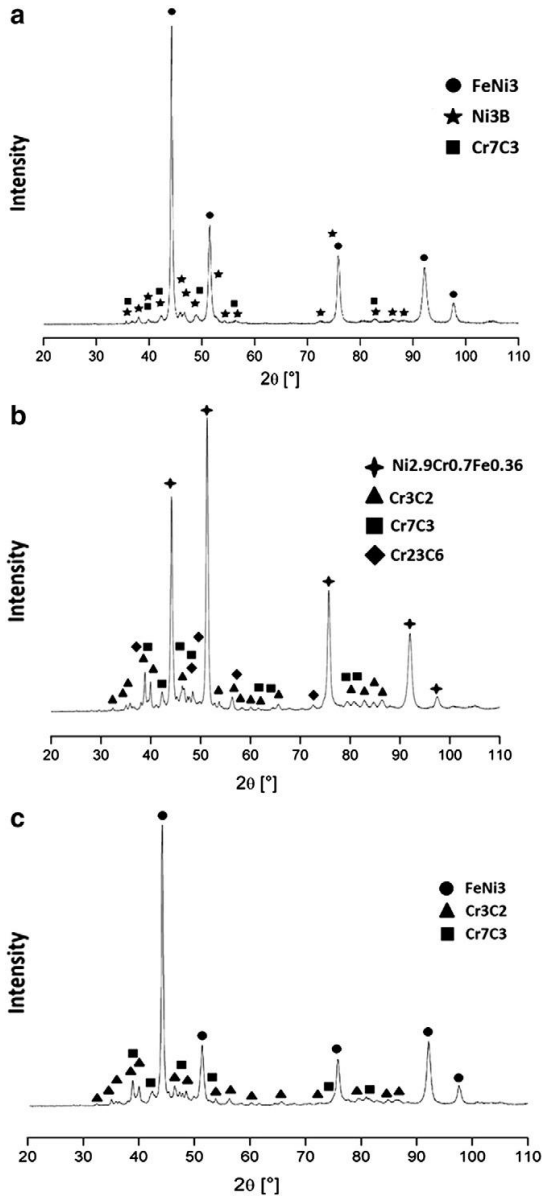


Fig. 3. XRD patterns: a) NiCrBSi hardfacing; b) Cr_3C_2 reinforced hardfacing; c) Cr_3C_2 -Ni reinforced hardfacing.

Fig. 4b shows the microstructure of the Cr_3C_2 (Sulzer Metco 70C-NS) reinforced hardfacing. The micrograph reveals the presence of a high amount of re-precipitated spine-like carbides (Cr_7C_3) resulting from the extensive carbide dissolution in the matrix. The coating microstructure is in good correlation with earlier reported observations [14,15].

Fig. 4c illustrates the microstructure of the coating produced from cermet powder in combination with NiCrBSi matrix. The microstructure of this coating can be characterised by three apparent phases: hard-phase-rich hypereutectic matrix material, some amount of dissolved and re-precipitated Cr_7C_3 carbides, and a certain content of particles of

the initial cermet particles homogeneously distributed throughout the matrix. It is assumed that the nickel binder in the cermet particles protects the primary carbides from dissolution and helps keep the particles in the original composition. SEM images of the structure (Fig. 5) show Ni binder (labelled as Matrix) between the primary carbides. According to the EDS analysis, the metallic Ni-based binder phases of the cermets consist of nickel–chromium solid solution. This is in good correlation with analysis of bulk Cr_3C_2 -Ni cermet [24].

Growth and formation of spine-like carbides occur mostly between the matrix and cermet particles. No re-precipitated carbides were found inside the cermet phase (Fig. 5b). The cermet particles (Fig. 5c) consist of agglomerates of 2–5 μm sized Cr_3C_2 and Cr_7C_3 particles embedded into the metal matrix, i.e. the commonly reported structure of the reactive sintered Cr_3C_2 -Ni cermets [23,25].

3.2. Hardness

Vickers hardness of the (compound) NiCrBSi alloy is 375 ± 6 HV10. The Cr_3C_2 reinforced coating shows a hardness of 569 ± 13 HV10, while the cermet particles reinforced hardfacing reveals a hardness value of 730 ± 110 HV10. The hardness of multiphase materials is influenced to a great extent by microstructural features. The increase in hardness of the Cr_3C_2 -Ni reinforced coating is due to a high content of uniformly distributed cermet particles. However, because of the microstructural complexity of the PTA coatings a wide spread of hardness values is demonstrated. To obtain more information on hardness and modulus of each individual phase the nanoindentation method was applied.

The hot hardness of the NiCrBSi alloy is 380 ± 40 HV10 at temperatures below 550°C and rapidly decreases with increase in temperature. The hardness measurements in the hardfacings under consideration represent a composite hardness of hardphases and binder. Fig. 6 illustrates HV10 results for Cr_3C_2 and Cr_3C_2 -Ni reinforced NiCrBSi hardfacings. The hardness values for both materials slightly decrease in the temperature range from 20°C to 500°C . Rapid decrease in hardness starts from 600°C ; at the temperature of 700°C the hardness is lower than 400 HV for both Cr_3C_2 and Cr_3C_2 -Ni reinforced NiCrBSi hardfacings.

3.3. Nanoindentation

Measuring the intrinsic properties of each phase separately provides information on the spatial heterogeneity in local material properties and serves as guidance to process engineering and advanced materials design [26]. Micro-mechanical properties of the phases (hardness and reduced Young's modulus) were determined by nanoindentation measurements and statistically analysed using bubble graphic presentation. The reduced Young's modulus (E_r) is described by the equation:

$$1/E_r = (1-\nu_i^2)/E_i + (1-\nu_s^2)/E_s,$$

where ν is the Poisson's ratio, the index i denotes the values for the indenter tip and the index s denotes the ones for the sample. The indenter term for the diamond tip can be neglected in the present investigation; the term $1-\nu_s^2$ introduces a deviation from E_s in the order of 10%.

The main goal of nanoindentation measurements in the present research was to compare the differences in mechanical properties of Cr_3C_2 and Cr_3C_2 -Ni reinforced hardfacings. It was suggested that changes in the microstructure could lead to changes of the properties, especially in hardphases.

Fig. 7a illustrates the load–displacement curves obtained for carbides and matrix. As expected, carbides exhibit a typical elastic behaviour, while matrix alloy shows some plasticity. The scanning

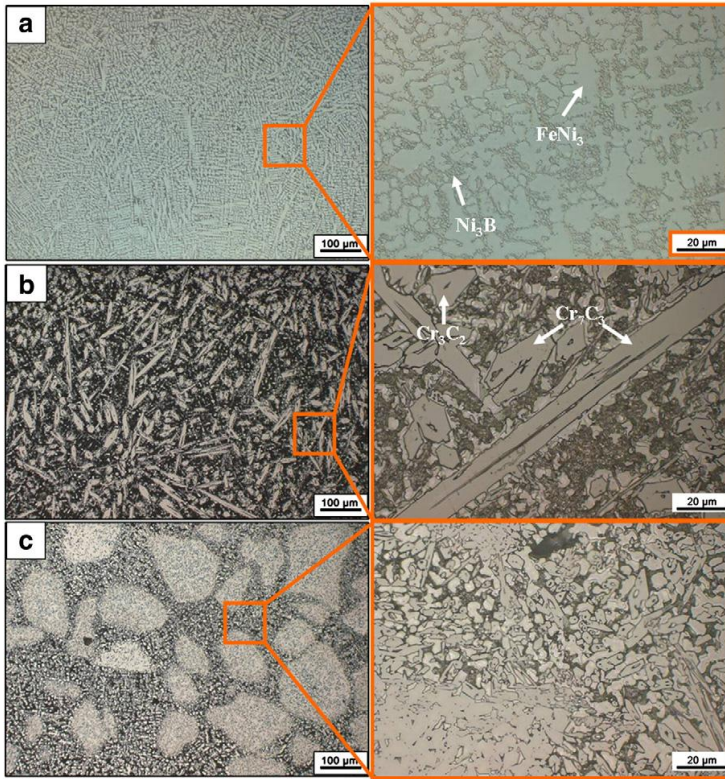


Fig. 4. OM cross-sectional images of the hardfacings: a) NiCrBSi matrix; b) Cr_3C_2 reinforced coating; c) Cr_3C_2 -Ni reinforced coating.

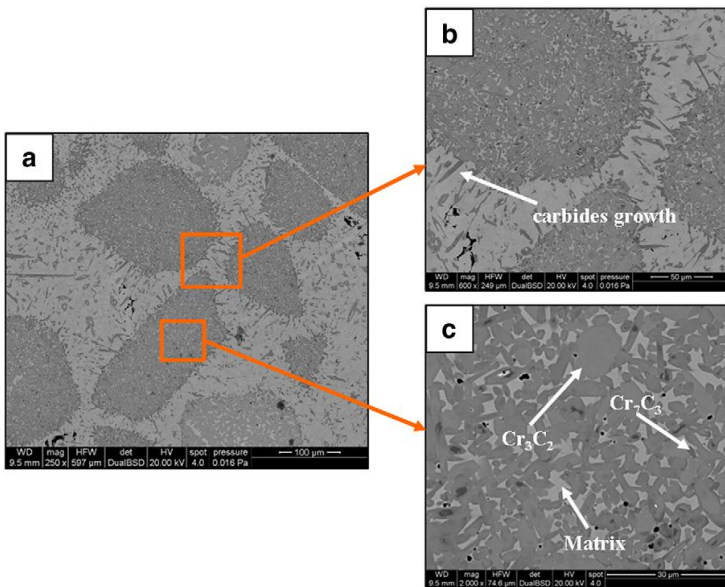


Fig. 5. SEM images of Cr_3C_2 -Ni particle reinforced NiCrBSi hardfacing: a) overview; b) interface between particles and matrix; c) inner structure of the particles.

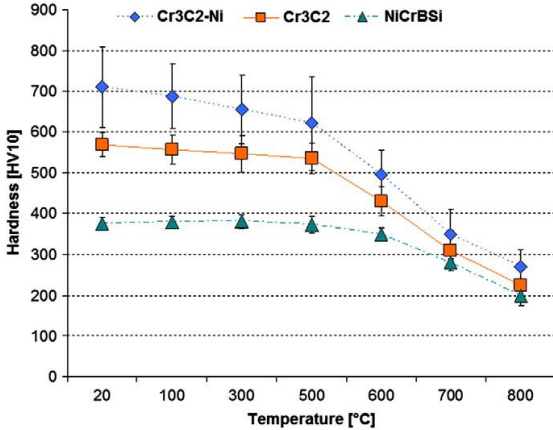


Fig. 6. Hot hardness distribution curves for “Cr₃C₂” – coating reinforced with standard Cr₃C₂ particles; “Cr₃C₂-Ni” – coating reinforced with cermet particles; “NiCrBSi” – NiCrBSi matrix hardfacing.

probe microscopy (SPM) image of a residual indent (Fig. 7b) demonstrates that there is no significant pile-up around the indentation site of the carbides, confirming that the Oliver and Pharr method [22] yields valid estimates of the contact area and, therefore, provides reliable parameters for the hard particles.

The bubble chart of reduced modulus of elasticity vs. hardness for the constituents in Cr₃C₂ reinforced coating is shown in Fig. 8a. A mean nanoindentation hardness of 5.5 ± 1.2 GPa and a reduced elastic modulus varying between 250 and 300 GPa were measured in the matrix phase. The rather high hardness of the matrix phase can be explained by extensive carbide precipitations resulting in isolated or agglomerated groups of small particles that serve as the dispersion strengthening particulates to harden the matrix alloy. Also, due to solid solution strengthening generated by extensive carbide dissolution during PTA cladding, chromium and carbon distort the nickel lattice, inhibiting the motion of dislocations [22]. In Fig. 8a “Cr₃C₂” corresponds to undissolved Cr₃C₂ particles which are found in the matrix. Those phases show a compact distribution of the measured values of both hardness and elastic modulus with average values of 25 ± 1.5 GPa for hardness and 274 ± 11 GPa for reduced Young’s modulus. “M7C₃” corresponds to the re-precipitated spine-like hard-phases which show a high spread of the measured values, probably

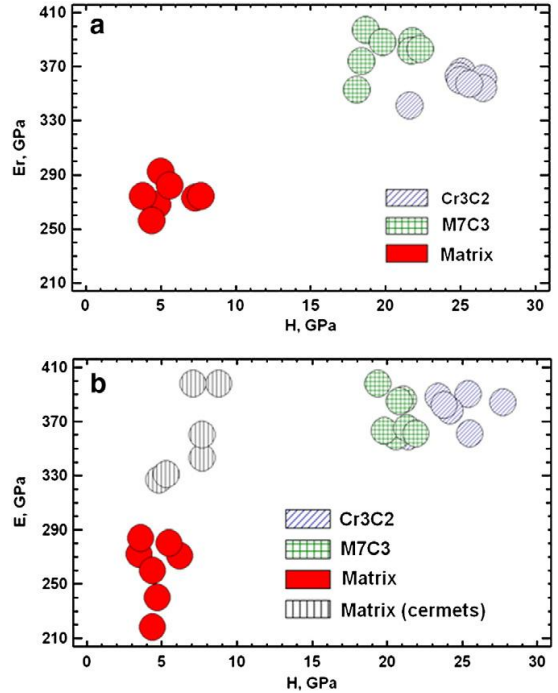


Fig. 8. a) Nanoindentation measurements for Cr₃C₂ reinforced coating; b) nanoindentation measurements for Cr₃C₂-Ni reinforced coating.

due to partially completed re-precipitation processes and the presence of undissolved carbides. It should be noted that these nanoindentation values have a good correlation with the previously reported data [27,28], where Cr₃C₂ polymorphs were shown to exhibit a higher hardness compared to Cr₇C₃.

Nanoindentation results obtained for the Cr₃C₂-Ni reinforced coating are presented in Fig. 8b. The hardness values of the matrix phase are comparable with the matrix values for the Cr₃C₂ reinforced coating, indicating similar processes of matrix development during PTA cladding. The wide data spread can be explained with substantial microstructural and compositional variations in the as-sprayed coatings, e.g.

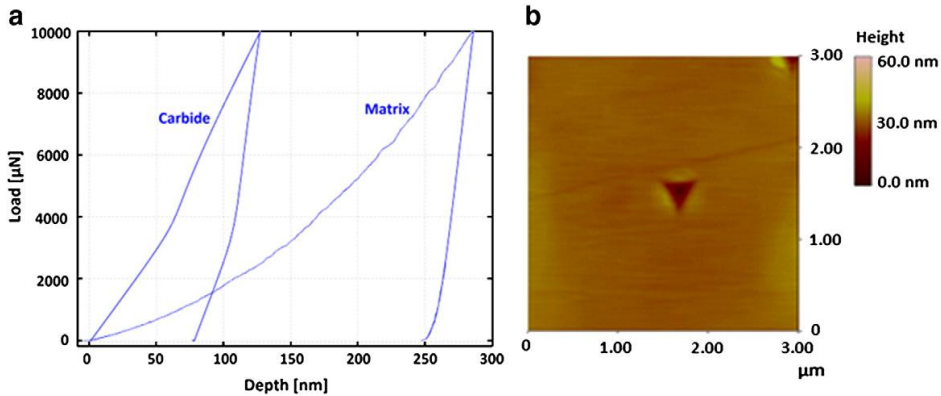


Fig. 7. a) Typical experimental load-displacement curve of matrix and carbide particles in coating; b) SPM image of the nanoindentation imprint in ceramic phase.

visibly less precipitation content in the matrix due to minimal dissolution of chromium carbides. In Fig. 8b “Matrix (cermet)” corresponds to the binder phase in the cermet particles. Both hardness and reduced modulus are higher for the nickel based matrix in the cermet particles compared to those in the coatings’ matrix. This could reflect an increase in the effective hardness due to the small mean free path between carbides of the constrained material. The high degree of contiguity of carbide particles results in a higher hardness of the material. The wide data scatter can be explained by diffusion of chromium and carbon into the binder matrix and inhomogeneous distribution of solute elements throughout the matrix [24]. The primary chromium hardphases Cr_3C_2 have a mean reduced Young’s modulus of 378 ± 13 GPa and a hardness range from 21 GPa up to 28 GPa. This high spread of hardness values can be attributed to the presence of Cr_7C_3 particles (which appear during sintering of the C_3C_2 -Ni bulk as a result of decarburisation of Cr_3C_2 [23,24]) that are undistinguishable under SPM while they differ in properties. “M7C3” corresponds to the apparent phase of re-precipitated spine-like hardphases and the values are comparable to those found in the Cr_3C_2 reinforced coating.

The results obtained by nanoindentation measurements reveal no significant difference between the mechanical properties of both (Cr_3C_2 and Cr_3C_2 -Ni) reinforced hardfacings for matrix region. However, the presence of inter-metallic phase “Matrix (cermet)” in Cr_3C_2 -Ni reinforced hardfacing may lead to the considerably different wear behaviour of this coating.

3.4. Impact-abrasive wear of the coatings

It is well known that abrasive wear behaviour is mainly influenced by material hardness and microstructural features [1,21,29]. However, in conditions where impact loading is a dominating factor, increased plasticity and fine particle hardphases uniformly distributed in the matrix result in improved wear resistance [21]. Therefore, it can be assumed that hardfacings reinforced with chromium carbide based cermet particles could be an alternative to the commercially used tungsten carbide reinforced coatings, especially at temperatures exceeding 500 °C.

The impact-abrasive wear behaviour of the hardfacings has been evaluated using the HT-CIAT technique [21]. Tests were conducted at different temperatures to study the effect of temperature on wear performance of the materials. Fig. 9 shows the volumetric wear of the coatings tested at room temperature, 300 °C, 550 °C and 700 °C.

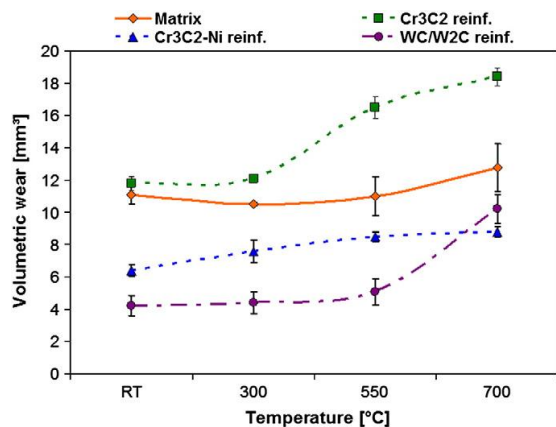


Fig. 9. Impact-abrasive wear of the tested coatings: “Matrix” – NiCrBSi matrix without reinforcement; “ Cr_3C_2 reinf.” – coating reinforced with standard Cr_3C_2 particles; “ Cr_3C_2 -Ni reinf.” – coating reinforced with cermet particles; “WC/W₂C reinf.” – NiCrBSi matrix reinforced with 60 wt.% WC/W₂C particles.

A commercially used multiphase coating with NiCrBSi matrix and 60 wt.% of fused WC/W₂C hardphases was taken as a reference material. Properties and wear behaviour of the reference material are described elsewhere [30].

The wear behaviour of the NiCrBSi matrix without any reinforcement was also evaluated (labelled as “Matrix” in Fig. 9; chemical composition is described in Section 2.1). This alloy shows relatively constant volumetric wear up to 550 °C testing temperature. The increase of wear at a temperature of 700 °C reflects the softening of the metallic matrix resulting in more pronounced abrasive attack. The reinforcement of NiCrBSi matrix with Cr_3C_2 hardphases results in a slight increase in volumetric wear at temperatures up to 300 °C. At higher temperatures the wear rate rapidly increased up to a maximum value of ~ 18 mm³ at 700 °C.

The lowest volume loss was found for NiCrBSi matrix reinforced with Cr_3C_2 -Ni tested at all temperatures under consideration. Relatively small increase in wear loss was detected with increase in testing temperature up to 700 °C (Fig. 9), still wear resistance was twice higher compared to Cr_3C_2 reinforced coatings. The better performance of the reference hardfacing (60 wt.% WC/W₂C in Ni-basis) at temperatures below 700 °C is obvious, however, at the highest testing temperature the volumetric wear is increased by $\sim 20\%$ as compared to Cr_3C_2 -Ni cermet reinforced coatings due to excessive oxidation and rapid degradation of the material. It should be outlined that at high testing temperatures the surface oxidation processes and formation of mechanical mixed layers significantly influence the wear behaviour. SEM investigation has revealed the presence of oxides on the surface of all investigated hardfacings. In fact, the detailed analysis and discussion on the oxidation behaviour of Cr_3C_2 -Ni reinforced hardfacings are topics of another research.

The performance of chromium carbide reinforced coatings in high temperature applications is strongly affected by the developed microstructure [18]. Processing routes allowing minimisation of carbide dissolution are expected to produce composites with effective wear resistance at high temperatures. The cermet particles reinforced coatings exhibit improved wear resistance under impact/abrasion conditions because of the fine carbides in un-dissolved Cr_3C_2 and Cr_7C_3 and the short mean free path length in the cermet particles, which are uniformly distributed throughout the metallic matrix and acting effectively as large reinforced inclusions.

SEM micrographs in Fig. 10 show the worn surface of the coatings after HT-CIAT testing at room temperature. The main wear mechanism identified in Cr_3C_2 reinforced coatings (Fig. 9a) is extensive plastic deformation with large flakes and pile-ups of laterally displaced material. The ductility of the matrix increased with temperature and the material as a whole exhibits predominantly plastic deformation. The increase in wear rate at temperatures of 550 °C and 700 °C is in a good agreement with softening effects of the matrix and with the hot hardness results [30].

For the homogeneously distributed cermet particles (Cr_3C_2 -Ni) in the NiCrBSi matrix less plastic deformation of the matrix can be detected on the worn surface (Fig. 10b). Furthermore, the cermet particles show only local damage and brittle carbide fracture or intergranular cracking are evident only within the impact site. Hardphases themselves tend to remain in their original form (marked in Fig. 10b) serving as effective reinforcements preventing severe deformation and chipping of the matrix and resulting, therefore, in an increase in wear resistance of the coating. Cracks which appear during cyclic impact can affect the hardfacing only locally inside the few micro sized carbides. Another reason for increased wear resistance can be correlated with the properties of the matrix inside the cermet phase. Hardfacings reinforced with Cr_3C_2 -Ni show less carbides “pulling out” because the mechanical properties of the metallic binder in the Cr_3C_2 -Ni reinforcing particles are very close to the mechanical properties of the NiCrBSi matrix, as was detected by nanoindentation measurements.

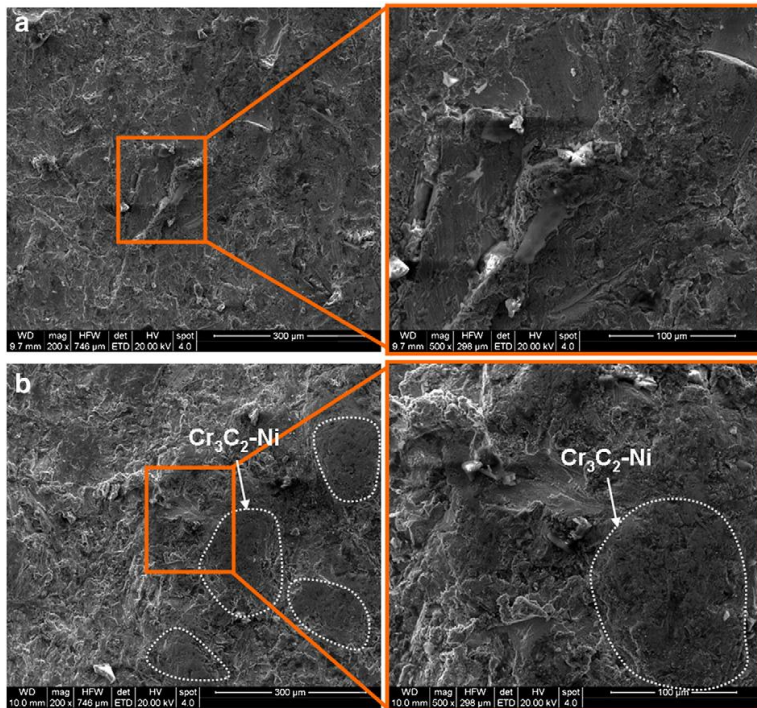


Fig. 10. Worn surface of hardfacings at room temperature: a) Cr_3C_2 reinforced coating; b) $\text{Cr}_3\text{C}_2\text{-Ni}$ reinforced coating.

4. Conclusions

Based on the study within this work, the following conclusions can be drawn:

1. Chromium carbide-based cermet particles can be successfully applied to the fabrication of wear resistant hardfacings using the PTA technology.
2. Minimal carbide dissolution occurs during PTA processing of the composite hardfacings reinforced from cermet particles. The resulting coating is characterised by homogeneous distribution of cermet particles throughout the matrix.
3. In spite of comparable mechanical properties of the Cr_3C_2 and $\text{Cr}_3\text{C}_2\text{-Ni}$ reinforced hardfacings, the distinctly different microstructures result in different wear behaviours of the coatings.
4. The coatings developed are an attractive candidate material for high temperature applications. The wear rate at 700 °C is lower for the $\text{Cr}_3\text{C}_2\text{-Ni}$ reinforced hardfacing as compared to the commercially used $\text{WC/W}_2\text{C}$ reinforced NiCrBSi coating. At the same time the wear resistance of the $\text{Cr}_3\text{C}_2\text{-Ni}$ reinforced coating shows high temperature stability up to 700 °C with negligible wear rate growth.

It also has to be mentioned that further process optimisation is required for the production of PTA hardfacings with high reliability.

Acknowledgements

This work was funded by the “Austrian Comet-Program” (governmental funding program for pre-competitive research) via the Austrian Research Promotion Agency (FFG) and the TecNet Capital GmbH (Province of Niederösterreich) and has been carried out within the “Austrian Centre

of Competence for Tribology” (AC2T research GmbH) in cooperation with Tallinn University of Technology under ESF grant N 8211. This work has been also partially supported by graduate school “Functional materials and technologies” receiving funding from the European Social Fund under project 1.2.0401.09-0079 in Estonia. It was also partially supported with EFRE funding within the project “OnLab”.

The authors are also grateful to Dr. A. Gavrilović from CEST competence centre and Dipl.-Ing. S. H. Gerdehi from TU Vienna for their help with XRD and SEM analyses.

References

- [1] I. Hussainova, I. Jasiuk, M. Sardela, M. Antonov, *Wear* 267 (2009) 152.
- [2] M. Antonov, I. Hussainova, R. Veinthal, J. Pirso, *Tribol. Int.* 46 (2012) 261.
- [3] M. Stack, M. Antonov, I. Hussainova, *J. Phys. D: Appl. Phys.* 39 (2006) 3165.
- [4] S. Matthews, B.B. James, M. Hyland, *Wear* 203 (2009) 1144.
- [5] M. Roy, A. Pauschitz, R. Polak, F. Franek, *Tribol. Int.* 39 (2006) 29.
- [6] N. Espallargas, J. Berget, J.M. Guilemany, A.V. Benedetti, P.H. Suegama, *Surf. Coat. Technol.* 202 (2008) 1405.
- [7] D.E. Wolfe, T.J. Eden, J.K. Potter, A.P. Jaroh, *J. Therm. Spray Technol.* 15 (2006) 400.
- [8] J. Wilden, J.P. Bergmann, H. Frank, *J. Therm. Spray Technol.* 15 (2006) 779.
- [9] B.G. Mellor, *Surface Coatings for Protection against Wear*, Woodhead Publishing Limited, Cambridge, 2006.
- [10] J.F. Flores, A. Neville, N. Kapur, A. Gnanavelu, *Wear* 267 (2009) 213.
- [11] R.L. Deuis, J.M. Yellup, C. Subramanian, *Compos. Sci. Technol.* 58 (1998) 299.
- [12] C. Katsich, E. Badisch, *Surf. Coat. Technol.* 206 (2011) 1062.
- [13] J. Nurminen, J. Nötkki, P. Vuoristo, *Int. J. Refract. Met. Hard Mater.* 27 (2009) 472.
- [14] Y.P. Kathuria, *Surf. Coat. Technol.* 140 (2001) 195.
- [15] Z. Dawei, T. Li, T.C. Lei, *Surf. Coat. Technol.* 110 (1998) 81.
- [16] Z. Dawei, T.C. Lei, F.J. Li, *Wear* 251 (2001) 1372.
- [17] Z. Huang, Q. Hou, P. Wang, *Surf. Coat. Technol.* 202 (2008) 2993.
- [18] S. Matthews, B. James, M. Hyland, *Corros. Sci.* 51 (2009) 1172.
- [19] S. Matthews, M. Hyland, B. James, *Acta Mater.* 51 (2003) 4267.
- [20] A. Zikin, I. Hussainova, H. Winkelmann, P. Kulu, E. Badisch, *Int. J. Heat Treat. Surf. Eng.* 6 (2012), <http://dx.doi.org/10.1179/1749514811Z.0000000004>.
- [21] H. Winkelmann, E. Badisch, M. Kirchgaßner, H. Danning, *Tribol. Lett.* 34 (2009) 155.

- [22] G.M. Pharr, W.C. Oliver, F.R. Brotzen, *J. Mater. Res.* 7 (1992) 613.
- [23] J. Pirso, M. Viljus, S. Letunovits, K. Juhani, *Int. J. Refract. Met. Hard Mater.* 24 (2006) 263.
- [24] I. Hussainova, I. Jasiuk, X. Du, M. Antonov, *Int. J. Mater. Prod. Technol.* 40 (2011) 58.
- [25] I. Hussainova, J. Pirso, M. Antonov, K. Juhani, S. Letunovits, *Wear* 263 (2007) 905.
- [26] I. Hussainova, E. Hamed, I. Jasiuk, *Mech. Compos. Mater.* 46 (2011) 667.
- [27] C. Jiang, *Appl. Phys. Lett.* 92 (2008) 041909.
- [28] K. Hirota, K. Mitani, M. Yoshinaka, O. Yamaguchi, *Mater. Sci. Eng.* 399 (2005) 154.
- [29] I. Hussainova, M. Antonov, *Int. J. Mater. Prod. Technol.* 28 (2007) 361.
- [30] H. Winkelmann, E. Badisch, M. Varga, H. Danninger, *Tribol. Lett.* 37 (2010) 419.

PUBLICATION III

Zikin, A., Badisch, E., Hussainova, I., Tomastik, C., Danninger, H.,
Characterisation of TiC-NiMo reinforced Ni-based hardfacing, *Surf. Coat.
Technol.* In press. DOI: <http://dx.doi.org/10.1016/j.surfcoat.2013.02.027>³

³ Copyright 2013, reprinted with permission from Elsevier



Contents lists available at SciVerse ScienceDirect

Surface & Coatings Technology

journal homepage: www.elsevier.com/locate/surfcoat

Characterisation of TiC–NiMo reinforced Ni-based hardfacing

A. Zikin^{a,b,*}, E. Badisch^a, I. Hussainova^b, C. Tomastik^a, H. Danninger^c^a AC2T research GmbH, Excellence Centre of Tribology, Viktor-Kalpan-Straße 2D, 2700 Wiener Neustadt, Austria^b Department of Materials Engineering, Tallinn University of Technology (TUT), Ehitajate tee 5, 19086 Tallinn, Estonia^c Institute of Chemical Technologies and Analytics, Vienna University of Technology, Getreidemarkt 9/164-CT 1060 Wien, Austria

ARTICLE INFO

Available online xxxx

Keywords:

Hardfacing

PTA

Cermet

Nanoindentation

Scratching

Three body abrasion

ABSTRACT

In the present study, TiC–NiMo composites were remilled to particle size of 250–315 μm and used as reinforcements for NiCrBSi alloy by plasma transferred arc hardfacing process. The manufactured hardfacing alloy was characterised in terms of microstructure, mechanical properties and abrasive wear resistance. Deposition results indicate good quality thick coating with uniform distribution of hard cermet (TiC–NiMo) particles in the matrix, minimum level of hard particle dissolution and low porosity of the hardfacing. Cermet particles remain in initial form and consist of agglomerates (TiC and (Ti,Mo)C grains) embedded into Ni-based matrix. The mechanical properties of the TiC and (Ti,Mo)C phases measured by nanoindentation are very similar exhibiting a narrow distribution. The nano-scratching test reveals excellent bonding between the matrix and cermets in the hardfacing. No crack propagation was found in the interface matrix/hard phase region.

The abrasive wear results ensure the promising features of TiC–NiMo reinforcements for Ni-based alloys. Produced coatings showed excellent performance under high-stress abrasion with wear values lower than for industrially used WC/W₂C reinforced coatings.

© 2013 Elsevier B.V. All rights reserved.

1. Introduction

Coatings and surface treatments have proved to be a successful approach for increasing machinery lifespan by preventing severe wear and corrosion of working tools [1–3]. One of the attractive surface treatment methods is hardfacing by welding technique. This method offers the ability to apply thick protective coatings metallurgically bonded to the substrate material. Many hardfacing techniques such as laser cladding, gas-tungsten arc welding (GTAW), gas-metal arc welding (GMAW) and plasma transferred arc (PTA) are widely employed for deposition of a protective layer on a surface of a bulk material subjected to severe working conditions [4–6]. The most common coatings applied by hardfacing are metal matrix composites (MMCs) consisting of Ni, Co or Fe-based matrix, and reinforced with hard ceramic particles such as tungsten carbides [5,7,8]. Tungsten carbide based hard metals are widely used in tribo-conditions because of their high abrasion and combined impact/abrasion wear resistance [9,10]. However, due to their poor oxidation resistance at elevated temperatures, WC-based composites are a less than ideal choice for tooling parts exposed to temperatures exceeding 550 °C [11].

Titanium carbide (TiC) can be considered as an attractive reinforcement for MMCs because of its high hardness, quite low density,

good oxidation resistance and high wear resistance in erosion and abrasion environments [12–15].

Several attempts have been made to apply titanium carbide powders by hardfacing using different processing methods. For the powder feeding method, TiC-based powder and metal matrix powder are delivered into the laser or plasma beam, melted and deposited onto the substrate [4,5,16]. This method enables a uniform distribution of primary hard phases in the matrix and results in low carbide dissolution. Alternative methods include mixing TiC and metal matrix, pre-placing the powder mixture on the surface of the substrate with the help of an organic binder and forming a coating layer to be clad [17,18]. The coatings deposited by these techniques are mostly characterised by formation of a gradient distribution of hard phase and are highly affected by dilution and its influence on the microstructure of the final product.

A promising method for the reinforcement of metal matrix with TiC particles using laser cladding involves in-situ synthesis of TiC by reaction of titanium and graphite during laser processing [19,20]. Such hardfacings are characterised by excellent metallurgical bonding between the coating and the substrate and the high quality of the deposited material. However, because of TiC's low density, a uniform distribution of hard phases is not easily achieved. During solidification, the TiC particles show a gradient distribution in the matrix with respect to size and volume fraction [20].

Although titanium carbides are widely applied as reinforcements using different cladding technologies, there is a lack of information about processing of recycled TiC-based cermets as reinforcements for a nickel-based matrix with the PTA process.

* Corresponding author at: AC2T research GmbH, Excellence Centre of Tribology, Viktor-Kalpan-Straße 2D, 2700 Wiener Neustadt, Austria. Tel.: +43 2622 81600 322; fax: +43 2622 81600 99.

E-mail address: zikin@ac2t.at (A. Zikin).

In the present study, titanium carbide reinforced hardfacings have been produced by the PTA technique using the powder feeding method. The precursor materials used were re-milled TiC-20% Ni:Mo (2:1) cermet added into the NiCrBSi matrix alloy. The coatings have been deposited onto an austenitic steel substrate. The main objectives of the work were: (i) to deposit NiCrBSi hardfacing coatings reinforced by TiC–NiMo cermet particles; (ii) to examine the microstructure and mechanical properties of the developed hardfacings; and (iii) to study the wear resistance of the coatings under three body abrasive wear conditions.

2. Experimental details

2.1. Powders

Pre-processed powder of titanium carbide based and nickel-molybdenum bonded cermet particles was used in the present study. These cermet particles were re-milled from the bulk of TiC-20 wt.% Ni:Mo (2:1) and then sieved to obtain the fraction 150... 310 μm using collision milling method. To obtain cermet particles with the predetermined granulometry, multistage milling (up to 16 times) was used [21]. A representative SEM micrograph of the powder is shown in Fig. 1. NiCrBSi alloy powder (0.2% C, 4% Cr, 1% B, 2.5% Si, 2% Fe, rest Ni) with particle size of 50 ... 150 μm was used as a matrix material for the PTA process.

2.2. Plasma transferred arc hardfacing

PTA hardfacing of TiC–NiMo particles in combination with NiCrBSi matrix was carried out using a EuTronic® Gap 3001 DC apparatus. Austenitic stainless 1.4301 steel was used as a substrate. The coating thickness was set to 2.0–2.5 mm. The coating of the identical matrix alloy with the same volume percentage of WC/W₂C reinforcements (Castolin Eutectic EuTroLoy PG 6503 alloy) was used as reference material for the wear testing.

2.3. Characterisation

Prior to testing, the samples were cut from large pieces, ground and subsequently polished using 1 μm diamond paste. A comprehensive microstructural evaluation of the plasma hardfacing was performed by optical microscopy (OM) with a digital camera (MEF4A, Leica Microsystem) and scanning electron microscopy (SEM Philips XL 30 FEG), equipped with an energy dispersive X-ray analyser (EDX) with Dual BSD detector and operating at an accelerating voltage of 20 kV. For EDX quantification the standardless EDAX ZAF quantification method was used. The microstructural examination (OM) was conducted on the samples etched with a solution of HF and HNO₃ in volume ratio 1:12 at room temperature for 2 s.

X-ray diffraction (XRD) experiments were performed on an X-Pert nanodiffractometer (PANalytical, Netherlands) in continuous mode using CuK α radiation in Bragg–Brentano geometry at 40 kV and 30 mA. The diffractometer was equipped with a secondary graphite monochromator, automatic divergence slits and a scintillation counter.

The hardness was determined by standard Vickers hardness testing at a load of 50 kgf (HV50). Average hardness values were calculated from 8 indents per specimen. The choice of such a high load was conditioned by the microstructural features of multiphase hardfacings, where under load of 10 kgf (10HV) a large scatter of hardness values for similar multiphase structures was obtained [22].

To evaluate the mechanical properties of constituent phases, nanoindentation measurements were performed using a Hysitron Triboindenter TI900 (Minneapolis, MN, USA) equipped with a diamond Berkovich indentation tip with 100 nm tip radius. The load cycle comprised loading for 5 s to reach the peak load of 10 mN and subsequent unloading for 5 s. The load vs. depth curves were analysed to determine the reduced elastic modulus and hardness using the procedure described elsewhere [23].

Nano-scratch testing was also performed with the Hysitron Triboindenter TI900 using the Berkovich tip as described above. The load during the scratches was set to a constant value of 5 mN. The length of all scratches was 20 μm with a scratch rate of 0.2 $\mu\text{m}/\text{s}$.

2.4. Wear testing

The abrasive wear performance was evaluated using three-body abrasion tester by variation of testing conditions: a) use of a dry-sand rubber wheel according to ASTM G65 requirements; b) application of a steel wheel to simulate high-stress wear behaviour of materials. Rotation speed, normal load and sliding distance were kept constant at 200 rpm, 130 N and 4309 m, respectively. Ottawa silica sand with particle size of 212–300 μm was used as abrasive. Before and after testing each specimen was cleaned with acetone, dried and weighed. At least three tests were run for each material to determine the wear resistance.

3. Results and discussion

3.1. Deposition

Deposits of the TiC–NiMo and NiCrBSi alloy powders in the ratio of 40:60 vol.% were processed onto an austenitic stainless steel substrate. The selection of proportion for PTA hardfacings can be attributed to the low density of TiC-based reinforcements, where 40 vol.% of hard phases was suggested to be optimal for uniform hard particles distribution [24].

Two separately controlled powder feeders were used for the adjustment of the required powder ratio. The powders were transported

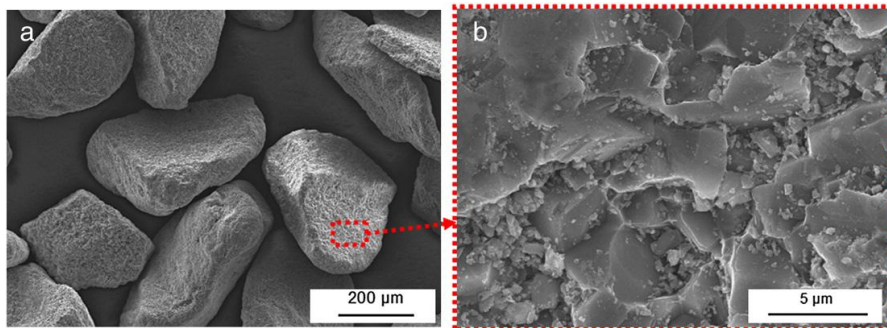


Fig. 1. SEM images of TiC–NiMo particles: (a) overview; (b) surface of the particle.

internally through the welding torch with the help of a carrier gas and then introduced into a molten weld pool which after solidification formed a metallurgically bonded layer on the surface of the base metal as schematically shown in Fig. 2.

Optimised hardfacing process parameters are listed in Table 1. The parameters of deposition of TiC–NiMo phase are influenced by certain porosity; high welding energy (welding current up to 100 A and high plasma gas flow rate) is required to overcome this problem and minimise porosity level in a welding seam. Due to low density of TiC–NiMo reinforcements ($\sim 5.5 \text{ g/cm}^3$), which is significantly lower than density of nickel-based alloy ($\sim 8.5 \text{ g/cm}^3$), cermet particles float upward in the molten pool during solidification and almost no cermet particles remain at the close proximity to a coating base. The high carrier gas flow and pressure rates were found to improve the distribution of hard particles during deposition.

Fig. 3 illustrates the TiC–NiMo reinforced NiCrBSi weld overlay. The OM examination reveals a uniform distribution of hard phases in the matrix, negligible porosity of the hardfaced layer and overall good quality of the welding seam with minimal dilution with the substrate of less than 5% according to the quantitative analysis. The obtained coating seems to be metallurgically well bonded to the austenite substrate.

3.2. Microstructural analysis

Fig. 4 illustrates the microstructure of the cermet particle reinforced hardfacing. The following apparent phases were detected: dendritic Ni-based matrix, TiC-based precipitates of less than $2 \mu\text{m}$ in diameter, and TiC–NiMo cermet grains. Both hard phases were homogeneously distributed throughout the matrix. The nickel binder in the cermet particles is assumed to protect the primary carbides from dissolution.

The XRD pattern of TiC–NiMo reinforced NiCrBSi hardfacing is presented in Fig. 5. The analysis reveals five crystalline phases: Ni-rich dendritic matrix – $\gamma(\text{Fe,Ni})$; $(\text{Fe, Ni, Mo})_{23}\text{B}_6$, which is the most probable Fe–Ni–B hard phase located in dendrites with some traces of Mo in the crystal lattice; TiC phase; non-stoichiometric carbide $\text{Ti}_{0.92}\text{Mo}_{0.02}\text{C}_{0.6}$; and $(\text{Mo, Ti})\text{C}$. Formation of solid solutions of Mo in the TiC lattice results in development of so-called core-rim

Table 1
Main parameters of PTA processing.

Parameter	Value
Welding current	80–100 A
Oscillation speed	20–25 mm/s
Oscillation width	20 mm
Welding speed	1.0–1.2 mm/s
Substrate material	Austenitic steel (1.4301)
Substrate thickness	5 mm
Distance torch/part	8 mm
Plasma gas	Ar; 1.7 l/m
Shielding gas	Ar/H ₂ ; 15 l/m
Carrier gas	Ar/H ₂ ; 2 l/min

structured grains consisting of a TiC core surrounded by the rim of $(\text{Ti,Mo})\text{C}$ [25–27].

Fig. 6 presents SEM micrographs of the TiC–NiMo reinforced hardfacing. The PTA welding process does not significantly influence the structure and composition of the cermet particles. However, it is found that besides a high amount of TiC-based spherical precipitates (Fig. 6d), TiC diffusing from the cermet zone to the matrix during deposition the structure of cermet particles along the interface (Fig. 6b) differs from the microstructure of the cermet particles at the core (Fig. 6c). The particles near the interface are partially dissolved showing decrease in grain size and modification in their shape. However, partially dissolved grains are still core-rim structured TiC– $(\text{Ti,Mo})\text{C}$ particles as confirmed by the EDX analysis of spots 1 and 2 indicated in Fig. 6b and c and shown in Table 2.

Table 2 identifies the chemical composition (wt. %) of TiC–NiMo reinforced hardfacing examined with energy dispersive X-ray (EDX) analysis. Results presented in Table 2 show average values of at least 5 spot analyses. The corresponding EDX spots are labelled with numbers in Fig. 6. Spot 1 corresponds to the core part of the TiC-based grain and shows only Ti and C, i.e. a TiC phase. Spot 2 was taken at the rim part of the TiC-based grain and shows the presence of Mo with a concentration varying between 4 and 12 wt.%. This distribution of elements, verified at approximately 5 spots taken at the rim part, confirms the presence of the $(\text{Ti,Mo})\text{C}$ phase, which according to the XRD results can be non-stoichiometric carbide

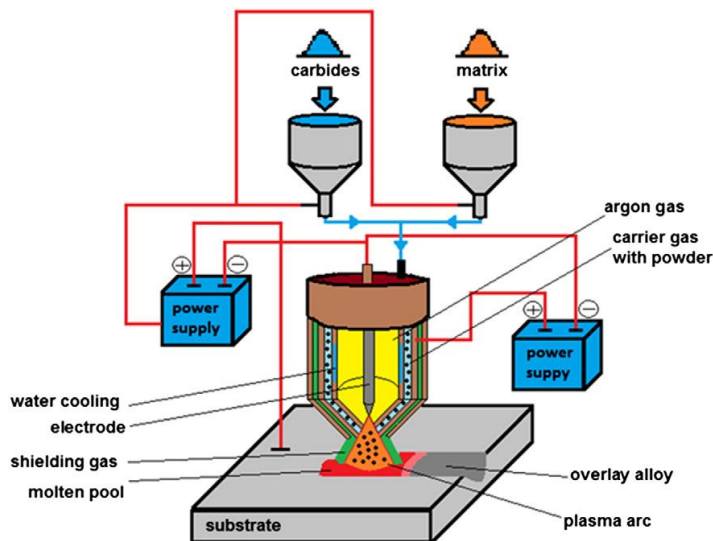


Fig. 2. Schematic representation of the PTA hardfacing process with application of two separate powder feed units.

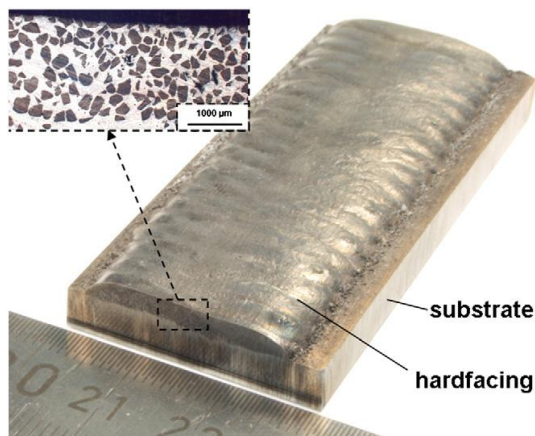


Fig. 3. Weld seam analysis of TiC–NiMo reinforced NiCrBSi hardfacing.

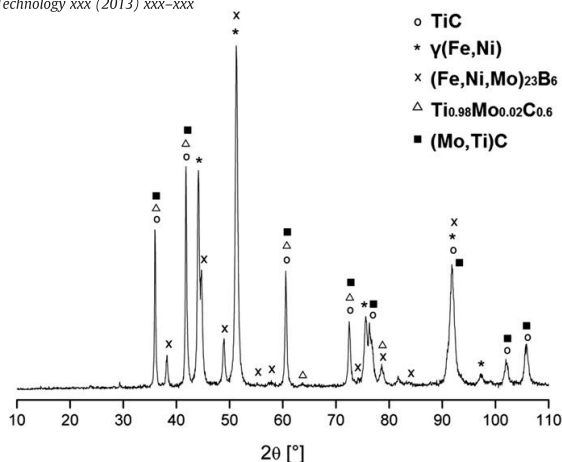


Fig. 5. XRD pattern of the TiC–NiMo reinforced NiCrBSi hardfacing.

form $\text{Ti}_{0.92}\text{Mo}_{0.02}\text{C}_{0.6}$ or in the form $(\text{Mo}, \text{Ti})\text{C}$. The binder phase inside the cermet particle can be described as a complex Ni-based matrix (spot 3 in Fig. 6). However it should be outlined that the signals from points 2 and 3 may be overlapped because of relatively low spatial resolution of the device. That can also explain the presence of Ti and Mo in the matrix. Spot 4 shows the chemical composition of the TiC-based precipitates in the matrix. An unexpectedly high Cr content was found according to EDX measurements. Most probably chromium in the form of chromium carbide diffuses from the matrix to the re-precipitated $(\text{Ti}, \text{Mo})\text{C}$ grains during the solidification process. High solubility of chromium and carbon in TiC during rapid heating/cooling process resulting in the formation of metastable phases and solid solutions at temperatures above 1500 K has been discussed in [28].

3.3. Mechanical properties

3.3.1. Hardness

The measured Vickers hardness of the pure NiCrBSi matrix was $365 \pm 15 \text{ HV}_{50}$, which is in good agreement with the previous study [22]. The macro hardness of the TiC–NiMo reinforced hardfacing is $571 \pm 25 \text{ HV}_{50}$. The hardness increase is probably due to the high content of uniformly distributed cermet particles and TiC-based precipitations.

3.3.2. Nanoindentation

Micro-mechanical properties (hardness and reduced Young's modulus) were determined by nanoindentation

measurements and statistically analysed. The reduced Young's modulus (E_r) is described by following equation:

$$1/E_r = (1-\nu_i^2)/E_i + (1-\nu_s^2)/E_s,$$

where ν is the Poisson's ratio, the index i denotes the values for the indenter tip and the index s is the ones for the sample. The indenter term for the diamond tip can be neglected in the present investigation. The elastic modulus was recalculated assuming a Poisson's ratio of 0.21 for the carbide phases and 0.3 for the matrix phases. Selected Poisson's ratios introduce an error for E of less than 10% and are found to be representative for the similar cermet materials [29].

Fig. 7 illustrates the typical load–displacement curves obtained for the different phases in the tested hardfacing. The curves are labelled correspondingly to the phases: “carbide” corresponds to the TiC phase in the cermet zone of the hardfacing (Fig. 6a; it should be noted that it was not possible to distinguish the core and rim zones using scanning probe microscopy (SPM) and, therefore, the $(\text{Ti}, \text{Mo})\text{C}$ phase is also defined as “carbide”); the label “precipit.” corresponds to the TiC-based precipitates in the matrix as shown in Fig. 6d; “dendrite” corresponds to the dendritic precipitates in the matrix, identified as complex boride phase by XRD analysis; “binder” corresponds to the complex matrix phase inside the cermet zone (Fig. 6b, c, white colour); and “matrix” corresponds to the $\gamma(\text{Fe}, \text{Ni})$ phase (Fig. 4d). The corresponding hardness and reduced Young's modulus variations for the defined phases are presented in a bubble chart in Fig. 8. Carbide and precipitate phases show similar hardness with the mean values of $33.7 \pm 1.7 \text{ GPa}$ and $32.9 \pm 2.2 \text{ GPa}$, respectively.

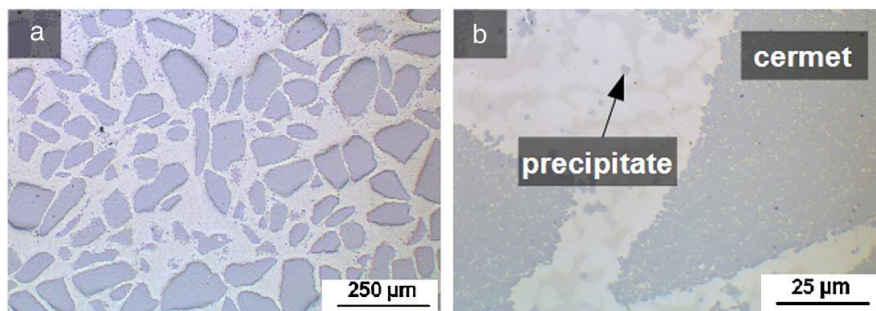


Fig. 4. OM images of the hardfacings: (a) and (b) TiC–NiMo cermet particles reinforced NiCrBSi hardfacing.

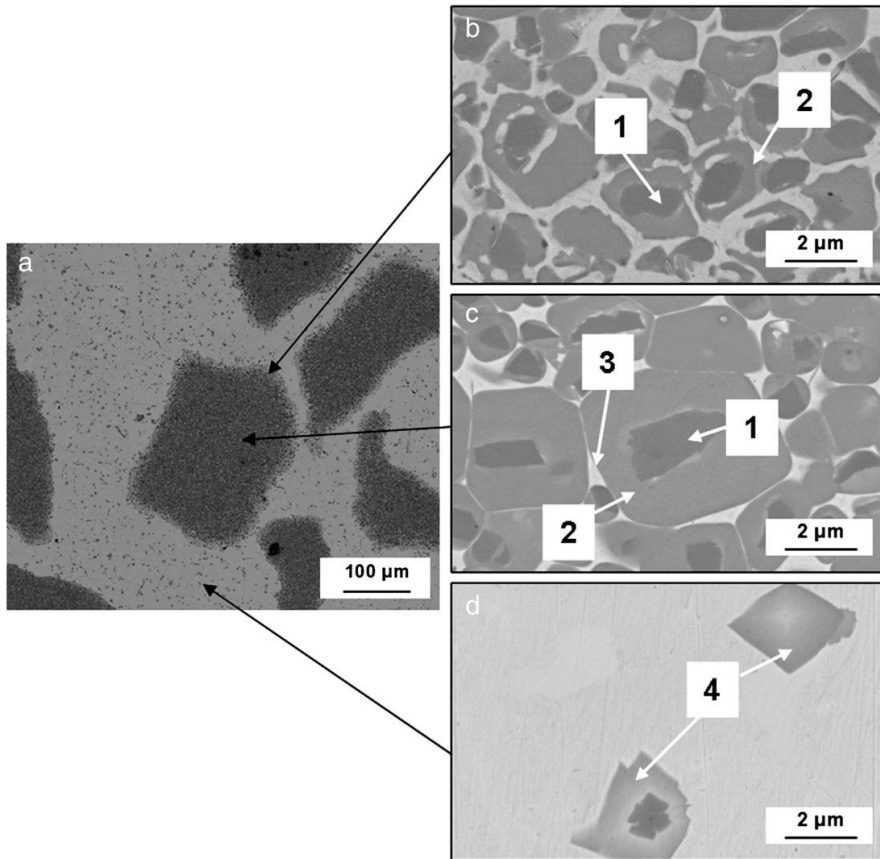


Fig. 6. SEM micrographs of the TiC–NiMo reinforced NiCrBSi hardfacing: (a) overview microstructure; (b) interphase cermet/matrix region; (c) interior of the cermet particle; (d) matrix region with TiC-based precipitates.

The measured Young's modulus for the precipitate phase varies between 275 and 330 GPa, whereas the measured Young's modulus for the carbide phase shows the mean value of 377 ± 10 GPa.

Narrow distribution of the hardness and Young's modulus results observed for the carbide phase in the bubble chart (Fig. 8) allows the conclusion that the mechanical properties of the TiC and (Ti,Mo)C phases are very similar. Previous nanoindentation investigations done on the TiC–NiMo bulk materials show comparable elastic properties of the carbides as measured in present work [30].

The measured hardness value of the binder phase is 6.6 ± 0.6 GPa, and the mean measured Young's modulus is 273 ± 10 GPa. The binder phase shows higher hardness values compared to the matrix phase with a hardness of 4.6 ± 0.2 GPa. This is in good agreement with the microstructural analysis of the deposited hardfacing, where some dissolution of TiC and Mo in the Ni binder takes place,

Table 2

Chemical composition of the TiC–NiMo reinforced hardfacing in different zones.

Spot	Ti (wt. %)	Mo	Ni	Fe	C	Cr
1	74 ± 2	–	–	–	26 ± 2	–
2	65 ± 1	8 ± 4	–	–	27 ± 5	–
3	12 ± 1	4 ± 2	64 ± 5	7 ± 2	7 ± 1	6 ± 3
4	53 ± 2	9 ± 2	10 ± 1	–	20 ± 4	8 ± 1

as shown in Table 2. However, this also leads to changes in the phase plasticity, as can be observed from the load–displacement curve in Fig. 7. The measured Young's modulus for the $\gamma(\text{Fe,Ni})$ phase is 217 ± 10 GPa, which is more than 30% lower than for the

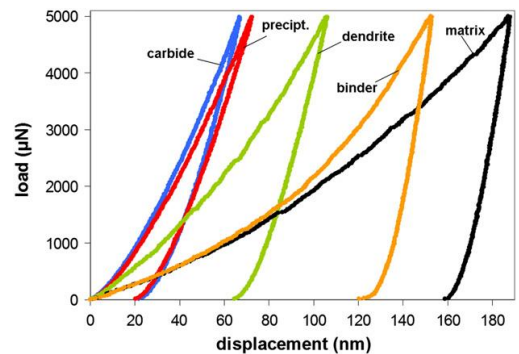


Fig. 7. Typical load–displacement curves obtained for the different phases in the tested TiC–NiMo reinforced NiCrBSi hardfacing (Designations: carbide – TiC and (Ti,Mo)C phase; precip. – TiC-based precipitates in matrix; dendrite – complex boride phase; binder – Ni-binder between carbide particles in the cermet zone; matrix – main matrix phase defined as $\gamma(\text{Fe,Ni})$).

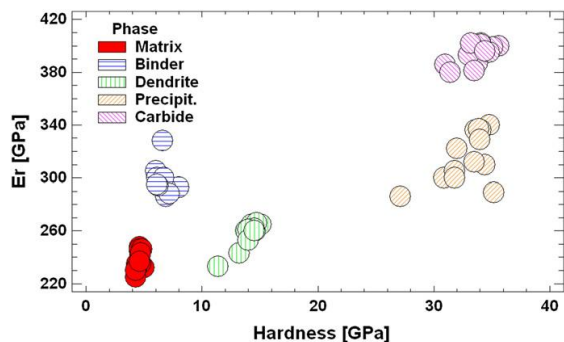


Fig. 8. Calculated modulus of elasticity (E_r) vs. hardness (H) of different phases in the TiC–NiMo reinforced NiCrBSi hardfacing measured by nanoindentation.

binder phase. However, it is worth noticing that pile-ups around the indents occurring in ductile materials influence the contact area calculations that lead to overestimation of hardness and Young's modulus.

The Fe–Ni–B hard phase labelled as “dendrite” and located in dendrites of the NiCrBSi matrix exhibits a mean hardness of 14.1 ± 0.9 GPa and calculated Young's modulus of 249 ± 10 GPa. This complex boride phase together with the TiC-based precipitates is responsible for the increased compound macro hardness of the hardfacing.

3.4. Nano-scratching

In order to characterise the response of the TiC–NiMo reinforced NiCrBSi hardfacing to initial abrasive attack, nano-scratch tests were performed. Nano-scratching of multiphase materials helps to gain knowledge and in-situ understanding of wear-related properties of hard reinforcements and metal matrices [31,32].

In the current research, a constant load nano-scratch technique was used in order to compare the damage of various phases in the composite. Nano-scratches have been performed in the matrix region to simulate scratch behaviour of matrix and TiC-based precipitates. Furthermore, the bonding behaviour of precipitations in the NiCrBSi matrix was the focus of the study. As a second step, scratch properties of the cermet particles themselves have been evaluated and correlated to matrix scratch behaviour. In each region two scratches were performed to verify consistent behaviour for each phase. The presented results are exemplary evaluations from one scratch for each region.

The SPM image of nano-scratch mark across NiCrBSi matrix and TiC-based precipitate is presented in Fig. 9. Fig. 9b traces the profiles across the scratch line. A maximum depth of ~200 nm can be seen for

the matrix scratch, whereas in the TiC-based precipitate the penetration of the indenter was measured to be ~20–30 nm. Compared to a ductile micro-ploughing mechanism in the matrix, the precipitate behaves in a less ductile micro-cutting way. The precipitate dissection of ~60 nm can be correlated to the specimen polishing procedure (Fig. 9b).

Fig. 10 shows the results of similar tests performed in the cermet zone. As mentioned before, in the present work it was not possible to separate the TiC and (Ti,Mo)C phases in the nanoindentation and nano-scratch investigation; however, the nano-scratch does not show visible variations within the carbide grain, as shown in Fig. 10a, indicating no significant mechanical differences between two phases. The presence of the Ni binder between the carbide grains highly influences the scratch. The 2D cross sections of the scratch mark clearly resolve both phases. The scratch depth differs for binder and carbide phases and was measured to be ~120–150 nm and ~20–30 nm, respectively. Comparing quantitative scratch analysis (Figs. 9 and 10) and nanoindentation measurements (Fig. 8), a good correlation can be found. For example, the scratch profiles for precipitate and carbide phases are very similar with almost the same depth. Also, the binder phase differs from the matrix phase and shows higher resistance against plastic deformation although both can be easily pulled out during scratching.

In order to investigate the hard phase/matrix bonding properties, SEM examinations were done in the scratch interface region (Fig. 11) High magnification SEM image in Fig. 11a shows a typical matrix/hard phase transition zone. In this transition zone no tendency of crack formation can be detected, which can be explained by ductile behaviour of the matrix (the matrix was ploughed) and good bonding of the hard phase to the matrix. The nano-scratch of the cermet zone is shown in Fig. 11b. Extensive binder deformation/ploughing resists crack initiation and propagation although can result in materials chipping after multiple scratch actions.

3.5. Abrasive wear behaviour

Wear tests exploiting steel and rubber wheels were carried out to reproduce three-body abrasion process. Quantitative wear analysis was performed by determination of volume loss, Fig. 12. The relative wear resistance of the TiC–NiMo reinforced hardfacing was compared to conventionally used Ni-based reference hardfacing consisting of 40 vol.% of WC/W₂C particles (Castolin Eutectic EuTroLoy PG 6503 alloy). Generally, both materials under investigation indicate low wear values; however, conventionally used tungsten carbide reinforced coating shows approximately 40% higher wear resistance.

The volumetric wear values of the materials tested with steel wheel are drawn on the abscissa. Wear of the commercially used WC/W₂C reinforced alloy is significantly increased (almost by a factor

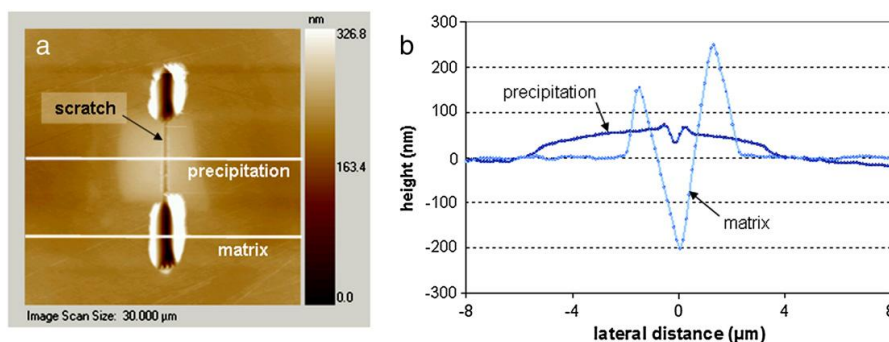


Fig. 9. Nano-scratch across NiCrBSi matrix and TiC-based precipitate at 5 mN normal load: (a) Scanning probe microscopy (SPM) image of $30 \times 30 \mu\text{m}$ (horizontal lines correspond to the 2D cross section); (b) 2D cross section profiles of the nano-scratch as measured by SPM.

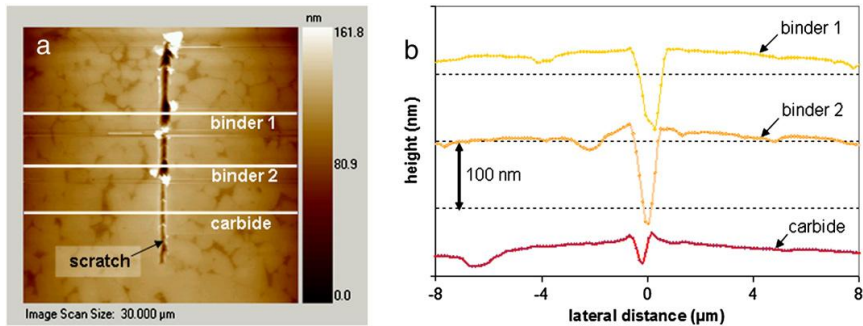


Fig. 10. Nano-scratch in cermet particle at 5 mN normal load: (a) SPM image of scratch (horizontal lines correspond to the 2D cross section); (b) 2D cross section profiles of the nano-scratch as measured by SPM.

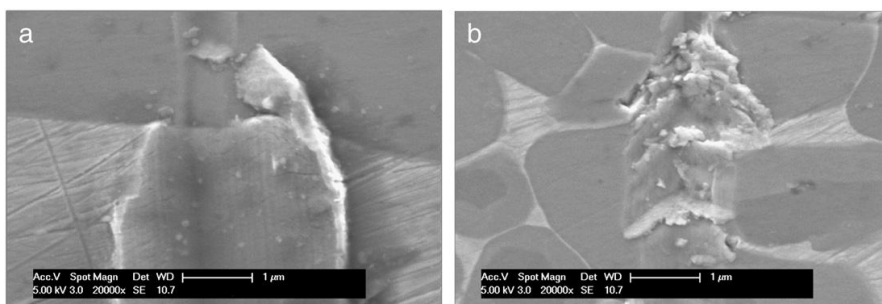


Fig. 11. High magnification SEM images of the scratch marks: (a) interface between NiCrBSi matrix and TiC-based precipitate (scratch direction bottom up); (b) scratch mark within a cermet particle.

of three), while wear of TiC–NiMo reinforced coating remains at almost the same low level.

It is well known that abrasive wear behaviour is strongly influenced by material hardness and microstructural features [33]. Under conditions of three-body abrasion several wear mechanisms can dominate depending on material of a testing wheel. Exploitation of a rubber wheel simulates low stress abrasion, while application of a steel wheel results in a high stress mode of abrasion characterised by other mechanisms of material removal as compared to mechanisms operating at low stress wear mode. To study the wear mechanisms, SEM surface sectional images of the worn areas were examined as shown in Fig. 13. High performance of WC/W₂C reinforced alloy under testing with a rubber wheel is in a good correlation with previous studies [6,7], where the high matrix hardness and dense distribution of coarse primary carbides ensure excellent wear resistance (Fig. 13a). Moreover, the secondary precipitations in matrix do not negatively influence the low-stress abrasion resistance and no cracks were detected by scanning electron microscopy. For the TiC–NiMo reinforced alloy the increase in wear rate can be attributed to low hardness of the matrix material. The titanium carbide based precipitates are small enough for successful protection of the matrix against coarse silica abrasive particles (Fig. 13c). The dominant wear mechanisms in this case are ploughing and cutting of ductile Ni-based matrix. Additionally, the inter-particle distances between cermet reinforcements are large that leads to the formation of hills in cermet supported areas of the matrix.

The behaviour of a material in a rotating wheel abrasion test depends not only on the intrinsic properties of the test piece itself, but also on the conditions of the test [34]. Application of a steel wheel can cause a significant fragmentation of abrasive particles or their embedment into the surface of base material [35]. Certain ductility

and specific microstructural arrangement are required to increase the abrasive wear resistance of multiphase materials. For the WC/W₂C reinforced hardfacing (Fig. 13b) the brittle fracture of both primary carbides and matrix precipitates was observed; extensive cracking and subsequent chip removal explain a significant increase in wear rate by a factor of three. Compared to the brittle fracture behaviour of the Ni-based reference hardfacing consisting of 40 vol.% of WC/W₂C particles, the TiC–NiMo reinforced alloy performs in a more ductile way (Fig. 13d), where no well pronounced brittle fracture of hard particles was detected; neither matrix precipitates nor cermet particles indicate extensive crack formation. These results can be also correlated with the data obtained during nano-scratching, where no cracking of hard particles was detected.

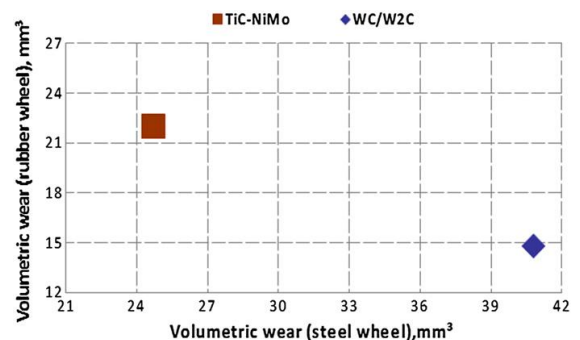


Fig. 12. Three-body abrasion volumetric wear: abscissa – steel wheel test; ordinate – rubber wheel test.

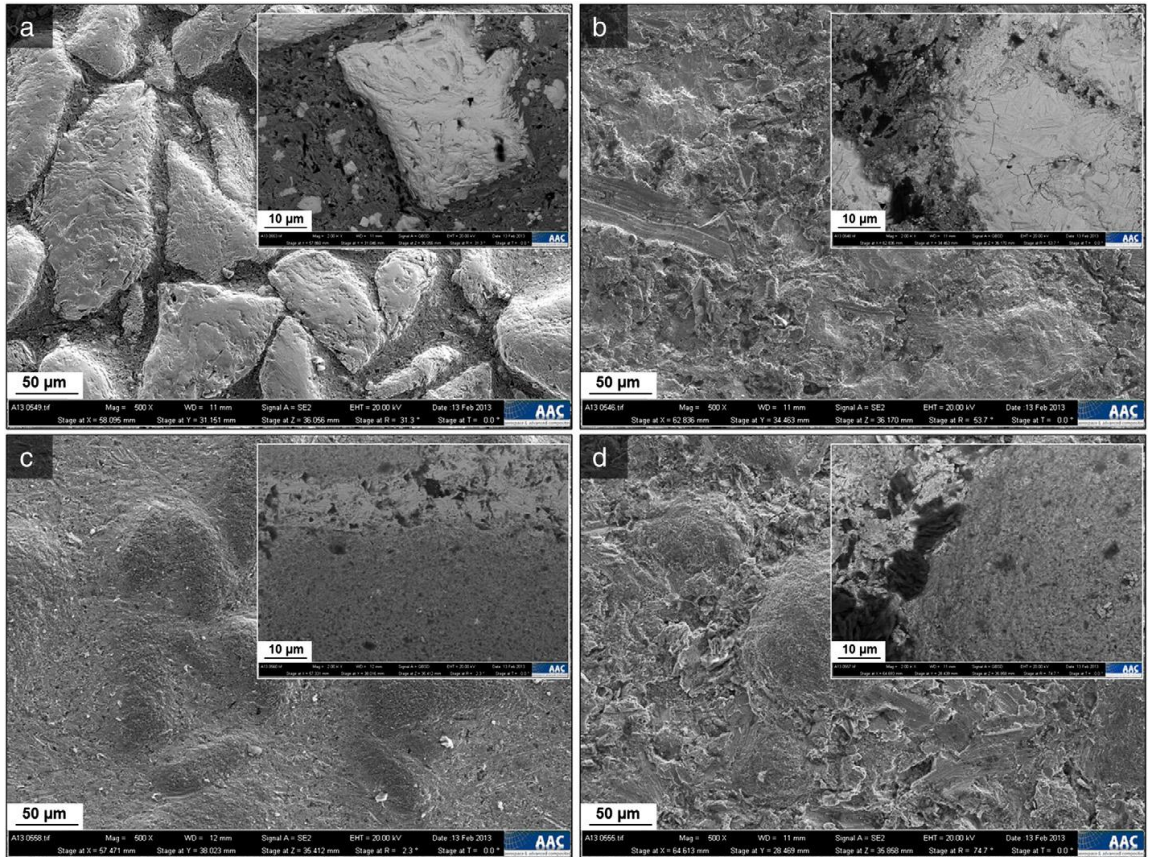


Fig. 13. SEM micrographs of worn hardfacing surfaces after three-body abrasion tests: a) and b) WC/W₂C reinforced coating – rubber and steel wheel; c) and d) TiC–NiMo reinforced coating – rubber and steel wheel.

4. Conclusions

Based on the study within this work, the following conclusions can be drawn:

- The titanium carbide based cermet particles recycled from TiC–Mo₂C–Ni composites' scrap and applied for hardfacings deposition using the PTA technology can be successfully used for deposition of thick coatings characterised by uniform distribution of constituents and low level porosity.
- The mechanical properties of the TiC and (Ti,Mo)C phases measured by nanoindentation are very similar exhibiting a narrow distribution of the hardness and Young's modulus values. Both carbide and precipitate phases indicate similar high hardness values, whereas the precipitate phase has significantly lower Young' modulus.
- The nano-scratching test reveals excellent bonding between the matrix and cermets in the hardfacing. No extensive cracking was detected in the interface matrix/hard phase region.
- The performance of the TiC–NiMo reinforced hardfacings under low stress three-body abrasion is lower as compared to the commercially used WC/W₂C reinforced coatings. Wear mechanisms operating in TiC–NiMo reinforced alloy are matrix material ploughing and cutting. Fine structured TiC-based precipitates do not provide sufficient protection against coarse abrasive particles.
- Under high-stress three-body abrasion TiC–NiMo reinforced hardfacings show significantly higher wear resistance as compared

to commercially used WC/W₂C reinforced coatings. The tungsten carbide reinforced coating shows brittle fracture of the coarse primary carbides and secondary precipitates, while fine-grained structure of TiC–NiMo reinforcements is not subjected to extensive cracking during the test.

Acknowledgements

This work was funded by the "Austrian Comet-Program" (governmental funding program for pre-competitive research) via the Austrian Research Promotion Agency (FFG) and the TecNet Capital GmbH (Province of Niederösterreich) and has been carried out within the "Austrian Center of Competence for Tribology" (AC2T research GmbH) in cooperation with Tallinn University of Technology and Vienna University of Technology. Part of this work was supported with EFRE funding and with support of the country of Lower Austria within the project "Onlab". This work has been also partially supported by graduate school "Functional materials and technologies", receiving funding from the European Social Fund under project 1.2.0401.09-0079 in Estonia. The authors would like to acknowledge Estonian Science Foundation under grant ETF 8211 for the support of the study.

The authors are also grateful to Dmitriy Goljandin, MSc, and Der-Liang Yung, MSc, from Tallinn University of Technology for their contribution into research and to Dr. Christian Jogl from AAC (Aerospace & Advanced Composites GmbH) for the support with SEM images.

References

- [1] B.G. Mellor, *Surface Coatings for Protection Against Wear*, Chapter 9, Woodhead Publishing Limited, Cambridge, 2006, p. 302.
- [2] R. Chattopadhyay, Kluwer Academic Publishers, New York, 2004, p. 1.
- [3] E. Badisch, C. Katsich, H. Winkelman, F. Franek, M. Roy, *Tribol. Int.* 43 (2010) 1234.
- [4] R.L. Deuis, J.M. Yellup, C. Subramanian, *Compos. Sci. Technol.* 58 (1998) 299.
- [5] J. Nurminen, J. Nötkki, P. Vuoristo, *Int. J. Refract. Met. Hard Mater* 27 (2009) 472.
- [6] M. Kirchgäßner, E. Badisch, F. Franek, *Wear* 265 (2008) 772.
- [7] C. Katsich, E. Badisch, *Surf. Coat. Technol.* 206 (2011) 1062.
- [8] S. Chatterjee, T.K. Pal, *Wear* 261 (2006) 1069.
- [9] S. Ndlovu, *The Wear Properties of Tungsten Carbide-Cobalt Hardmetals from the nanoscale up to the Macroscopic Scale*, PhD thesis, Erlangen, 2009.
- [10] I. Hussainova, *Wear* 258 (2005) 357.
- [11] J. Kuzmanovic, *WC-W2C Particle Reinforced Powder Metallurgy Iron and Nickel Matrix Composites Produced by Pressing and Sintering*, MSc thesis, Vienna TU, 2011.
- [12] S. Cardinal, A. Malchere, V. Garnier, G. Fantozzi, *Int. J. Refract. Met. Hard Mater* 27 (2009) 521.
- [13] I. Hussainova, *Wear* 255 (2003) 121.
- [14] J. Kübarssepp, H. Klaasen, J. Pirso, *Wear* 249 (2001) 229.
- [15] M. Antonov, I. Hussainova, *Tribol. Int.* (2009) 1566.
- [16] Y.P. Kathuria, *Surf. Coat. Technol.* 140 (2001) 195.
- [17] R.L. Sun, Y.W. Lei, W. Niu, *Surf. Coat. Technol.* 203 (2009) 1395.
- [18] S. Yang, M. Zhong, W. Liu, *Mater. Sci. Eng. A* 343 (2003) 57.
- [19] X.H. Wang, S.L. Song, Z.D. Zou, S.Y. Qu, *Mater. Sci. Eng. A* 441 (2006) 60.
- [20] S. Yang, N. Chen, W. Liu, M. Zhong, Z. Wang, H. Kokawa, *Surf. Coat. Technol.* 183 (2004) 254.
- [21] P. Kulu, S. Zimakov, *Surf. Coat. Technol.* 130 (2000) 46.
- [22] A. Zikin, I. Hussainova, C. Katsich, E. Badisch, C. Tomastik, *Surf. Coat. Technol.* 206 (2012) 4270.
- [23] G.M. Pharr, W.C. Oliver, F.R. Brotzen, *J. Mater. Res.* 7 (1992) 613.
- [24] A. Zikin, S. Ilo, P. Kulu, I. Hussainova, C. Katsich, E. Badisch, *Mater. Sci. Medžiagotyra* 18 (2012) 12.
- [25] Y.K. Kim, J.H. Shim, Y.W. Cho, H.S. Yang, J.K. Park, *Int. J. Refract. Met. Hard Mater* 22 (2004) 193.
- [26] I. Hussainova, A. Kolesnikova, M. Hussainov, A. Romanov, *Wear* 267 (2009) 177.
- [27] Z. Liu, L. Zhao, Y. Bao, B. Li, *Adv. Mater. Res.* 194–196 (2011) 1785.
- [28] A.O. Kunrath, I.E. Reimans, J.J. Moore, *J. Alloys Compd.* 329 (2001) 131.
- [29] I. Hussainova, E. Hamed, I. Jasiuk, *Mech. Compos. Mater.* 46 (2011) 667.
- [30] F. Sergejev, E. Kummari, M. Viljus, *Procedia Eng.* 10 (2011) 2873.
- [31] H. Berns, *Wear* 181–183 (1995) 271.
- [32] M.G. Gee, A. Gant, B. Roebuck, *Wear* 263 (2007) 137.
- [33] H. Winkelman, E. Badisch, M. Kirchgäßner, H. Danninger, *Tribol. Lett.* 34 (2009) 155.
- [34] S. Wirojanupatump, P.H. Shipway, *Wear* 239 (2000) 91.
- [35] M. Antonov, I. Hussainova, R. Veinthal, J. Pirso, *Tribol. Int.* 46 (2012) 261.

PUBLICATION IV

Zikin, A., Antonov, M., Hussainova, I., Katona, L., Gavrilovic, A., High temperature wear of cermet particle reinforced NiCrBSi Hardfacings, *Tribol. Inter.* In press. DOI: <http://dx.doi.org/10.1016/j.triboint.2012.08.013>⁴

⁴ Copyright 2012, reprinted with permission from Elsevier



Contents lists available at SciVerse ScienceDirect

Tribology International

journal homepage: www.elsevier.com/locate/triboint

High temperature wear of cermet particle reinforced NiCrBSi hardfacings

A. Zikin^{a,b,*}, M. Antonov^b, I. Hussainova^b, L. Katona^a, A. Gavrilović^c

^a AC2T research GmbH, Viktor-Kaplan-Straße 2, 2700 Wiener Neustadt, Austria

^b Department of Materials Engineering, Tallinn University of Technology, Ehitajate tee 5, 19086 Tallinn, Estonia

^c CEST Centre of Electrochemical Surface Technology, Viktor-Kaplan Strasse 2, 2700 Wiener Neustadt, Austria

ARTICLE INFO

Article history:

Received 2 May 2012

Received in revised form

30 July 2012

Accepted 21 August 2012

Keywords:

High temperature wear

Erosion wear

Impact damage

Weld overlay coating

ABSTRACT

The aim of the current study was to investigate erosive and impact/abrasive wear behaviour of TiC–NiMo and Cr₃C₂–Ni reinforced NiCrBSi hardfacings at temperatures up to 700 °C.

Coatings were produced using plasma transferred arc cladding process. It was shown that the high temperature wear behaviour of TiC–NiMo and Cr₃C₂–Ni NiCrBSi hardfacings is influenced by oxidation. The formation of mechanical mixed layers and oxide films was observed for both investigated coatings. TiC–NiMo and Cr₃C₂–Ni reinforced hardfacings show high wear resistance at all testing temperatures for both impact/abrasion and erosion conditions.

© 2012 Elsevier Ltd. All rights reserved.

1. Introduction

The ceramic–metal composites or cermets are widely used in many industrial applications where high wear resistance is required. They combine properties of both ceramics (high temperature stability and hardness) and metals (deformability). This set of properties makes cermets attractive candidates for applications in aggressive high temperature environments. Corrosion-oxidation resistance and wear behaviour at high temperature for TiC and Cr₃C₂-based cermets are widely studied [1–6]. In oxidising environment and at high temperature wear behaviour is influenced by rate of oxidation, adhesion of oxide layers and their resistance against impact. It was shown [1–6] that TiC- as well as Cr₃C₂-based materials can be considered as suitable alternatives for WC-Co hardmetals due to their high temperature wear resistance and corrosion/oxidation stability.

Erosion and impact/abrasion wear are commonly occurring problems in industry, for example in mining and agricultural applications. Erosion rate of composite materials is mainly affected by abrasive particle impact velocity, angle of impingement, particle size/shape and intrinsic microstructural features of material such as reinforcements content, homogeneity of phase distribution and bonding strength between constituents, etc. [7,8]. Impact/abrasion is a complex wear process requiring outstanding material properties. For parts subjected to abrasive action the most influential factors are hardness of both hardphases and matrix material, content of

hardphases and nature of precipitations [9–11]. Impact wear rate is less dependent on hardness; while the size, shape and distribution of hardphases are of high importance [12,13].

For composite materials with ductile binder an important contribution to wear resistance at elevated temperatures is attributed to development of a mechanically mixed layer (MML). Well developed MMLs were found on the surface of many cermets and metal matrix composites after erosion and impact/abrasion tests [4,14,15]. MML usually form during 3-body contact wear in the metal matrix, which is getting softer with increasing testing temperature. The erodent materials (for example SiO₂) get embedded to the soft matrix and get mixed with it, forming a tribo-composite layer [15]. Mechanical properties of such tribo-layers differ from the bulk body properties and, therefore, surface integrity strongly affects the wear resistance of materials.

Recently hardfacing by welding has become a commonly used technique for improvement of material performance in extreme (high temperature, impact/abrasion, erosion, etc.) conditions [16–18]. The possibility to apply hardfacing selectively and in pre-determined thickness to suit exact requirements in combating wear makes this method very attractive and cost effective [10,19].

WC/W₂C particles are the most common hardphases applied by hardfacing process as reinforcements for Ni-based matrix. Such structures reveal sufficient mechanical properties and provide high wear resistance at both impact and abrasion conditions [17]. However, the temperature of 550 °C remains a limiting factor for the high temperature applications of WC/W₂C phase as reinforcements.

In order to overcome problems caused by oxidation, cermet particles (TiC–NiMo and Cr₃C₂–Ni) are proposed as an alternative to WC/W₂C. The main objectives of this work are (1) to study

* Corresponding author at: AC2T research GmbH, Viktor-Kaplan-Straße 2, 2700 Wiener Neustadt, Austria. Tel.: +43 2622 81600 322; fax: +43 2622 81600 99.

E-mail address: zikin@ac2t.at (A. Zikin).

impact/abrasion and erosion resistance of the developed cermet particle reinforced double-structured hardfacings at high temperatures; and (2) to examine wear and oxidation mechanisms operating for the materials under consideration.

2. Experimental details

2.1. Materials

Two types of advanced hardfacings produced by plasma transferred arc (PTA) process were analysed and compared. The hardfacings were produced out of cermet particles $\text{Cr}_3\text{C}_2\text{-Ni}$ or TiC-NiMo and NiCrBSi matrix powder with a ratio of 40/60 vol%. The compositions of the precursor powders are presented in Table 1.

2.2. High temperature cyclic impact abrasion (HT-CIAT)

The wear rates of the hardfacings were evaluated with cyclic impact abrasion tester (HT-CIAT) developed at the Austrian Center of Competence for Tribology (AC2T, Austria). The samples were mounted at 45° to the horizon, cyclically hit by a plunger at a given frequency in combination with an abrasive flow between the sample and the plunger (Fig. 1) [12].

Samples were cleaned in an ultrasonic bath with isopropanol, dried and weighed before and after testing. Quantitative wear characterisation was conducted by measuring the gravimetric mass

loss of the testing specimens. Tribo-tests parameters are listed in Table 2.

After tests completion the topography of the worn surfaces was analysed by SEM Philips XL 30 FEG equipped with an energy dispersive X-ray analyser. The cross-section images were examined by optical microscopy (OM, MEF4A, Leica Microsystem). OM imaging was performed on samples etched with a solution of HF and HNO_3 with a ratio of 1:12 at room temperature for 10 s.

2.3. High temperature erosion

Erosion tests were performed on a centrifugal particle accelerator described elsewhere [6,12]. The test parameters are listed in Table 3. Before and after testing each specimen was cleaned

Table 2
HT-CIAT test conditions.

Parameter	Value
Impact energy (J)	0.8
Impact angle (deg.)	45
Frequency (Hz)	2
Testing cycles	7200
Abrasive material	SiO_2
Abrasive flow (g s^{-1})	3
Abrasive size, shape (mm)	0.4–0.9, angular
Abrasive hardness (HV1)	1000–1200
Test temperatures ($^\circ\text{C}$)	20, 350, 550, 700

Table 1
Initial powder data.

Powder	Source	Grain size (μm)	Chemical composition (wt%)
Ni-based matrix	Castolin 16221	50–150	0.2% C, 4% Cr, 1% B, 2.5% Si, 2% Fe, 1% Al, rest Ni
TiC–NiMo	Milled from bulk	150–310	80% TiC, 20% Ni:Mo 2:1
$\text{Cr}_3\text{C}_2\text{-Ni}$	Milled from bulk	150–310	80% Cr_3C_2 , 20% Ni

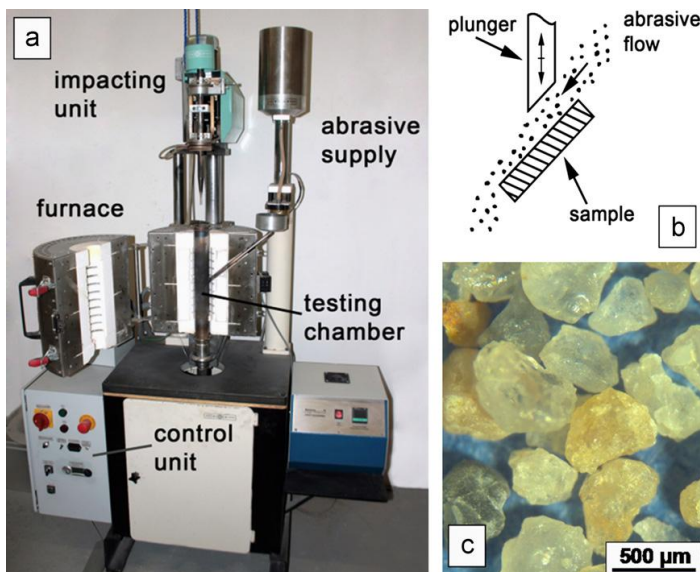


Fig. 1. (a) High temperature cyclic impact abrasion tester (HT-CIAT); (b) testing principle (45° impact angle with abrasives tested) and (c) abrasive silica particles.

with acetone, dried and weighed. At least three tests were run for each material to determine the erosion resistance. After test completion the cross-sectional images and the elemental composition of the worn surfaces were analysed by SEM/EDS.

2.4. Macro-hardness

Vickers hardness test rig [12] specially developed by AC2T was used to measure the hardness of materials at high temperatures. The diagonals of the indent marks were measured by OM. Testing chamber was kept under vacuum to exclude oxidation during the test. All samples were loaded by 10 kg to measure HV10. The mean value of hardness at each test temperature was calculated by averaging of the results obtained on at least 8 indents.

2.5. XRD and XPS analysis

XRD experiments were performed on an X-Pert powder diffractometer (PANalytical, Netherlands) equipped with a secondary graphite monochromator, automatic divergence slits and a scintillation counter. The measurements were performed using $\text{CuK}\alpha$ radiation in Bragg–Brentano geometry at 40 V and 30 mA, in continuous mode, in 2θ range from 20° to 110° .

Relative weight contributions (wt%) for each crystalline phase as well as crystallite size were obtained with the help of Rietveld refinement procedure by using the commercial software TOPAS V3 [20].

XPS experiments were performed on a Theta Probe[®] spectrometer (Thermo Fisher Scientific, UK) using monochromated $\text{AlK}\alpha$ X-ray source with the photon energy of 1486.6 eV. The vacuum chamber had a pressure of $\sim 10^{-10}$ mbar during the measurement. Survey spectra were recorded for binding energies between -10 and 1350 eV with a pass energy of 200 eV, the total dwell time of 0.25 s per point and step size of 1 eV to determine the elements present in the particular measurement. For elements of special interest measurements of higher resolution were also performed. The pass energy was set to 50 eV, the total dwell time per point to 0.75 s and the step size to 0.1 eV. The standard software of the Theta Probe was used to evaluate the spectra. The evaluation of the data was done with help of The National Institute of Standards and Technology (NIST) database.

3. Results and discussion

3.1. Microstructural analysis of hardfacings

The microstructures of the two hardfacings are illustrated in Fig. 2. Fig. 2a presents the microstructure of NiCrBSi-based hardfacing reinforced by Cr_3C_2 -Ni. The coatings consist of at least three apparent phases: hardphases-rich hypereutectic matrix material, some amount of dissolved and re-precipitated M_7C_3 and Cr_3C_2 (spine-like) carbides, and grains of the precursor cermet particles homogeneously distributed throughout the matrix. The cermet particles represent agglomerates of 2–5 μm sized chromium carbides (Cr_3C_2 and Cr_7C_3 grains) embedded into the nickel binder, i.e. the commonly reported structure of the

Table 3
Erosion test conditions.

Parameter	Values
Impact velocity (m s^{-1})	50
Impact angles (deg.)	30, 90
Erodent	SiO_2
Erodent size, shape (mm)	0.1–0.3, angular
Total weight of erodent (kg)	6
Test temperature ($^\circ\text{C}$)	20, 350, 550, 650

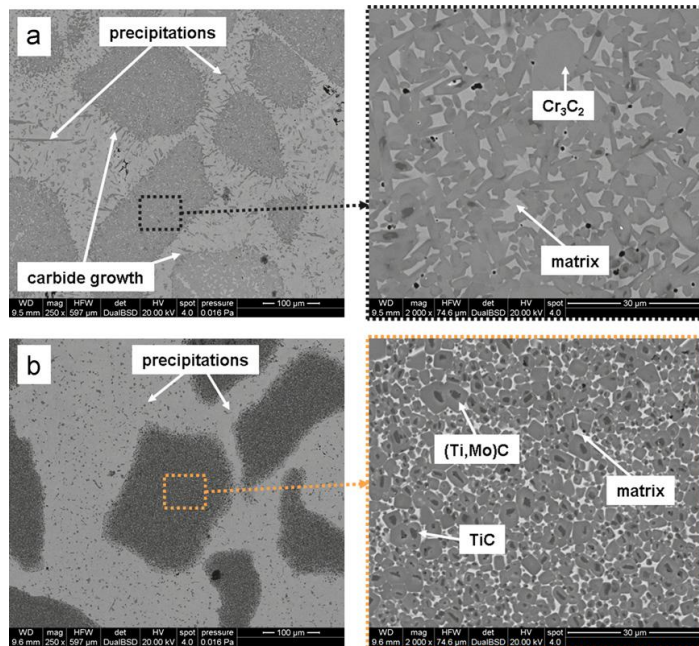


Fig. 2. SEM micrographs: (a) Cr_3C_2 -Ni reinforced NiCrBSi hardfacing and (b) TiC-NiMo reinforced NiCrBSi hardfacing.

reactive sintered $\text{Cr}_3\text{C}_2\text{-Ni}$ cermets [21]. The detailed microstructural analysis of these coatings is described elsewhere [22,23].

Fig. 2b shows the microstructure of TiC–NiMo reinforced hardfacing. SEM imaging revealed homogeneously distributed cermet particles throughout a Ni-based matrix. The cermet particles themselves consist of three main phases: core-rim structured carbides of TiC core surrounded by a rim of double carbide (Ti, Mo)C and Ni-based alloy binder. In the case of TiC–NiMo reinforced hardfacing, no measurable carbide growth was detected during PTA processing. Precipitations in the matrix were of rounded shape of less than 1 μm in diameter and uniformly distributed throughout the dendritic matrix.

3.2. Hot hardness

The hardness of the NiCrBSi matrix material is 380 ± 40 HV10 at temperatures below 550 °C and rapidly decreased with increase in temperature. The hardness measurements in the hardfacings under consideration represent a composite hardness of hard phases and binder. Fig. 3 illustrates HV10 results for TiC–NiMo and $\text{Cr}_3\text{C}_2\text{-Ni}$ reinforced NiCrBSi hardfacings. For both materials similar compound hardness values were found at room temperature (~ 650 HV10). The hardness values stay at the same level for both materials in the temperature range from 20 °C to 300 °C and then start slightly to decrease in the interval between 300 °C and 600 °C. Rapid decrease in hardness for both hardfacings starts from 700 °C; at this temperature the hardness is lower than 400 HV. Both materials tested at the highest temperature show the comparable sharp hardness drop, which implies the degradation point for the matrix material.

The demonstrated considerable distribution (including standard deviations) of the mean hardness values for TiC–NiMo and $\text{Cr}_3\text{C}_2\text{-Ni}$ reinforced NiCrBSi hardfacings can be explained with microstructural complexity of the PTA coatings.

3.3. Impact/abrasive wear of the hardfacings

It is well known that abrasive wear behaviour is strongly influenced by material hardness and microstructural features [12,24]. However, in conditions with dominating impact load, an improvement in wear resistance can be obtained by applying ductile matrixes with fine uniformly distributed hard phases [12,22]. Therefore, it can be assumed that hardfacings reinforced with cermet particles could be an alternative to the commercially

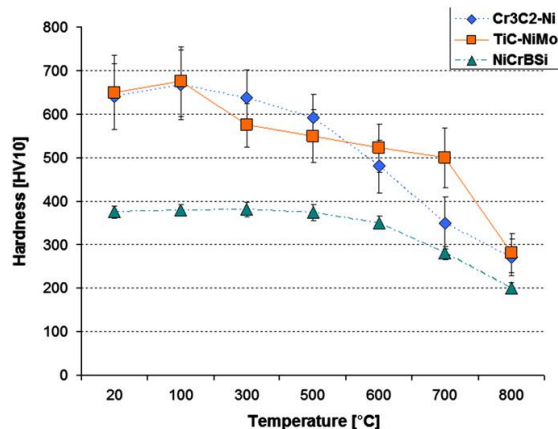


Fig. 3. Hot hardness distribution curves for NiCrBSi matrix alloy, TiC–NiMo and $\text{Cr}_3\text{C}_2\text{-Ni}$ reinforced NiCrBSi hardfacing.

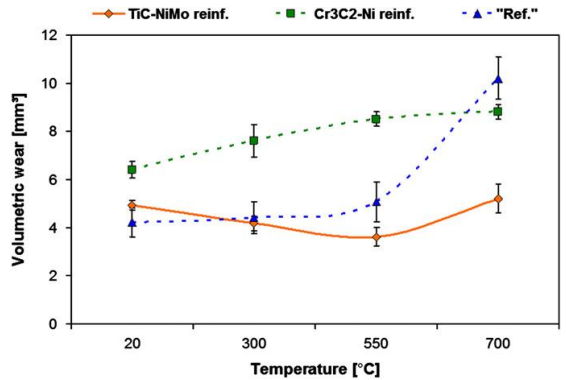


Fig. 4. Volumetric wear values after HT-CIAT testing for TiC–NiMo and $\text{Cr}_3\text{C}_2\text{-Ni}$ reinforced NiCrBSi hardfacings. “Ref.”—commercially used WC/W₂C reinforced NiCrBSi hardfacing.

used tungsten carbide reinforced coatings, especially at temperatures exceeding 550 °C.

Fig. 4 shows the volumetric wear of the coatings tested at room temperature, 300 °C, 550 °C and 700 °C. Commercially used multiphase coatings with Ni-based matrix and 60 wt% of fused WC/W₂C hardphases were taken as a reference material (labelled “Ref.”). Properties and wear behaviour of the reference material are described elsewhere [14].

Good performance of the reference hardfacing at temperatures below 550 °C is evident; however, the volumetric wear increased significantly with increase in temperature, which can be attributed to hardphases oxidation and excessive fracture of the material [14]. In comparison, $\text{Cr}_3\text{C}_2\text{-Ni}$ and TiC–NiMo reinforced hardfacings have better wear and oxidation resistance up to 700 °C.

$\text{Cr}_3\text{C}_2\text{-Ni}$ reinforced hardfacings show some increase in wear rate with increase in temperature, which is mainly the result from both the matrix softening and fracture of chromium carbide precipitations. However, the system remains stable with only 20% wear rate increase in the interval between 20 °C and 700 °C.

TiC–NiMo reinforced hardfacings show promising impact/abrasion resistance with low volumetric wear values. Additionally, in the temperature interval between 20 °C and 550 °C, the wear rate decreases by 20%. This can be explained by the formation of mechanically mixed tribo-layers of fused silica dust and softened Ni-based matrix. At 700 °C oxidation of the matrix material becomes significant leading to increase in wear rate. At the highest testing temperature TiC–NiMo reinforced hardfacing has two times higher wear resistance than the “Ref” hardfacing.

3.3.1. $\text{Cr}_3\text{C}_2\text{-Ni}$ reinforced NiCrBSi hardfacings

Fig. 5 illustrates cross-section OM micrographs of $\text{Cr}_3\text{C}_2\text{-Ni}$ and TiC–NiMo reinforced coatings after cyclic impact testing.

For the $\text{Cr}_3\text{C}_2\text{-Ni}$ reinforced coating at low testing temperature (Fig. 5a) a uniform wear of material surface was observed. Matrix regions contain high amount of precipitations, which correspond to broken abrasive particles. Similar fracture mechanisms also occur in cermet zones of the material. With increase in testing temperature the presence of SiO_2 particles in the sub-surface layer of hardfacing is detected (Fig. 5b). The main mechanism of surface layer formation during impact/abrasion testing is indentation of silica dust into the soft matrix between cermet grains. For the $\text{Cr}_3\text{C}_2\text{-Ni}$ reinforced hardfacing the presence of SiO_2 particles is also found in the cermet zones (Fig. 6a–c).

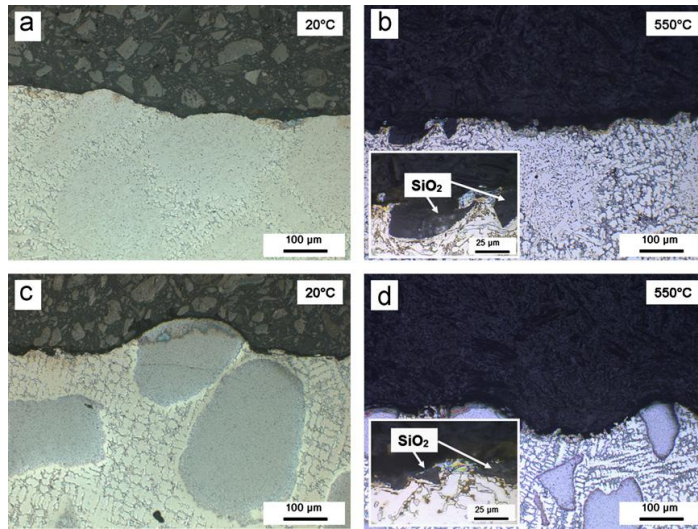


Fig. 5. OM cross-sectional images after HT-CIAT testing: (a) Cr_3C_2 -Ni reinforced NiCrBSi hardfacing at 20 °C; (b) Cr_3C_2 -Ni reinforced hardfacing at 550 °C; (c) TiC-NiMo reinforced NiCrBSi hardfacing at 20 °C and (d) TiC-NiMo reinforced hardfacing at 550 °C.

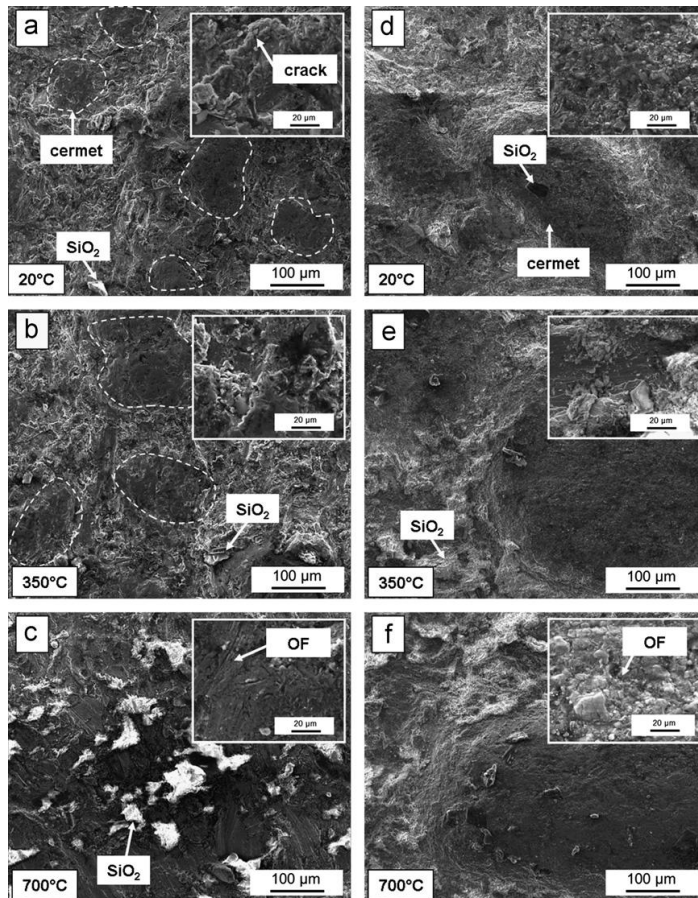


Fig. 6. SEM micrographs of worn surface after HT-CIAT testing: (a–c) Cr_3C_2 -Ni reinforced NiCrBSi hardfacing at 20 °C, 350 °C and 700 °C; (d–f) TiC-NiMo reinforced NiCrBSi hardfacing at 20 °C, 350 °C and 700 °C.

Trans- and inter-granular cracking results in subsequent removal of the carbides and materials chips from the surface especially when subjected to high testing temperatures. This could be one of the reasons of surface degradation. The $\text{Cr}_3\text{C}_2\text{-Ni}$ reinforced hardfacing at 700°C shows intensive plastic deformation and formation of oxide films with only fine crashed ceramic particles found on the surface (Fig. 6c).

3.3.2. TiC–NiMo reinforced NiCrBSi hardfacings

For the TiC–NiMo reinforced coatings the wear predominantly takes place in the matrix material by continuous removal of the plastic binder. Cermet particles exhibit less damage and the hardfacing is characterised by elevations and depressions on the surface (Fig. 5c). Increasing in testing temperature results in development of well pronounced layers of SiO_2 particles in the sub-surface region of the hardfacing (Fig. 5d). Fig. 6d–e illustrates the surface transformation of TiC–NiMo reinforced coating at different temperatures after cyclic impact/abrasion testing. It is determined that with increase in temperature more than 50% of the hardfacing surface (almost all matrix regions and some cermet zones) is covered by SiO_2 particles. Low amount of precipitations in the matrix and their sub-micron size facilitate the penetration of silica into the soft matrix. At the highest test temperature (700°C), the adhesion between silica particles and matrix is getting weaker due to oxidation of matrix resulting in wear rate increase.

The surface of cermet zones in TiC–NiMo reinforced hardfacing shows formation of oxide films at high testing temperatures (Fig. 6e).

3.4. Erosive wear of the hardfacings

Solid particle erosion of composite materials depends on many factors including mechanical properties of the target and erodent as well as the impact parameters. The angle of impingement along with other test conditions determines the mechanisms and, therefore, the rates of materials damage. For ductile alloys the oblique impact of the particles causes severe plastic strain at the impact site and material removes from the surface by ploughing and abrasive cutting when the localized strain exceeds the materials strain-to-failure limit. Brittle materials suffer from intensive cracking highly promoted at normal angle of impact. Depending on combination of factors, the mechanism of material removal during erosion of composites may be described as mixed mode of material damage. The maximum erosion rate of the cermets is usually observed at an impact angle of $75\text{--}90^\circ$ [25]. Double-structured advanced hardfacings are proposed as cost-effective coatings for protection against erosion in the whole range of impact angles. Volumetric wear rates are shown in Fig. 7. All tests were performed with a constant impact velocity of 50 m/s. On the abscissa the volumetric wear rate of the materials at the impact angle of 30° is drawn. The ordinate shows the wear rate of the tested materials at the impact angle of 90° .

3.4.1. $\text{Cr}_3\text{C}_2\text{-Ni}$ reinforced NiCrBSi hardfacing

Cr_3C_2 based cermet with 40 wt% of pure Ni binder was used as reference material (labelled "Ref"). Erosive wear of this cermet is almost twice higher under normal angle of impact as compared to that obtained under oblique impact conditions. $\text{Cr}_3\text{C}_2\text{-Ni}$ reinforced hardfacings having almost twice less content of hard ceramic phase are performing similarly well as reference material. $\text{Cr}_3\text{C}_2\text{-Ni}$ reinforced hardfacings are clad on a substrate with formation of the needle-like carbide precipitations reducing plasticity of the binder and also serving as a source of cracking under impact. Nickel binder has sufficient oxidation resistance but experiences softening that accelerates embedment of crushed

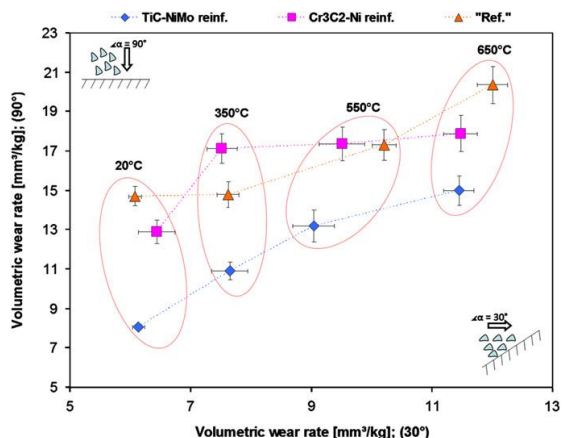


Fig. 7. Volumetric wear rates after erosion testing for TiC–NiMo and $\text{Cr}_3\text{C}_2\text{-Ni}$ reinforced NiCrBSi hardfacing at constant impact velocity of 50 m/s. "Ref"— Cr_3C_2 solid cermet with 40 wt% of Ni binder. Abscissa—volumetric wear rate of the materials at the impact angle of 30° ; ordinate—volumetric wear rate of the materials at the impact angle of 90° .

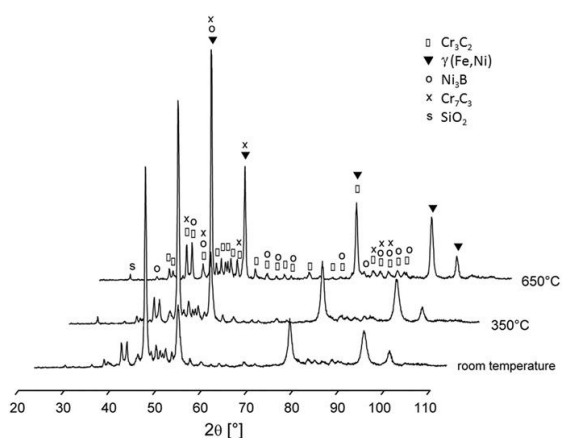


Fig. 8. XRD patterns for $\text{Cr}_3\text{C}_2\text{-Ni}$ reinforced NiCrBSi hardfacing at three different temperatures: 20°C , 350°C and 650°C .

abrasive particles, deformation of material and development of mechanically mixed tribo-layer (MML) consisting of wear debris, highly deformed matrix alloy, oxides and fused silica. Performance of the hardfacings under consideration is good at both impact angles and test temperature of 650°C . The tribo-layer formed on the wear surface may protect the material from removal and rapid oxidation.

Fig. 8 shows corresponding XRD patterns of $\text{Cr}_3\text{C}_2\text{-Ni}$ reinforced samples eroded at three different temperatures: 20°C , 350°C and 650°C . Quantitative XRD analysis of the $\text{Cr}_3\text{C}_2\text{-Ni}$ reinforced hardfacing has revealed five crystalline phases: Cr_3C_2 , $\gamma(\text{Fe,Ni})$, Ni_3B , Cr_7C_3 and SiO_2 . $\gamma(\text{Fe,Ni})$ phase composes the major amount (around $60 \pm 5\text{ wt}\%$) at all testing temperatures. The amount of the Cr_7C_3 phase decreases with increase in temperature from $\sim 8\text{ wt}\%$ at 20°C to $\sim 2\text{ wt}\%$ at 650°C . The relative weight contribution of the Cr_3C_2 phase was found to be around $33 \pm 3\text{ wt}\%$ for all samples eroded at different temperatures. Ni_3B phase also decreases with increasing testing temperature from $\sim 11\text{ wt}\%$ at 20°C to $\sim 2\text{ wt}\%$ at 650°C . The relative weight contribution of the erodent particles debris

(SiO₂ phase) increases with the temperature from ~2 wt% at 20 °C up to ~5 wt% at 650 °C. The changes in relative weight of some phases can be contributed to the development of oxide layers in the matrix region. The Ni₃B and Cr₇C₃ phases are located in the NiCrBSi matrix and their reduction with increasing temperature is associated with softening of matrix and substitution it by the silica particles. XRD measurements detect no oxides on the surface of the eroded hardfacing.

3.4.2. TiC–NiMo reinforced NiCrBSi hardfacing

Spherical carbide precipitations, which work as matrix hardening precipitation, in TiC–NiMo reinforced hardfacings serve as much less severe stress concentrator. The wear rates under normal and oblique impact angles are very similar indicating that double structuring along with right material constituent and coating procedure selection may provide improved wear resistance compared to conventional cermets.

Fig. 9 shows corresponding XRD patterns of TiC–NiMo reinforced samples eroded at three different temperatures: 20 °C, 350 °C and 650 °C. For the TiC–NiMo reinforced hardfacing, six crystalline phases were detected: TiC, the intermetallic matrix γ (Fe,Ni), (Fe, Ni, Mo)₂₃B₆, which is the most probable Fe–Ni–B hardphase with some traces of Mo in the crystal lattice, (Mo, Ti)C₂, SiO₂ and non-stoichiometric carbide Ti_{0.92}Mo_{0.02}C_{0.6}.

γ (Fe,Ni) phase composes the major amount (~55 ± 5 wt%) at all testing temperatures. The relative weight contribution of TiC crystalline phase was ~15 wt% and Ti_{0.92}Mo_{0.02}C_{0.6} phase ~12 wt% over the whole temperature range. The (Mo, Ti)C₂ crystalline phase

appears in traces 3 ± 1 wt%. The Fe–Ni–Mo–B solid solution is recognised as a (Fe, Ni, Mo)₂₃B₆ cubic crystalline phase contributing in the range from 11 ± 2 wt% at room temperature, to 4 ± 1 wt% for the sample eroded at 650 °C. The relative weight contribution of the eroded particles debris (SiO₂ phase) increases with the temperature from ~2 wt% at 20 °C up to ~10 wt% at 650 °C. As for Cr₃C₂–Ni reinforced hardfacing, the XRD measurements reveal no oxide layers on the surface of TiC–NiMo reinforced coating.

3.4.3. Erosive wear mechanisms of Cr₃C₂–Ni and TiC–NiMo reinforced hardfacings

Wear mechanism of double-structured coatings is schematically depicted in Fig. 10 and supported by SEM micrographs of the single impact craters and worn surfaces (Figs. 11, 12 and 13).

The main erosive wear mechanisms operating at given conditions are:

- ploughing and cutting of NiCrBSi matrix (Fig. 11a,c);
- squeezing of a metal binder in cermet particles to the surface with formation of the rigid supporting compacted layer and top layer with higher metal content;
- selective removal of a matrix binder from cermet particles by crashed abrasive particles pushed by the stream of particles;
- fracturing and/or fragmentation of carbides (less intensive for TiC–NiMo particles reinforced claddings as compared to Cr₃C₂–Ni reinforced ones, Fig. 11a–d);
- removal of the whole ceramic particles insufficiently supported by metal matrix;
- embedment of crushed abrasive particles mainly into the NiCrBSi binder alloy (Fig. 12);
- intermixing of cermet and NiCrBSi binder constituents with formation of well developed MML consisting of wear debris, fused silica dust, finely dispersed different oxides and highly deformed matrix alloy (Fig. 12);
- interaction of abrasive particles with formed oxide films at testing temperature of 650 °C (Fig. 12).

Cross-sectional SEM images of the materials under consideration after testing at temperature of 650 °C, Fig. 14, show the correlation between mechanisms marked out in Fig. 10 for both hardfacings. Fig. 14 illustrates the high magnitude SEM images of TiC–NiMo (a—matrix region, b—cermet region) and Cr₃C₂–Ni (c—matrix region, d—cermet region) reinforced hardfacings after erosion tests at temperature of 650 °C. For both materials in the matrix region the presence of SiO₂ particles at the sub-surface layer is clearly identified. Cracking of Cr₃C₂ particles exhibits

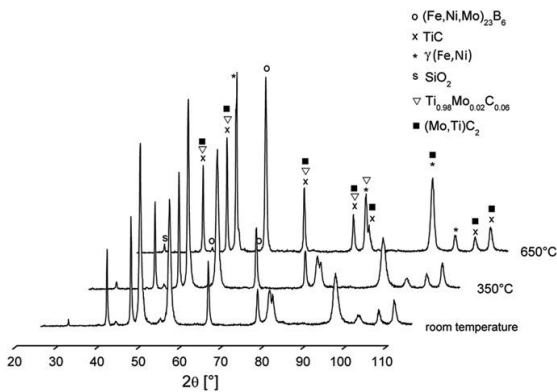


Fig. 9. XRD patterns for TiC–NiMo reinforced NiCrBSi hardfacing at three different temperatures: 20 °C, 350 °C and 650 °C.

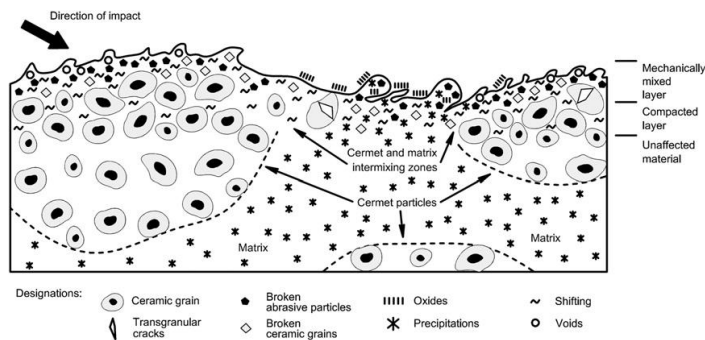


Fig. 10. Features of cermet reinforced NiCrBSi hardfacings during erosive wear.

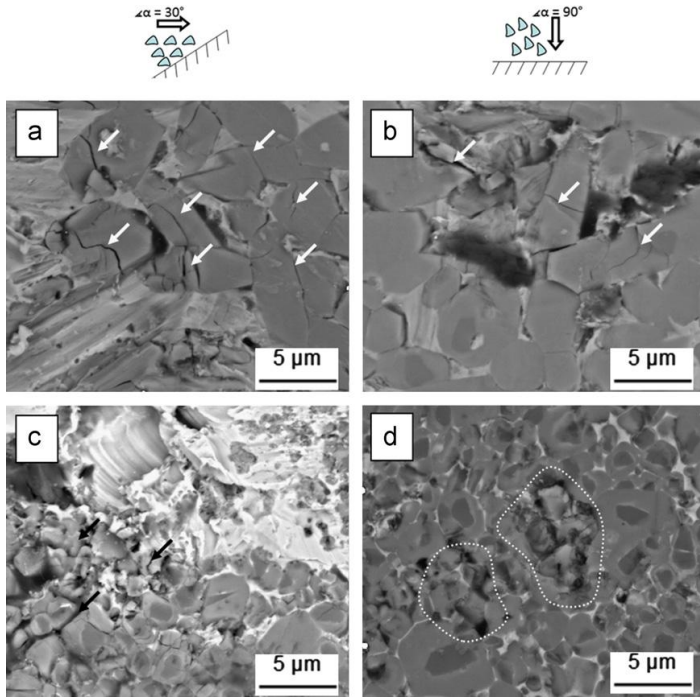


Fig. 11. SEM micrographs of single impact crater: (a) and (c) $\text{Cr}_3\text{C}_2\text{-Ni}$ reinforced NiCrBSi hardfacing; (b) and (d) TiC-NiMo reinforced NiCrBSi hardfacing.

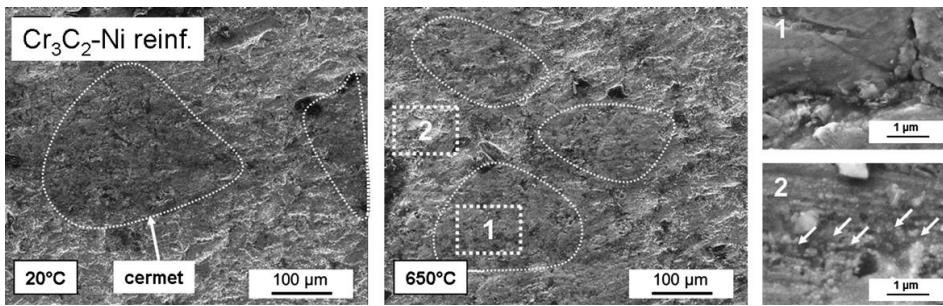


Fig. 12. SEM micrographs of worn surface after erosion testing for $\text{Cr}_3\text{C}_2\text{-Ni}$ reinforced NiCrBSi hardfacing at 20 °C and 650 °C; 1—cermet zone; 2—matrix zone.

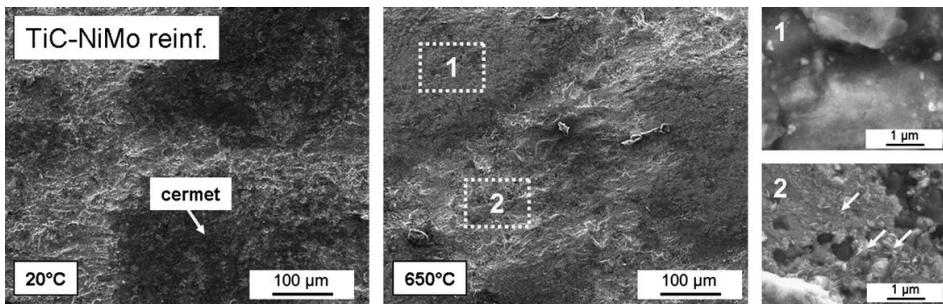


Fig. 13. SEM micrographs of worn surface after erosion testing for TiC-NiMo reinforced NiCrBSi hardfacing at 20 °C and 650 °C; 1—cermet zone; 2—matrix zone.

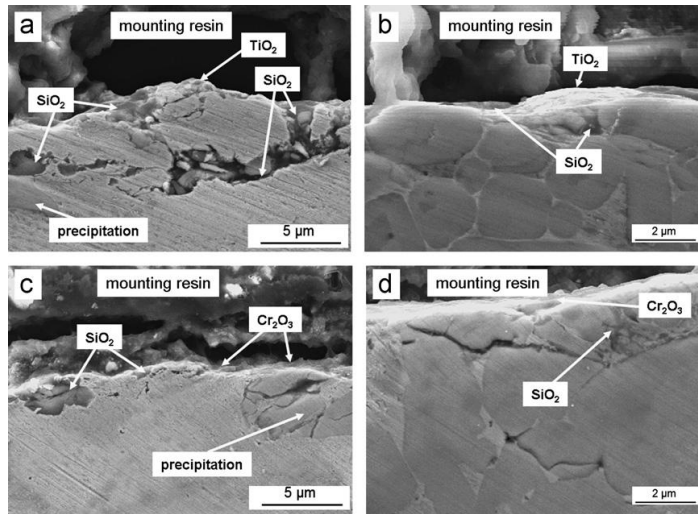


Fig. 14. SEM cross-sectional images after erosion testing at 650 °C: (a) TiC–NiMo reinforced NiCrBSi hardfacing matrix region; (b) TiC–NiMo reinforced NiCrBSi hardfacing cermet region; (c) Cr₃C₂–Ni reinforced NiCrBSi hardfacing matrix region and (d) Cr₃C₂–Ni reinforced NiCrBSi hardfacing cermet region.

more brittle mode compared to TiC particles. For the both hardfacings formation of oxide layers was detected.

It is well known, that at elevated temperatures the erosion wear is governed by the synergy of erosion and oxidation. Basically, there are four different erosion mechanisms at high temperature [26]. The hardfacings under investigation (Fig. 14) can be related to the oxide erosion model, where both processes play significant role and the formation of composite so called MML occurs, comprising the bulk metal and broken pieces of silica particles and oxide scale [26].

3.5. Oxidation during high temperature erosion

During erosion the formation of oxide products on the surface can significantly affect wear resistance of materials. Under high test temperature (650 °C and higher) the development of oxide films in cermet zones (Figs. 12 and 13—labelled 1) and also oxide growth in the matrix regions (Figs. 12 and 13—labelled 2); was detected for both investigated hardfacing. XRD analysis was unable to detect oxides on the surface of investigated materials. This can be explained with low thickness of formed oxide layers. Therefore, to analyse the surface oxidation on nano-scale XPS measurements were conducted.

3.5.1. Oxidation of Cr₃C₂–Ni reinforced hardfacing during erosion testing

Fig. 15 shows XPS patterns for the samples eroded at temperatures of 20 °C, 350 °C, 550 °C and 650 °C. The data from the matrix region of Cr₃C₂–Ni reinforced sample (Fig. 15a) indicate the presence of five main elements and their phases in the matrix. The binding energies (BE) for Ni are measured at 852.7 eV and 870.0 eV. Both peaks correspond to elemental Ni (spectral lines 2p_{3/2} and 2p_{1/2}, respectively). Pure Ni occupy ~34 wt% of the tested surface at 20 °C. At elevated temperature, the peak in the Ni is shifted, showing a value of 854.2 eV. This corresponds to the formation of nickel oxide (NiO). The peaks for NiO appear at temperature of 350 °C with ~8 wt% from the tested surface and increase to content of ~10 wt% at 650 °C.

The BE for elemental Fe shows the presence of iron oxides at all tested temperatures with different iron oxide peaks (FeO, Fe₂O₃).

At testing temperature of 20 °C and 350 °C iron oxides occupy ~25 wt% of the surface and this values decreases to ~17 wt% at 650 °C. For the elemental Cr at 20 °C two peaks have been observed at a BE of 583.3 eV and 574.7 eV, respectively. Both correspond to elemental Cr (2p spectral lines), but can also correspond to chromium carbide. In fact, those two peaks occupy ~25 wt% of tested surface and disappear at testing temperature of 350 °C. Increased testing temperature leads the formation of two different chromium oxides with BEs at 576.6 eV (Cr₂O₃) and 578.0 eV (CrO₃). The amount of Cr₂O₃ is ~16 wt% at 350 °C and 550 °C and decreases to ~10 wt% at testing temperature of 650 °C. The CrO₃ phase occupy ~3 wt% of tested surface at 350 °C and 550 °C. At testing temperature of 650 °C the amount of phase CrO₃ increases to ~12 wt%. This can be correlated to reaction of Cr₂O₃ with O₂ and its further oxidation. The phenomenon is widely studied [27,28] and usually happens at temperatures above 1000 °C. This is also a limiting factor for the application of Cr-based systems. The formation of CrO₃ could be explained with high flash temperatures under impact of silica particle onto the sample surface. Those temperatures are significantly higher than the testing temperature that makes the further oxidation of Cr₂O₃ possible.

The analysis of the elemental boron shows no peaks at room temperature. However, starting from 350 °C the formation of B₂O₃ (BE of 192.8 eV) was detected. The content of boron oxide increases with temperature (from ~16 wt% at 350 °C to ~25 wt% at 650 °C). The boron forms a protective boron oxide coating being stable up to 1000 °C [29]. The Si region shows the presence of silica abrasive particles on the sample surface. The BE of 103.5 eV corresponds to SiO₂. The content of SiO₂ increases in the temperature interval between 20 °C (~18 wt%) and 550 °C (~34 wt%). This can be explained with softening of the matrix. At 650 °C the content of silica phase is ~20 wt%. It is hard to explain the high content of SiO₂ at temperature of 550 °C and normally it should stay on the same constant level of approximately 20 wt%. Most probably it can be contributed to the measurements mistake.

In the cermet zone of Cr₃C₂–Ni reinforced hardfacing, three main elements were found during the XPS measurements (Fig. 15b). All three of them (Ni, Cr and Si) indicate the same phases as in the matrix region with Cr₂O₃ being dominate phase (~40 wt%) in the interval between 350 °C and 650 °C. Because of large chromium

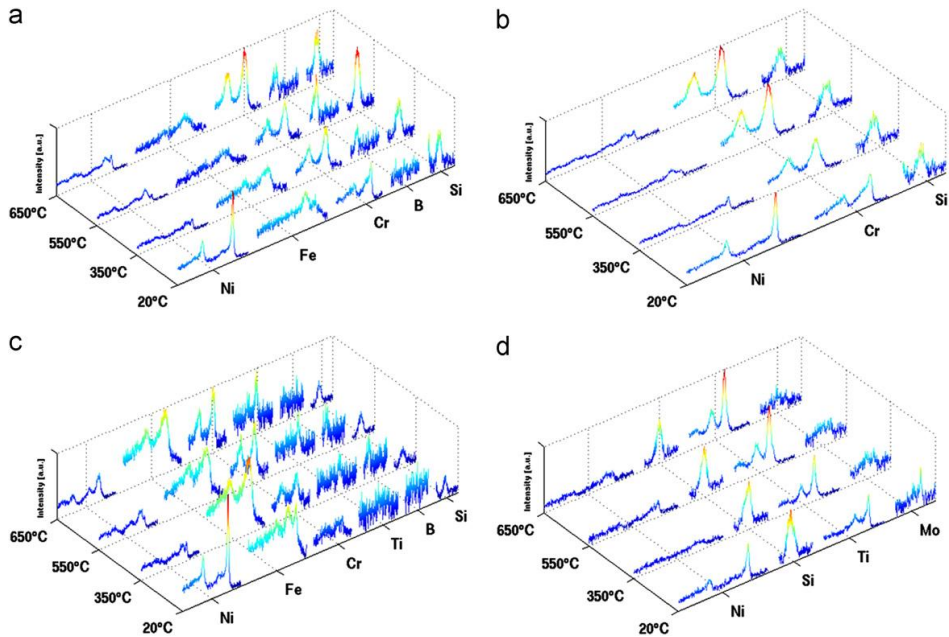


Fig. 15. XPS patterns for samples eroded at the four different temperatures: 20 °C, 350 °C, 550 °C and 650 °C: (a) and (b) Cr_3C_2 -Ni reinforced NiCrBSi hardfacing (matrix and cermet zone); (c) and (d) TiC-NiMo reinforced NiCrBSi hardfacing (matrix and cermet zone).

reservoir the external scale consist of Cr_2O_3 also acting as a barrier against further oxidation.

At the highest testing temperature Cr_2O_3 and SiO_2 are the main phases presented in the surface of Cr_3C_2 -Ni reinforced hardfacing and they mostly influence the wear behaviour. Chromium oxides and silica particles form a mixed composite layer protecting surface from further oxidation, which can result, for example, in more ductile behaviour of the hardfacing—only slight wear rate growth at elevated temperatures and impact angle of 90 °C (Fig. 7) is observed.

3.5.2. Oxidation of TiC-NiMo reinforced hardfacing during erosion testing

The XPS patterns from matrix region of TiC-NiMo reinforced hardfacing eroded at the temperatures of 20 °C, 350 °C, 550 °C and 650 °C are presented in Fig. 15.

At testing temperature of 20 °C the main elements in cermet zone of TiC-NiMo reinforced hardfacing (Fig. 15d) and their phases are Ni (~30 wt%) and Ti (~20 wt%) with BE of 454.9 eV (TiC phase). The other elements or phases presented on surface correspond to Cr (~10 wt%), Mo (~5 wt%), iron oxides (~15 wt%) and SiO_2 (~20 wt%). With increase of testing temperature peak for elemental Ti is shifted showing the BE of 459.0 eV (TiO_2). Content of TiO_2 remains approximately on the same (~50 wt%) level for all testing temperatures in the interval between 350 °C and 650 °C. This is in a good correlation with [30] studying oxidation of TiC in oxygen. Growth of TiO_2 inhibits formation of NiO. Only ~5 wt% of nickel oxide was found on the surface in the temperature interval between 350 °C and 650 °C. The high content of SiO_2 (~30 wt%) at temperatures higher than 350 °C corresponds to silica particles dust, which most probably interacts with the metal binder between TiC grains. The presence of Mo in the binder leads to the formation of Ti-Mo double carbides as it was shown by XRD analysis (Fig. 9). However, at high temperatures molybdenum oxidises with formation of MoO_2 (BE of 228.8 eV).

This oxide forms at temperature of 350 °C and is presented also at testing temperatures of 550 °C and 650 °C. The content of this phase remains constant (~4 wt%) at elevated temperatures. Iron oxides are also present on the surface of eroded sample at high temperatures with constant (~10 wt%) content in the temperature interval between 350 °C and 650 °C.

XPS analysis of the matrix region (Fig. 15c) at 20 °C indicates that the main elements and their phases are Ni (~40 wt%), SiO_2 (~20 wt%), iron and iron oxides (~30 wt%), and Cr (~8 wt%). For TiC-NiMo reinforced coating unexpected high content of iron oxides was detected also at elevated temperatures. At testing temperatures in the interval between 350 °C and 650 °C content of iron oxides is ~40 wt%. The content of chromium and nickel oxides in the same interval is ~6 wt% and ~18 wt%, respectively. Some amount of B_2O_3 (~5 wt%) is detected in the interval between 350 °C and 550 °C. At testing temperature of 650 °C boron peaks disappear. The presence of TiO_2 is detected starting from a temperature of 550 °C with ~5 wt% of titanium dioxide increasing up to ~20 wt% at a temperature of 650 °C. The content of SiO_2 on the surface remains on the same high concentration of 20–25 wt% up to the highest testing temperature. XRD analysis shows that the content of the SiO_2 below the surface is higher at elevated temperature due to softening of the matrix. Content of silica on the surface (measured by XPS) remains the same with some local variations. This may be explained by the smearing of the metal matrix over the silica particles.

4. Conclusions

Based on the study within this work, the following conclusions can be drawn:

1. The degradation of the NiCrBSi matrix at temperatures above 700 °C is a main limiting factor for the application of the TiC-NiMo and Cr_3C_2 -Ni cermet reinforced coatings.

2. For hardfacings under consideration the significant decrease in hardness is observed in the temperature interval between 700 °C and 800 °C.
3. Both cermet reinforced hardfacings are an attractive candidates for applications in impact/abrasive conditions, especially at high (> 550 °C) temperatures. The volumetric wear rate values for the TiC–NiMo and Cr₃C₂–Ni reinforced coatings are significantly lower compared with WC/W₂C reinforced hardfacings at testing temperature of 700 °C.
4. The erosion wear results show a low dependence of the TiC–NiMo reinforced coating on the impact angles. Hardfacing reveals high wear resistance at shallow as well as normal angles of impact. Cr₃C₂–Ni reinforced hardfacing show good wear resistance only at shallow impact angle.
5. Cross-sectional erosive wear analysis of samples tested at temperature of 650 °C (Fig. 14) combined with XPS surface analysis allows to conclude, that at high temperatures oxidation is one of the most wear influencing factors. For both hardfacings investigated, formed oxide and mechanically mixed layers protect the surface from the degradation and provide wear resistance.

Acknowledgements

This work was funded by the “Austrian Comet-Program” (governmental funding program for pre-competitive research) via the Austrian Research Promotion Agency (FFG) and the TecNet Capital GmbH (Province of Niederösterreich) and has been carried out within the “Austrian Center of Competence for Tribology” (AC2T Research GmbH) in cooperation with Tallinn University of Technology and partly supported by graduate school “Functional materials and technologies”, receiving funding from the European Social Fund under project 1.2.0401.09-0079 in Estonia and ESF Grants 8211 and 8850. Authors are also grateful to Sten Vinogradov and Dmitrij Goljandin MSc from Tallinn University of Technology for powders preparation.

References

- [1] Matthews S, James B, Hyland M. The role of microstructure in the high temperature oxidation mechanism of Cr₃C₂–NiCr composite coatings. *Corrosion Science* 2009;51:1172–80.
- [2] Meng J, Lu J, Wang J, Yang S. Tribological behavior of TiCN-based cermets at elevated temperatures. *Materials Science and Engineering: A* 2006;418: 68–76.
- [3] Hussainova I, Pirso J, Antonov M, Juhani K. High temperature erosion of Ti(Mo)C–Ni cermets. *Wear* 2009;267:1894–9.
- [4] Antonov M, Hussainova I, Veinthal R, Pirso J. Effect of temperature and load on three-body abrasion of cermets and steel. *Tribology International* 2012;46:261–8.
- [5] Antonov M, Hussainova I, Kübarsepp J, Traksmaa R. Oxidation-abrasion of TiC-based cermets in SiC medium. *Wear* 2011;273:23–31.
- [6] Antonov M, Hussainova I, Pirso J, Volobujeva O. Assessment of mechanically mixed layer developing during high temperature erosion of cermets. *Wear* 2007;263:878–86.
- [7] Feng Z, Ball A. The erosion of four materials using seven erodents-towards an understanding. *Wear* 1999;233:674–84.
- [8] Hussainova I. Some aspects of solid particle erosion of cermets. *Tribology International* 2001;34:89–93.
- [9] Kirchgäßner M, Badisch E, Franek F. Behaviour of iron-based hardfacing alloys under abrasion and impact. *Wear* 2008;265:772–7.
- [10] Buchely MF, Gutierrez JC, Leon LM, Torro A. The effect of microstructure on abrasive wear of hardfacing alloys. *Wear* 2005;259:52–61.
- [11] Bressan JD, Daros DP, Sokolowki A, Mesquita RA, Barbosa CA. Influence of hardness on the wear resistance of 17-4 PH stainless steel evaluated by the pin-on-disc testing. *Materials Processing Technology* 2008;205:353–9.
- [12] Winkelmann H, Badisch E, Kirchgäßner M, Danninger H. Wear mechanisms at high temperature. Part 1: wear mechanisms of different Fe-based alloys. *Tribology Letters* 2009;34:155–66.
- [13] Winkelmann H, Varga M, Badisch E, Danninger H. Wear mechanisms at high temperature. Part 2: temperature effects on wear mechanisms in the erosion test. *Tribology Letters* 2009;34:167–75.
- [14] Winkelmann H, Badisch E, Varga M, Danninger H. Wear mechanisms at high temperatures. Part 3: changes wear mechanisms at high temperatures. *Tribology Letters* 2010;37:419–29.
- [15] Katsich C, Badisch E, Roy M, Heath GR, Franek F. Erosive wear of hardfaced Fe–Cr–C alloys at elevated temperature. *Wear* 2009;267:1856–64.
- [16] Deuis RL, Subramanian C, Yellup JM. Three-body abrasive wear of composite coatings in dry and wet environments. *Composites Science and Technology* 1998;58:299–309.
- [17] Katsich C, Badisch E. Effect of carbide degradation in a Ni-based hardfacing under abrasive and combined impact/abrasive conditions. *Surface and Coatings Technology* 2011;206:1062–8.
- [18] Mellor BG. *Surface coatings for protection against wear*. Cambridge: Woodhead Publishing Limited; 2006.
- [19] Badisch E, Kirchgäßner M. Influence of welding parameters on microstructure and wear behaviour of a typical NiCrBSi hardfacing alloy reinforced with tungsten carbide. *Surface and Coatings Technology* 2008;202:6016–22.
- [20] TOPAS V3. General profile and structure analysis software for powder diffraction data. Bruker AXS, Karlsruhe; 2005.
- [21] Pirso J, Viljus M, Letunovits S, Juhani K. Reactive carburizing sintering—a novel production method for high quality chromium carbide–nickel cermets. *International Journal of Refractory Metals and Hard Materials* 2006;24: 263–70.
- [22] Zikin A, Hussainova I, Katsich C, Badisch E, Tomastik C. Advanced chromium carbide-based hardfacings. *Surface and Coatings Technology* 2012;206: 4270–8.
- [23] Zikin A, Hussainova I, Winkelmann H, Kulu P, Badisch E. Plasma transferred arc hardfacings reinforced by chromium carbide based cermet particles. *International Journal on Heat Treatment and Surface Engineering* 2012;6: 88–92.
- [24] Hussainova I, Antonov M. Assessment of cermets performance in erosive media. *International Journal of Materials and Product Technology* 2007;28: 361–76.
- [25] Hussainova I, Kübarsepp J, Pirso J. Mechanical properties and features of erosion of cermets. *Wear* 2001;250:818–25.
- [26] Roy M. Elevated temperature erosive wear of metallic materials. *Journal of Physics D: Applied Physics* 2006;39:101–24.
- [27] Lai GY. *High-temperature corrosion and materials applications*. USA: ASM International 2007.
- [28] Bose S. *High temperature coatings*. UK: Elsevier; 2007.
- [29] Ashish J, Kitheri J, Anthonyamy S, Gupta GS. Kinetics of oxidation of boron powder. *Thermochimica Acta* 2011;514:67–73.
- [30] Lavrenko VA, Glebov LA, Pomitkin AP, Chuprina VG, Protsenk TG. High-temperature oxidation of titanium carbide in oxygen. *Oxidation of Metals* 1975;9:171–9.

PUBLICATION V

Rojacz, H., Zikin, A., Mozelt, C., Winkelmann, H., Badisch, E., High temperature corrosion studies of cermet particle reinforced NiCrBSi hardfacings, *Surf. Coat. Technol.* In press.

DOI: <http://dx.doi.org/10.1016/j.surfcoat.2013.02.009>⁵

⁵ Copyright 2013, reprinted with permission from Elsevier



High temperature corrosion studies of cermet particle reinforced NiCrBSi hardfacings

H. Rojacz^{a,*}, A. Zikin^{a,b}, C. Mozelt^a, H. Winkelmann^a, E. Badisch^a

^a AC2T research GmbH, Viktor-Kaplan-Straße 2, 2700 Wiener Neustadt, Austria

^b Department of Materials Engineering, Tallinn University of Technology, Ehitajate tee 5, 19086 Tallinn, Estonia

ARTICLE INFO

Article history:

Received 4 May 2012

Accepted in revised form 9 February 2013

Available online 24 February 2013

Keywords:

High temperature corrosion

Oxidation

Metal matrix composite

Hardfacing

Cermet

ABSTRACT

Metal matrix composite hardfacings provide various types of heat and wear resistant products. They are widely used in high temperature aggressive environments due to their excellent high temperature corrosion and wear resistance. In this study, Cr_3C_2 -Ni and TiC-NiMo particles were used to reinforce a NiCrBSi matrix in plasma transferred arc welding process. These cermet particle reinforced hardfacings were examined on their oxidation behaviour and high temperature corrosion in different solid salts to optimise the field of application under high temperature conditions. Corrosion behaviour in solid salts is strongly dependent on the corroding anion. Cr_3C_2 -Ni reinforced hardfacings behave better in oxidative and sulphate/phosphate environment, while TiC-NiMo hardfacings show better resistance against chlorine and carbonate ions up to 700 °C. Additionally, oxidation is no critical exposure for these types of hardfacings.

© 2013 Elsevier B.V. All rights reserved.

1. Introduction

In various types of industrial applications such as sintering plants for the sintering of iron ore and coke, gas turbines, boilers, combustion engines, etc., high temperature corrosion is one of the most crucial problems. Materials working in such applications require not only high abrasion and impact wear resistance, but also excellent high temperature corrosion or/and oxidation resistance. Otherwise they would degrade by high-temperature oxidation processes which lead to failure and a loss of operability.

Hardfacings produced by high-velocity oxy-fuel (HVOF) spraying are commonly used in industry for protection coatings against corrosion and wear [1–3]. They combine high density, increased thickness capability and good wear resistance [3]. However, the presence of inclusions in the HVOF coatings often impairs the mechanical properties and may reduce the corrosion resistance. Reinforcement of HVOF coatings with hard phases can also lead to increased porosity. Cermet particles in sprayed coatings provide low metallurgical bonding and cohesive strength within these coatings [4].

Therefore, the development of metallurgically bonded highly impervious hardfacings, which would work at elevated temperatures and provide oxidation, high temperature corrosion and wear resistance, is of high scientific and industrial interest. One such promising technology for hardfacings production is the plasma transferred arc (PTA) welding process. PTA welding is an efficient technology commonly used for the fabrication of wear resistant hardfacings. As a unique heat source for surface modification, PTA exhibits enormous potential because of its low cost (compared with other surface deposition processes), easy

operation and no need for any special surface treatment [1,5,6]. Furthermore, the PTA technique allows the production of high quality coatings, e.g. good metallurgical bonding and low levels of porosity, consisting of metal matrix and carbide hard phases [7].

In the present research, two commonly developed hardfacings [8,9] were analysed regarding their high temperature corrosion and oxidation resistance. Both hardfacings have already shown promising results in aggressive (impact/abrasive and erosive wear conditions) environments at elevated temperature [9]. But there still is a lack of information about the behaviour of these hardfacings in high temperature corrosive environments.

Above mentioned metal matrix composites (MMCs) have a NiCrBSi matrix reinforced with wear resistant hard phases. One coating contains hard and oxidation resistant Cr_3C_2 -Ni hard phases. The choice of chromium-based hard phases can be explained with excellent oxidation resistance combined with high abrasion resistance of such structures [10–13]. It is also known that Ni and Cr form mixed Ni and Cr oxides, i.e. NiCr_2O_4 (Ni-spinel), NiO and Cr_2O_3 in oxidative media [14]. Due to the hard phase content, selective corrosion of matrix and carbide is expected. The forms of corrosion on the Ni-based matrix and the carbides strongly depend on temperature conditions and the anions; however, the matrix should be expected to show excellent resistance against most anions [15–17]. The second mentioned material contains TiC-NiMo hard phases, which have even higher hardness and promising properties like low density and high melting point.

The main objectives of this current study are the investigation of high temperature corrosion and oxidation behaviour of Cr_3C_2 -Ni and TiC-NiMo reinforced NiCrBSi PTA hardfacings. High temperature corrosion behaviour in four different salts (NaCl, NaHCO_3 , Na_2HPO_4 and NaHSO_4) at temperatures up to 700 °C is studied. Results show

* Corresponding author. Tel.: +43 2622 81600171; fax: +43 2622 8160099.
E-mail address: rojacz@ac2t.at (H. Rojacz).

performance of the investigated hardfacings in different high temperature corrosive conditions.

2. Experimental details

2.1. Materials data

Two different hardfacings were used in the present research: Cr_3C_2 -Ni reinforced NiCrBSi self-fluxing alloy and TiC-NiMo reinforced NiCrBSi self-fluxing alloy. PTA hardfacing of TiC-NiMo and Cr_3C_2 -Ni particles in combination with NiCrBSi matrix was carried out using a EuTronic® Gap 3001 DC apparatus using optimised welding parameters [8]. To prevent oxidation of the substrate material at high temperature austenitic stainless steel was used as substrate. The coatings' thickness was set to 2.0–2.5 mm. The hardfacings were produced from cermet particle and matrix powder with a ratio of 40/60 vol.%. The compositions of the precursor powders are presented in Table 1. Detailed information on the production of the coatings and the process of recycling of carbide scrap (bulk material) used to produce the initial carbide powder can be found in previous literature by Zikin et al. [8,9].

2.2. High temperature corrosion tests in solid salts at 700 °C

High temperature corrosion and oxidation behaviour in solid salts were investigated in this study. As seen in different studies [18–20] influences of different anions at elevated temperature were examined. Sodium salts were chosen in order to keep the cation constant. The corrosion tests were performed at 700 °C to show stability against corrosion at high temperature and to correlate the findings with the oxidation behaviour of these hardfacings. Both, corrosion and oxidation tests were performed over a period of 24 h. Chosen anions were: hydrogen carbonate HCO_3^- , chlorine Cl^- , hydrogen phosphate HPO_4^{2-} and hydrogen sulphate HSO_4^- . The resulting salts were: sodium hydrogen carbonate NaHCO_3 , sodium chloride NaCl , di-sodium hydrogen phosphate Na_2HPO_4 and sodium hydrogen sulphate NaHSO_4 . For explicit oxidation, tests at the same temperature were carried out in air. After preparing the samples (fine grinded condition) of $7 \times 7 \times 2$ mm, they were cleaned with ethanol, weighed and put into small ceramic crucibles for assembly in the furnace. All samples were completely surrounded with 10 g of salts to guarantee full contact between the samples and the anions during high temperature corrosion tests at 700 °C. After the procedure the samples were extricated from the remaining salts with deionised water, subsequently filtered and fully dried, which enables to determine the real mass loss or gain of the materials investigated. The characterisation of the different corrosiveness was studied quantitatively by mass change of the materials. In addition qualitative analysis was performed with light microscope (LM – Leica MEF4A equipped with a Leica Microsystems digital camera), stereo microscope (SM – Olympus SZX16 with Progres C5 digital camera), scanning electron microscope (SEM – Philips XL 30 FEG) and energy dispersive X-ray spectroscopy (EDX – EDAX X-ray analyser). In addition metallographic cross sections of the corroded samples were prepared to analyse carbide degradation, formed layers and the corrosive behaviour of different phases from both materials investigated. The microstructural studies were performed on samples etched with a

solution of HF and HNO_3 in a volume ratio of 1:12 at room temperature for 10 s.

3. Results and discussion

3.1. Materials microstructural characterisation

In the present study, two different hardfacings produced by a similar PTA process were analysed regarding their high temperature corrosion and oxidation behaviour. The coatings were produced from a mixture of hard phases (Cr_3C_2 -Ni or TiC-NiMo) and NiCrBSi matrix powder. The XRD patterns of the Cr_3C_2 -Ni and TiC-NiMo reinforced hardfacings are shown in Fig. 1. Fig. 1a shows the XRD analysis of the Cr_3C_2 -Ni reinforced NiCrBSi alloy. Basically, three main phases could be detected: the matrix phase identified as γ -Fe, Ni reinforced with high content of Cr_3C_2 and M_7C_3 hard phases [8]. Fig. 1b presents the XRD analysis of the NiCrBSi matrix with the addition of 40 vol.% TiC-NiMo particles. In this case five main phases were detected: matrix phase – γ -Fe, Ni solid solution with some complex borides indicated as a phase $(\text{Fe,Ni,Mo})_{23}\text{B}_6$ and probably also carbo-borides as precipitations. TiC and $\text{Ti}_{0.98}\text{Mo}_{0.02}\text{C}_{0.6}$ are the main hard phases according to the XRD analysis. Some amount of complex phase $(\text{Mo,Ti})\text{C}_2$ was also detected. Fig. 2a illustrates the microstructure of the coating produced from Cr_3C_2 -Ni powder in

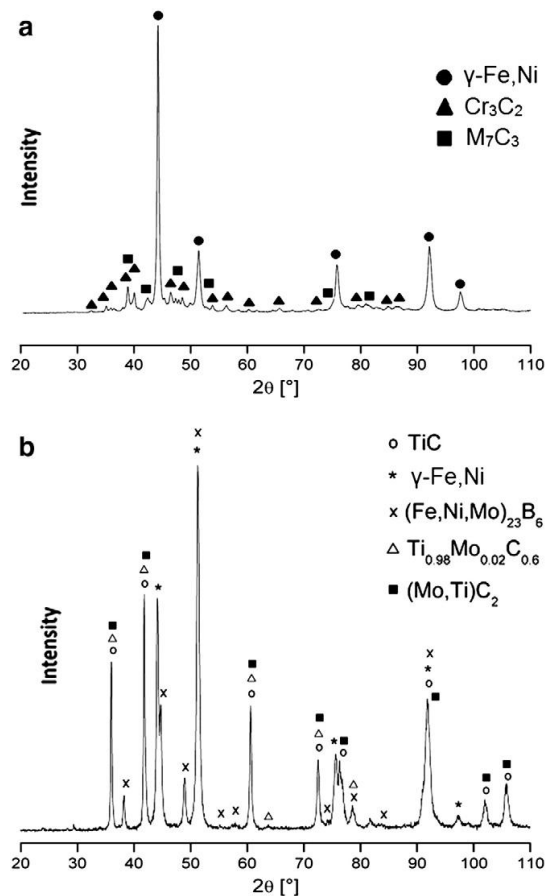


Fig. 1. XRD-patterns of the materials investigated: a) Cr_3C_2 -Ni particle reinforced; and b) TiC-NiMo particle reinforced.

Table 1
Initial welding powder data.

Powder	Source	Particle size, μm	Chemical composition, wt.%
Ni-based matrix	Castolin 16221	50–150	0.2% C, 4% Cr, 1% B, 2.5% Si, 2% Fe, rest Ni
TiC-NiMo	Recycled from bulk	150–310	80% TiC, 20% Ni:Mo 2:1
Cr_3C_2 -Ni	Recycled from bulk	150–310	80% Cr_3C_2 , 20% Ni

combination with the NiCrBSi matrix. The microstructure of this coating can be characterised by three apparent phases: hard phase-rich hypereutectic matrix material, some amount of dissolved and re-precipitated M_7C_3 (spine-like) carbides, and a certain content of grains of the initial cermet particles homogeneously distributed throughout the matrix. The cermet particles are constituted from agglomerates (2–5 μm sized Cr_3C_2 and M_7C_3 grains) embedded into nickel matrix, i.e. the commonly reported structure of the reactive sintered Cr_3C_2 -Ni cermet particles [21]. A detailed analysis of this hardfacing was previously presented by Zikin et al. [8,22]. Fig. 2b shows the microstructure of TiC-NiMo reinforced NiCrBSi hardfacing. SEM micrograph reveals the structure of the Ni-based dendritic matrix with homogeneous distribution of cermet particles and TiC-based rounded-shape precipitations. The cermet zone consists of TiC-Mo₂C-Ni phases and corresponds to typical co-rim structured hard grains surrounded by a tough metallic binder phase [23].

3.2. High temperature corrosion and oxidation studies

In the following subsections the effects of high temperature corrosion and oxidation of the investigated hardfacings are shown and discussed. Quantitative and qualitative analyses were performed to understand high temperature corrosion of the presented hardfacings, e.g. determination of mass changes and their comparison to different effects which took place during the thermal treatment in different corrosive media.

3.2.1. Mass changes due to thermal treatment

Hardfacings under investigation show both mass loss and gain due to decay of matrix or hard phases, or the forming of a corrosive layer. Qualitative effects will be discussed in the following sub items for a better understanding of gain or loss of mass. Fig. 3 highlights the percentage mass change of both samples in all tested media. This diagram shows the excellent oxidation behaviour of both hardfacings. It can be said that the combination of the NiCrBSi matrix and both chosen hard phases results in high oxidation resistance. Cr_3C_2 -Ni reinforced hardfacings lose mass due to oxidation (0.625 g/m^2). The oxidation of the cermet particle, which decreases the mass, is higher than the oxidation of the NiCrBSi matrix, which gains it. TiC-NiMo reinforced hardfacings also show excellent resistance of the matrix, but due to the low free Cr content in the NiCrBSi matrix and oxidation of TiC-based precipitations, they are less resistant against oxidation which leads to a mass gain of these samples of about 5 g/m^2 .

Cr_3C_2 -Ni reinforced hardfacing exhibits very low mass gain in phosphate (12.5 g/m^2) and high mass gain in sulphate (620 g/m^2) and chlorine ions (750 g/m^2), due to the massive growth of corrosion product layers. The only mass loss of these samples detected, took

place in carbonate environment. The mass loss of 170 g/m^2 derives from the decay of the cermet phases, which is stronger than the mass gain of the formed carbonate layer on NiCrBSi matrix.

TiC-NiMo reinforced hardfacings show high mass gain under chlorine condition (880 g/m^2), because of the forming of a thick chlorine layer and the dissolution of the NiMo binder in the cermet zones. TiC particles show high resistance against chlorine ions. Mass gain of these samples can be detected in carbonate (190 g/m^2) and phosphate (245 g/m^2) ions. High mass loss is seen under sulphate environment due to the total dissolution of the cermet particles, which is more influent on the mass change than the formed layer on the matrix. A slight mass increase (<1%) leads to the forming of a dense corrosive layer, which inhibits further corrosion attack. Mass increase at a higher rate (>2%) results in the forming of a porous layer which can spall off and further increase corrosion. Mass loss is far more problematic, due to the degradation of materials. Both, hard phases and matrix, can reveal degradation and decay at high levels. Excessive mass loss (>2%) probably indicates dropouts of cermet particles from the matrix. The above mentioned aspects and the quantitative analysis of the mass changes show that Cr_3C_2 -Ni reinforced hardfacings are highly resistant against phosphate environment at 700 °C, while TiC-NiMo reinforced hardfacings show good resistance against high temperature carbonate corrosion. Exposure to a high temperature chlorine environment results in strong mass increase for both investigated hardfacings. In contrast, exposure to a sulphate environment at 700 °C leads to high mass loss for TiC-NiMo reinforced hardfacings, probably due to degradation of the materials, while highly increasing the mass of the Cr_3C_2 -Ni reinforced samples by forming porous layers. Both hardfacings exhibit sufficient levels of oxidation resistance at 700 °C. To acquire a more detailed understanding of surface interactions with different corrosive media at 700 °C further investigations with precise microscopic analysis were elaborated.

3.2.2. Oxidation behaviour

The comparison of both materials investigated, as seen in Fig. 4 shows good stability against oxidation at 700 °C. In both cases the matrix shows very high resistance against oxidation, due to the forming of dense layers of NiO and NiCr_2O_4 in a thickness below the visibility with the SEM, which obstructs further oxidation [24]. Cr_3C_2 -Ni cermets show high resistance against corrosion because of the forming of Cr_2O_3 layers directionally into the cermet grain, while Ni and Cr in the matrix form a dense layer with oxygen from the surface. Both effects take place at the same time under elevated temperature conditions, which leads to a decrease or stop of oxidation. The formed oxide layer cannot be detected in the cross sections, while the TiC-NiMo cermets form a visible layer of about 2 μm thickness due to the high affinity of Ti to O.

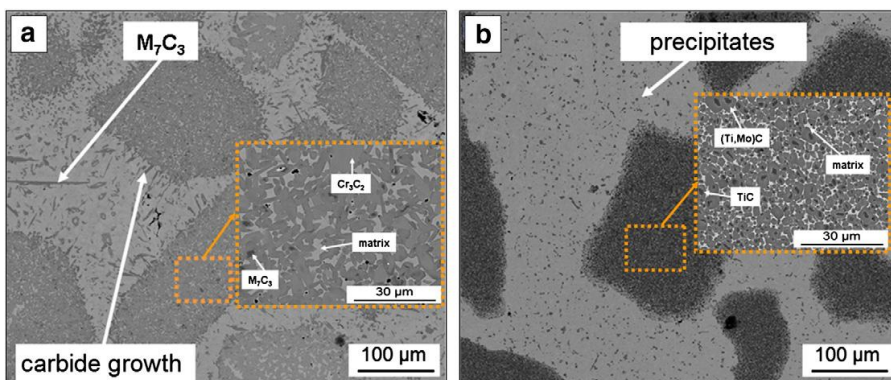


Fig. 2. SEM cross-section images of produced hardfacings: a) Cr_3C_2 -Ni particle reinforced; and b) TiC-NiMo particle reinforced.

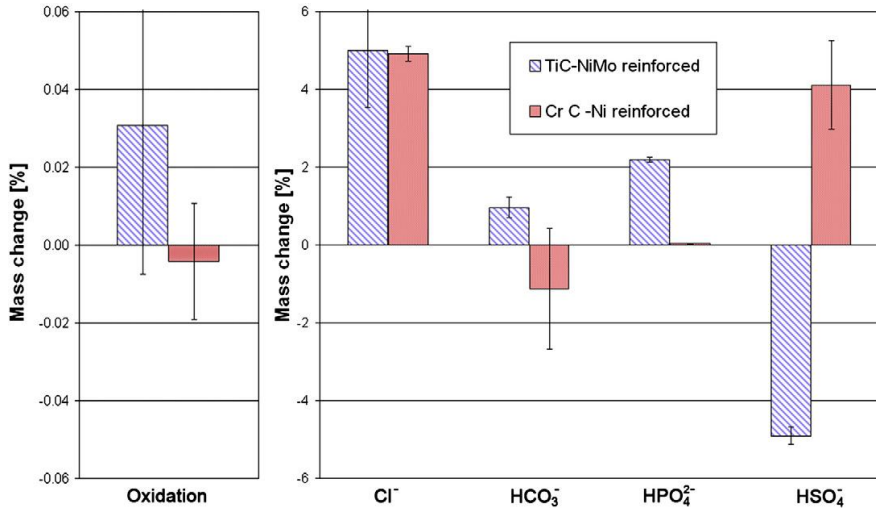


Fig. 3. Percentage mass changes of the materials investigated.

EDX-analysis, as seen in Fig. 4b, exhibits a mixed Ti-Ni-oxide layer. It can be said that both materials show very good resistance against oxidation at 700 °C due to the forming of very thin oxide layers, which obstruct further oxidation.

3.2.3. Stability against chlorine ions

Chlorine is highly corrosive to the Cr₃C₂-Ni reinforced samples, which leads to intergranular corrosion in the matrix and total decomposition and oxidation of the carbides. The formed chlorine layer of both of the samples cannot be seen in the cross sections because of the spalling off while performing the metallographic cross sections. As seen in Fig. 5a Cr₃C₂ oxidises, which is catalytic for the reaction with chlorine in high temperature environment. This leads to a chemical reaction from Cr₂O₃ to CrCl₃ and CO which brings about the decay of the hard phases [25]. As seen within the LM, these samples point out mostly CrCl₃ di-hydrate. TiC-NiMo shows better behaviour in this environment, because of the higher stability against intergranular corrosion, as seen in corrosion resistant steels [26,27].

Only the NiMo-binder of the TiC-NiMo hard phase degrades to NiCl₂ and more of MoCl₂, which leaves small amounts of Ni in the TiC-NiMo cermet particles as seen in Fig. 5b in detail. Due to the low carbide dissolution in the TiC-NiMo samples, the matrix shows much better behaviour in chlorine environment. There are no signs of intergranular corrosion. In high temperature chlorine environment TiC-NiMo as reinforcement for NiCrBSi matrix clearly is the better choice due to the increase of the resistance against intergranular corrosion.

3.2.4. Stability against carbonate ions

Carbonate ions encourage the forming of thick carbonate layers on both investigated samples. The dissolution of Cr₃C₂-Ni and the forming of a solid carbonate layer on the whole sample can be seen in Fig. 6a. Matrix and cermet particles form the layer equally. It can be said that the hydrogen carbonate anions decay to CO₂, H₂O and Na₂CO₃ which leads to corrosion under carbonic acid conditions. In combination with the present oxidation it leads to massive decay

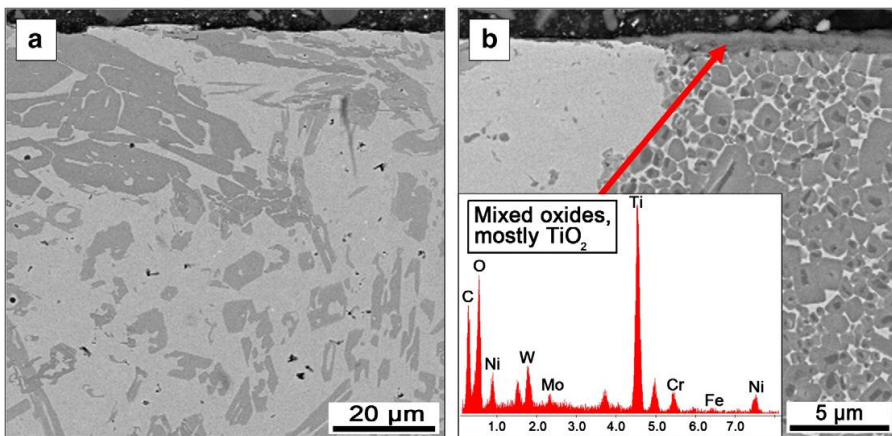


Fig. 4. SEM/EDX cross-sectional analysis of the materials investigated after oxidation tests at 700 °C for 24 h: a) Cr₃C₂-Ni particle reinforced; and b) TiC-NiMo particle reinforced.

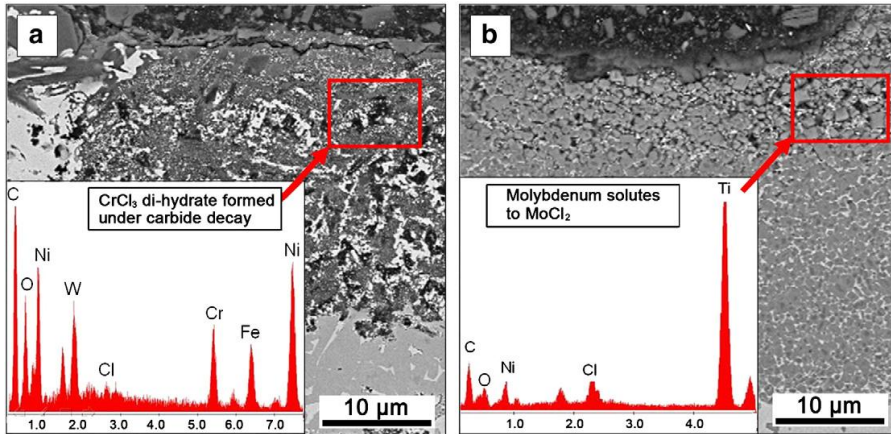


Fig. 5. SEM/EDX cross-sectional analysis of the materials investigated after corrosion tests in chlorine environment at 700 °C for 24 h: a) Cr_3C_2 -Ni particle reinforced; and b) TiC-NiMo particle reinforced.

of the surface. Different stages of film formation take place on the matrix in presence of TiC-NiMo reinforced hardfacing (Fig. 6b). The matrix forms a mixed Ni-Cr-oxide layer as seen on stainless steels, while the TiC transforms to TiCO_3 . On the outer side of the layer there is more Cr, and at the inner side more Ni can be detected which reliefs good correlation to the fundamentals of corrosion science [13]. The soluted carbides protect the matrix after oxidation with a layer of Cr oxides. Due to the low Ni binder amount in the cermet the hard phase is not protected against the alkaline corrosion, which leads to the dissolution into chromates. In this range of temperature according to Boudouard's equilibrium CO_2 and CO are present in equal parts. Ni reacts with the CO to $\text{Ni}(\text{CO})_4$ and NiO reacts with CO_2 to NiCO_3 , which leads to Ni decay and failure of the matrix [28]. Due to the mentioned facts it can be said that TiC-NiMo reinforced samples behave better in carbonate environment than those with Cr_3C_2 -Ni reinforcement.

3.2.5. Stability against phosphate ions

At 700 °C Na_2HPO_4 subverts to $\text{Na}_4\text{P}_2\text{O}_7$ under loss of H_2O . Simultaneously mixed phosphates with the alloying elements such as

Ni and Ti are formed under release of NaO or NaOH which leads to a basic corrosive species in addition to the phosphates [29]. On the Cr_3C_2 -Ni reinforced samples uniform corrosion is the dominant corrosion mechanism. This concludes on the basic corrosive species of NaO and NaOH and the not defined, locally changeable anodic and cathodic regions and the forming of a constant layer on the whole surface which is fundamental for uniform corrosion [26]. In phosphate environment, as seen in Fig. 7a, matrix and cermet particle corrode equally under forming of a phosphate/oxide-layer with a thickness of about 10 µm, which decreases further corrosion to a minimum due to parabolic growth of the layer. Due to the low affinity of Cr to P there is low corrosion on the surface.

The samples with TiC-NiMo hard phases do not show this effect. Both, the matrix and hard phase exhibits a coat of different phosphate layers as seen in Fig. 7b. Detailed analysis shows that Me_xP_y -compounds and phosphates from Ni, Cr, Ti and Fe are formed in the test. At the outer side of the mixed phosphate layer, a higher amount of Ni, than on the inside can be detected, where Ti-richer phases occur. The outer layer of these mixed phosphates is more porous than the inner layer, so the decay can be reduced by forming a more concrete layer at the inner

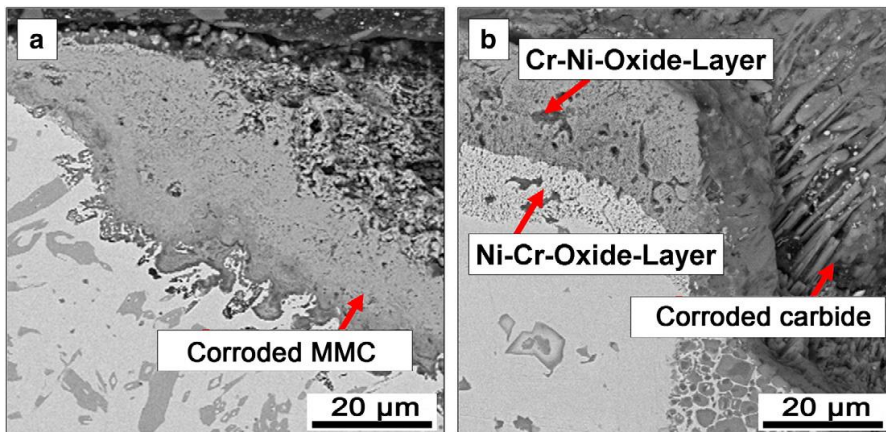


Fig. 6. SEM/EDX cross-sectional analysis of the materials investigated after corrosion tests in carbonate environment at 700 °C for 24 h: a) Cr_3C_2 -Ni particle reinforced; and b) TiC-NiMo particle reinforced.

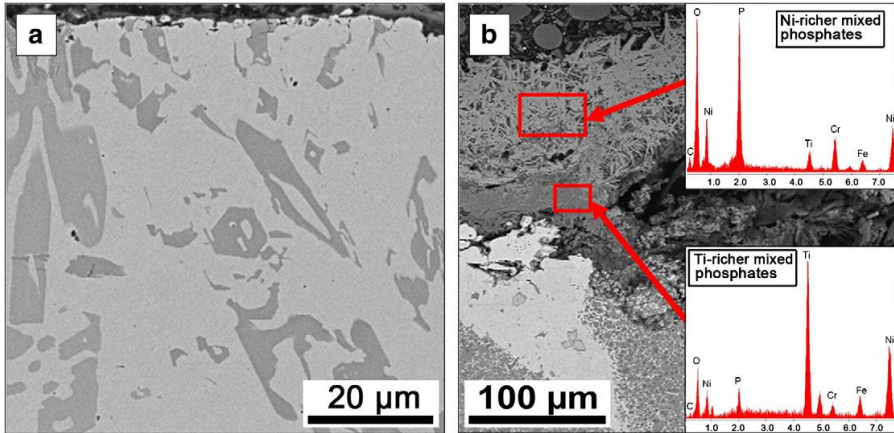


Fig. 7. SEM/EDX cross-sectional analysis of the materials investigated after corrosion tests in phosphate environment at 700 °C for 24 h: a) Cr_3C_2 -Ni particle reinforced; and b) TiC-NiMo particle reinforced.

side of these formed layers. The decay of the cermet particles is caused by the high affinity of Mo in the binder to P. This affects the decay of the TiC-NiMo hard phases and further corrodes the surrounding surface. Investigations show that Cr_3C_2 -Ni hard phases have better resistance against the high temperature phosphate environment.

3.2.6. Stability against sulphate ions

As a consequence of the high affinity of Ni to S there is uniform corrosion of the matrix in both types of samples. The decay of NaHSO_4 to Na_2SO_4 , SO_3^{2-} and H_2O via $\text{Na}_2\text{S}_2\text{O}_7$ and H_2O causes the release of free sulphur trioxide SO_3^{2-} which corrodes the matrix uniformly. Due to the Cr_3C_2 dissolution in the matrix, better behaviour is detected in these samples (Fig. 8a). In the case of the Cr_3C_2 -Ni particle reinforced samples the carbides are more resistant against sulphate corrosion than the NiCrBSi matrix. Due to the dissolution of the Cr_3C_2 -cermet particles and the formed chromium oxide layer on both, carbides and matrix, these MMCs are more stable than the TiC-NiMo reinforced samples. Mixed sulphate and oxide layers are formed when exceeding the temperature of degradation of the $\text{Na}_2\text{S}_2\text{O}_7$ to Na_2SO_4 and SO_3^{2-} . TiC-NiMo reinforced samples behave less resistant against sulphate because

of the missing Cr oxide layer. The TiC-NiMo hard phases, as seen in Fig. 8b, form a dense protection coating to decelerate corrosion, but the instability of the matrix leads to dropouts and corrosion on the whole carbide matrix interface. The typical behaviour of both samples in the high temperature sulphate environment is as expected unsatisfying. It can be seen that the Cr_3C_2 -Ni reinforced hardfacing behaves a little better than the TiC-NiMo reinforced samples. Both are still not resistant against sulphur corrosion.

3.2.7. Definition of restrictive high temperature corrosive environments

Considering the above mentioned qualitative and quantitative statements about the high temperature corrosion in different salts and oxidation we define fields of application for both, Cr_3C_2 -Ni and TiC-NiMo, hardfacings. Fig. 9 shows a graphical draw of the areas of resistance for different corrosive anions at 700 °C. As seen due to the mentioned facts, Cr_3C_2 -Ni reinforced hardfacings behave well in oxidative and sulphate/phosphate environment. Due to minimal mass gain in high temperature phosphate environment and the dense layer formed on the whole surface it can be said that this hardfacing is resistant against this exposure. The influence of sulphate

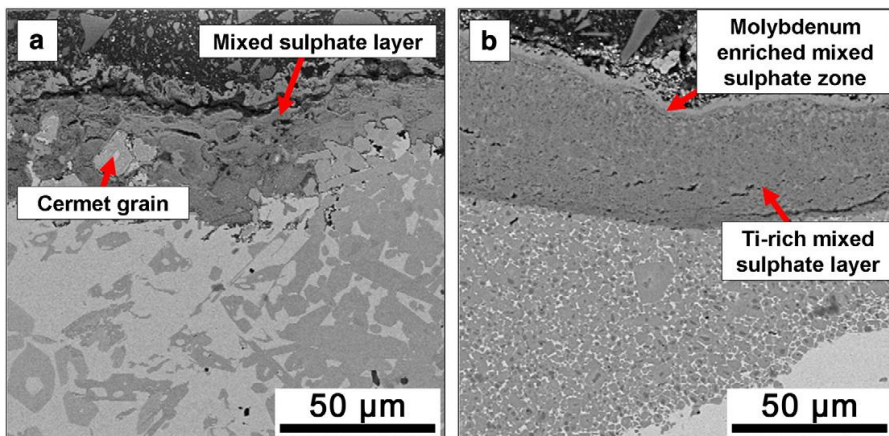


Fig. 8. SEM/EDX cross-sectional analysis of the materials investigated after corrosion tests in sulphate environment at 700 °C for 24 h: a) Cr_3C_2 -Ni particle reinforced; and b) TiC-NiMo particle reinforced.

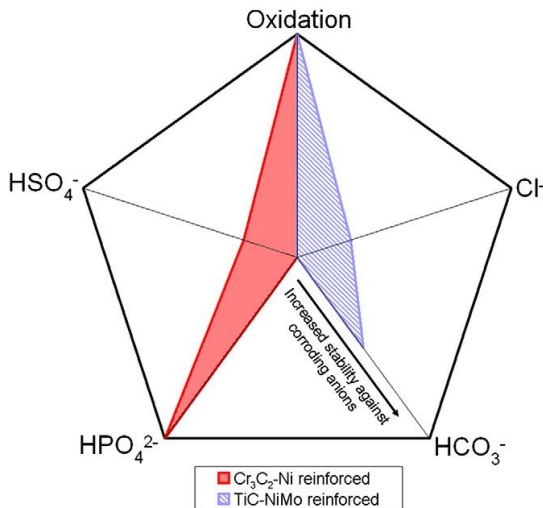


Fig. 9. Proposing the field of application in for $\text{Cr}_3\text{C}_2\text{-Ni}$ and TiC-NiMo reinforced hardfacings in different corrosive and oxidative media at a testing temperature of 700°C .

ions at 700°C is more problematic, but still a slight resistance due to the forming of moderately permeable layers, which decelerate but do not stop further corrosion, can be detected. TiC-NiMo hardfacings show good resistance against chlorine and carbonate ions at 700°C . Despite the high mass gain TiC-NiMo reinforced samples show better behaviour in chlorine condition because of the better stability of the cermet phases. Only the Ni-binder dissolves within the hard phases, while the TiC itself is inert to chlorine ions. The good resistance against high temperature carbonate corrosion can be inferred from the low mass gain; however, the greater part of the inhibiting effect derives from dense mixed Ni-Cr- or Cr-Ni-oxides, which further decrease corrosion. Both investigated cermet phases as reinforcement for the NiCrBSi matrix can be used in oxidative environment, because of their very low mass changes, and the forming of dense oxide layers, which decreases further oxidation to a minimum.

4. Conclusions

Based on the study within this work, the following conclusions can be drawn:

- High temperature corrosion tests of the investigated hardfacings show high dependence of the corrosion on the corroding anion. When reinforcing materials with cermet particles as hard phases it should be ensured that the hard phases are chosen according to the corrosive environment, otherwise the stability of those hardfacings cannot be assured. Material loss due to mechanical wear becomes negligible in comparison to corrosion if the wrong reinforcements are chosen.
- The $\text{Cr}_3\text{C}_2\text{-Ni}$ reinforced hardfacings exhibit good stability against oxidation and phosphate ions, while chlorine, sulphate and carbonate ions lead to high corrosion and in some cases degradation of the material. In the case of sulphate the $\text{Cr}_3\text{C}_2\text{-Ni}$ hard phases are more stable than the matrix, while carbonate is more radical to the NiCrBSi . Chlorine is highly aggressive to both, matrix and cermet reinforcements.

Intercrystalline corrosion due to chlorine leads to decay even down to a depth of $300\ \mu\text{m}$.

- For the TiC-NiMo reinforced samples in oxygen environment slight oxide films can be seen on the surface. Chlorine corrodes the matrix and the cermet binder, while the TiC itself is not decayed by chlorine. Phosphate and sulphate ions lead to total consumption of the hard phases and to massive corrosion products on the surface. Carbonate environment leads to mixed Ni and Cr oxides, which decreases further corrodibility.
- The field of application for both investigated hardfacings in dependence from the corrosive environment at 700°C was proposed. Both hardfacings show stability against oxidation, where protective oxide layers are formed. $\text{Cr}_3\text{C}_2\text{-Ni}$ reinforced hardfacings exhibit stronger resistance against sulphate and phosphate environment, while the TiC-NiMo hardfacings show better behaviour in chlorine and carbonate environment at 700°C .

Acknowledgements

This work was funded by the “Austrian Comet Program” (governmental funding programme for pre-competitive research) via the Austrian Research Promotion Agency (FFG) and the TecNet Capital GmbH (province of lower Austria) and has been carried out within the “Austrian Center of Competence for Tribology” (AC2T research GmbH).

References

- [1] B.G. Mellor, *Surface Coatings for Protection Against Wear*, Woodhead Publishing Limited, Cambridge, 2006, p. 83.
- [2] T.S. Sidhu, S. Prakash, R.D. Agrawal, *Surf. Coat. Technol.* 201 (2006) 1602.
- [3] T.S. Sidhu, R.D. Agrawal, S. Prakash, *Surf. Coat. Technol.* 198 (2005) 441.
- [4] W.-M. Zhao, Y. Wang, T. Han, K.-Y. Wu, J. Xue, *Surf. Coat. Technol.* 183 (2004) 118.
- [5] R. Chattopadhyay, *Advanced Thermally Assisted Surface Engineering Processes*, Springer, New York, 2004, p. 78.
- [6] R.L. Deus, J.M. Yellup, *Comput. Sci. Technol.* 58 (1998) 299.
- [7] C. Katsich, E. Badisch, *Surf. Coat. Technol.* 206 (2011) 1062.
- [8] A. Zikin, I. Hussainova, C. Katsich, E. Badisch, C. Tomastik, *Surf. Coat. Technol.* 206 (2012) 4270.
- [9] A. Zikin, M. Antonov, I. Hussainova, L. Katona, A. Gavrilovic, *Tribol. Int.* (2012), <http://dx.doi.org/10.1016/j.triboint.2012.08.013>.
- [10] M. Antonov, I. Hussainova, *Wear* 267 (2009) 1798.
- [11] J. Nurminen, J. Nakkki, P. Vuoristo, *Int. J. Refract. Met. Hard Mater.* 27 (2009) 472.
- [12] Z. Huang, Z. Hou, P. Wang, *Surf. Coat. Technol.* 202 (2008) 2993.
- [13] ASM International Handbook Committee, *Properties and Selection: Nonferrous Alloys and Special Purpose Materials*, ASM Handbooks, USA, 1990, p. 2691.
- [14] H. Xiaoxiao, L. Jinshan, H. Rui, B. Guanghai, F. Hengzhi, *Rare Met. Mater. Eng.* 39 (2010) 1908.
- [15] E. Bardal, *Corrosion and Protection*, Springer, London, 2003, p. 272.
- [16] P.A. Schweitzer, *Fundamentals of Metallic Corrosion – Atmospheric and Media Corrosion of Metal*, second ed., CRC Press, Boca Raton, 2007, p. 272.
- [17] P. Marcus, *Corrosion Mechanisms in Theory and Practice*, second ed., Marcel Dekker Inc., New York, 2002, p. 189.
- [18] L. Zheng, Z. Maicang, D. Jianxin, *Mater. Des.* 32 (2011) 1981.
- [19] C.C. Tsaur, J.C. Rock, C.J. Wang, Y.H. Su, *Mater. Chem. Phys.* 89 (2005) 445.
- [20] Y.S. Li, M. Spiegel, S. Shimada, *Mater. Chem. Phys.* 93 (2005) 217.
- [21] J. Pirso, M. Viljus, S. Letunovits, K. Juhani, *Int. J. Refract. Met. Hard Mater.* 24 (2006) 263.
- [22] A. Zikin, I. Hussainova, H. Winkelmann, P. Kulu, E. Badisch, *Int. J. Heat Treat. Surf. Eng.* 6 (2012) 88.
- [23] I. Hussainova, *Wear* 258 (2005) 357.
- [24] S. Bose, *High Temperature Coatings*, Butterworth-Heinemann, Burlington, 2007, p. 29.
- [25] W.J. Li, Y. Wang, C. Han, H.P. Tang, *Trans. Nonferrous Met. Soc. China* 21 (2011) 2617.
- [26] J.C. Korb, L. Olson, *Corrosion*, ASM Handbooks, USA, 1990, p. 265.
- [27] S.D. Cramer, L. Olson, *Corrosion: Fundamentals, Testing, and Protection*, ASM Handbooks, USA, 2003, p. 661.
- [28] G. Brauer, *Handbook of Preparative Inorganic Chemistry*, Academic Press, New York, 1965, p. 2691.
- [29] M.T. Averbuch-Pouchot, A. Durif, *Topics in Phosphate Chemistry*, World Scientific Publishing, London, 1996, p. 11.

CURRICULUM VITAE

1. Personal Data

Name	Arkadi Zikin
Date and place of birth	29.09.1985, Tallinn, Estonia
Email	arkzikin@gmail.com

2. Education

Education Institution	Graduation year	Education (field of study/degree)
Tallinn University of Technology (TTÜ)	2013	Ph.D studies, Materials Engineering
Tallinn University of Technology (TTÜ)	2010	M. Sc., Production Development and Production Engineering
Tallinn University of Technology (TTÜ)	2008	B. Sc., Production Development and Production Engineering
Fachhochschule Kiel	2007	Exchange studies, Mechanical Engineering
Tallinna Õismäe Vene Lütseum	2004	Secondary Education

3. Language competence/skills (fluent, average, basic skills)

Language	Level
Russian	Fluent
Estonian	Fluent
German	Fluent
English	Fluent

4. Special courses

Period	Educational or other organisation
2013 - Introduction to project management (16 hours)	AC ² T academy
2013 - Führungskräfte Seminar (16 hours)	AC ² T academy
2012 - Tribological materials and tribological coatings (32 hours)	Swedish Research School in Tribology

2011 - High temperature materials (48 hours)	TU Vienna
2010 - Towards Comprehensive Control of Wear (16 hours)	TWC Tampere

5. Professional employment

Period	Organisation	Position
2010-...	AC2T research GmbH	Senior scientist, project manager
2009-2010	Gomab	Technical officer
2008-2010	Letoro Grupp AS	Technical officer
2007-2008	Imco AS	Quality engineer (trainee)
2007-2007	Dräger Safety AG	Development engineer (trainee)

6. Research activity, including honours and thesis supervised

Honours & awards: 2012 - AC²T award for the highest scientific writing activities among all company workers

Main fields of research: Thick coatings for protection against wear and corrosion, PTA hardfacing, thermal spraying, laser cladding, process optimisation, material design, wear process, tribology

Amount of publications - 26 (source: www.etis.ee)

List of selected publications:

I. Hornung, J., Zikin, A., Pichelbauer, K., Kalin, M., Kirchgansbner, M., Influence of cooling speed on the microstructure and wear behaviour of hypereutectic Fe-Cr-C hardfacings, *Mat. Sci. Eng. A*, 2013, <http://dx.doi.org/10.1016/j.msea.2013.04.029>

II. Rojacz, H., Zikin, A., Mozelt, C., Winkelmann, H., Badisch, E., High temperature corrosion studies of cermet particle reinforced NiCrBSi hardfacings, *Surf. Coat. Technol.* 222, 2013, 90–96.

III. Zikin, A., Badisch, E., Hussainova, I., Tomastik, C., Danninger, H., Characterisation of TiC-NiMo reinforced Ni-based hardfacing, *Surf. Coat. Technol.* 2013, <http://dx.doi.org/10.1016/j.surfcoat.2013.02.027>

IV. Zikin, A., Hussainova, I., Katsich, C., Badisch, E., Tomastik, C., Advanced chromium carbide based hardfacings, *Surf. Coat. Technol.* 206, 2012, 4270–4278.

V. Zikin, A., Antonov, M., Hussainova, I., Katona, L., Gavrilovic, A., High temperature wear of cermet particle reinforced NiCrBSi Hardfacings, *Tribol. Inter.* <http://dx.doi.org/10.1016/j.triboint.2012.08.013>

VI. Veinthal, R., Sergejev, F., Zikin, A., Tarbe, R., Hornung, J., Abrasive impact wear and surface fatigue wear behaviour of Fe-Cr-C PTA overlays, *Wear*, 2013, In press. DOI: <http://dx.doi.org/10.1016/j.wear.2013.01.077>

VII. Kuzmanovic, J., Danninger, H., Gierl, C., Zbiral, J., Halwax, E., Zikin, A., Preparation and properties of sintered Fe and Ni based MMCs reinforced with fused tungsten carbide particles, *Powder Metall. Progress* 12, 2012, 84–98.

VIII. Veinthal, R., Zikin, A., Sarjas, H., Podgurski, V., Adoberg, E., Coatings and surface engineering - industry oriented research, *Estonian J. Eng.* 18-3, 2012, 176–184.

IX. Hussainova, I., Antonov, M., Zikin, A., Erosive wear of advanced composites based on WC, *Tribol. Inter.* 46, 2011, 254–260.

ELULOOKIRJELDUS

1. Isikuandmed

Ees- ja perekonnanimi
Sünniaeg ja -koht
E-posti aadress

Arkadi Zikin
29.09.1985, Tallinn, Estonia
arkzikin@gmail.com

2. Hariduskäik

Õppeasutus	Lõpetamise aeg	Haridus (eriala/kraad)
Tallinna Tehnikaülikool (TTÜ)	2013	Doktoriõpe, Mehhanotehnika
Tallinna Tehnikaülikool (TTÜ)	2010	Magistrikraad, tootearendus ja tootmistehnika
Tallinna Tehnikaülikool (TTÜ)	2008	Bakalaureusekraad, tootearendus ja tootmistehnika
Fachhochschule Kiel	2007	Välisõpe, masinaehitus
Tallinna Õismäe Vene Lütseum	2004	keskkool

3. Keelteoskus (alg-, kesk- või kõrgtase)

Keel	Tase
Vene	kõrg
Eesti	kõrg
Saksa	kõrg
Inglise	kõrg

4. Täiendusõpe

Õppimise aeg	Täiendusõppe korraldaja nimetus
2013 - Koolitus "Introduction to project management"	AC ² T academy
2013 - Koolitus "Führungskräfte"	AC ² T academy
2012 - PhD kursus "Tribological materials and tribological coatings"	Swedish Research School in Tribology
2011 - PhD kursus "High temperature materials"	TU Vienna
2010 - PhD kursus "Towards Comprehensive Control of Wear"	TWC Tampere

5. Teenistuskäik

Töötamise aeg	Tööandja nimetus	Ametikoht
2010 - ...	Austria triboloogia uurimiskeskus	vanemteadur
2009 - 2010	Gomab AG	tehniline insener
2008 - 2009	Letoro Group AS	tehniline insener
2007 - 2008	Imco AS	kvaliteediinsener
2007	Dräger Safety AG	arendusinsener

**DISSERTATIONS DEFENDED AT
TALLINN UNIVERSITY OF TECHNOLOGY ON
MECHANICAL ENGINEERING**

1. **Jakob Kübarsepp**. Steel-Bonded Hardmetals. 1992.
2. **Jakub Kõo**. Determination of Residual Stresses in Coatings & Coated Parts. 1994.
3. **Mart Tamre**. Tribocharacteristics of Journal Bearings Unlocated Axis. 1995.
4. **Paul Kallas**. Abrasive Erosion of Powder Materials. 1996.
5. **Jüri Pirso**. Titanium and Chromium Carbide Based Cermets. 1996.
6. **Heinrich Reshetnyak**. Hard Metals Serviceability in Sheet Metal Forming Operations. 1996.
7. **Arvi Kruusing**. Magnetic Microdevices and Their Fabrication methods. 1997.
8. **Roberto Carmona Davila**. Some Contributions to the Quality Control in Motor Car Industry. 1999.
9. **Harri Annuka**. Characterization and Application of TiC-Based Iron Alloys Bonded Cermets. 1999.
10. **Irina Hussainova**. Investigation of Particle-Wall Collision and Erosion Prediction. 1999.
11. **Edi Kulderknup**. Reliability and Uncertainty of Quality Measurement. 2000.
12. **Vitali Podgurski**. Laser Ablation and Thermal Evaporation of Thin Films and Structures. 2001.
13. **Igor Penkov**. Strength Investigation of Threaded Joints Under Static and Dynamic Loading. 2001.
14. **Martin Eerme**. Structural Modelling of Engineering Products and Realisation of Computer-Based Environment for Product Development. 2001.
15. **Toivo Tähemaa**. Assurance of Synergy and Competitive Dependability at Non-Safety-Critical Mechatronics Systems design. 2002.
16. **Jüri Resev**. Virtual Differential as Torque Distribution Control Unit in Automotive Propulsion Systems. 2002.
17. **Toomas Pihl**. Powder Coatings for Abrasive Wear. 2002.
18. **Sergei Letunovitš**. Tribology of Fine-Grained Cermets. 2003.
19. **Tatyana Karaulova**. Development of the Modelling Tool for the Analysis of the Production Process and its Entities for the SME. 2004.
20. **Grigori Nekrassov**. Development of an Intelligent Integrated Environment for Computer. 2004.
21. **Sergei Zimakov**. Novel Wear Resistant WC-Based Thermal Sprayed Coatings. 2004.

22. **Irina Preis.** Fatigue Performance and Mechanical Reliability of Cemented Carbides. 2004.
23. **Medhat Hussainov.** Effect of Solid Particles on Turbulence of Gas in Two-Phase Flows. 2005.
24. **Frid Kaljas.** Synergy-Based Approach to Design of the Interdisciplinary Systems. 2005.
25. **Dmitri Neshumayev.** Experimental and Numerical Investigation of Combined Heat Transfer Enhancement Technique in Gas-Heated Channels. 2005.
26. **Renno Veinthal.** Characterization and Modelling of Erosion Wear of Powder Composite Materials and Coatings. 2005.
27. **Sergei Tisler.** Deposition of Solid Particles from Aerosol Flow in Laminar Flat-Plate Boundary Layer. 2006.
28. **Tauno Otto.** Models for Monitoring of Technological Processes and Production Systems. 2006.
29. **Maksim Antonov.** Assessment of Cermets Performance in Aggressive Media. 2006.
30. **Tatjana Barashkova.** Research of the Effect of Correlation at the Measurement of Alternating Voltage. 2006.
31. **Jaan Kers.** Recycling of Composite Plastics. 2006.
32. **Raivo Sell.** Model Based Mechatronic Systems Modeling Methodology in Conceptual Design Stage. 2007.
33. **Hans Rämmal.** Experimental Methods for Sound Propagation Studies in Automotive Duct Systems. 2007.
34. **Meelis Pohlak.** Rapid Prototyping of Sheet Metal Components with Incremental Sheet Forming Technology. 2007.
35. **Priidu Peetsalu.** Microstructural Aspects of Thermal Sprayed WC-Co Coatings and Ni-Cr Coated Steels. 2007.
36. **Lauri Kollo.** Sinter/HIP Technology of TiC-Based Cermets. 2007.
37. **Andrei Dedov.** Assessment of Metal Condition and Remaining Life of In-service Power Plant Components Operating at High Temperature. 2007.
38. **Fjodor Sergejev.** Investigation of the Fatigue Mechanics Aspects of PM Hardmetals and Cermets. 2007.
39. **Eduard Ševtšenko.** Intelligent Decision Support System for the Network of Collaborative SME-s. 2007.
40. **Rünno Lumiste.** Networks and Innovation in Machinery and Electronics Industry and Enterprises (Estonian Case Studies). 2008.
41. **Kristo Karjust.** Integrated Product Development and Production Technology of Large Composite Plastic Products. 2008.
42. **Mart Saarna.** Fatigue Characteristics of PM Steels. 2008.

43. **Eduard Kimmari**. Exothermically Synthesized B₄C-Al Composites for Dry Sliding. 2008.
44. **Indrek Abiline**. Calibration Methods of Coating Thickness Gauges. 2008.
45. **Tiit Hindreus**. Synergy-Based Approach to Quality Assurance. 2009.
46. **Karl Raba**. Uncertainty Focused Product Improvement Models. 2009.
47. **Riho Tarbe**. Abrasive Impact Wear: Tester, Wear and Grindability Studies. 2009.
48. **Kristjan Juhani**. Reactive Sintered Chromium and Titanium Carbide-Based Cermets. 2009.
49. **Nadežda Dementjeva**. Energy Planning Model Analysis and Their Adaptability for Estonian Energy Sector. 2009.
50. **Igor Krupenski**. Numerical Simulation of Two-Phase Turbulent Flows in Ash Circulating Fluidized Bed. 2010.
51. **Aleksandr Hlebnikov**. The Analysis of Efficiency and Optimization of District Heating Networks in Estonia. 2010.
52. **Andres Petritšenko**. Vibration of Ladder Frames. 2010.
53. **Renee Joost**. Novel Methods for Hardmetal Production and Recycling. 2010.
54. **Andre Gregor**. Hard PVD Coatings for Tooling. 2010.
55. **Tõnu Roosaar**. Wear Performance of WC- and TiC-Based Ceramic-Metallic Composites. 2010.
56. **Alina Sivitski**. Sliding Wear of PVD Hard Coatings: Fatigue and Measurement Aspects. 2010.
57. **Sergei Kramanenko**. Fractal Approach for Multiple Project Management in Manufacturing Enterprises. 2010.
58. **Eduard Latõsov**. Model for the Analysis of Combined Heat and Power Production. 2011.
59. **Jürgen Riim**. Calibration Methods of Coating Thickness Standards. 2011.
60. **Andrei Surzhenkov**. Duplex Treatment of Steel Surface. 2011.
61. **Steffen Dahms**. Diffusion Welding of Different Materials. 2011.
62. **Birthe Matsi**. Research of Innovation Capacity Monitoring Methodology for Engineering Industry. 2011.
63. **Peeter Ross**. Data Sharing and Shared Workflow in Medical Imaging. 2011.
64. **Siim Link**. Reactivity of Woody and Herbaceous Biomass Chars. 2011.
65. **Kristjan Plamus**. The Impact of Oil Shale Calorific Value on CFB Boiler Thermal Efficiency and Environment. 2012.
66. **Aleksei Tšinjan**. Performance of Tool Materials in Blanking. 2012.
67. **Martinš Sarkans**. Synergy Deployment at Early Evaluation of Modularity of the Multi-Agent Production Systems. 2012.

68. **Sven Seiler**. Laboratory as a Service – A Holistic Framework for Remote and Virtual Labs. 2012.
69. **Tarmo Velsker**. Design Optimization of Steel and Glass Structures. 2012.
70. **Madis Tiik**. Access Rights and Organizational Management in Implementation of Estonian Electronic Health Record System. 2012.
71. **Marina Kostina**. Reliability Management of Manufacturing Processes in Machinery Enterprises. 2012.
72. **Robert Hudjakov**. Long-Range Navigation for Unmanned Off-Road Ground Vehicle. 2012.